

This is a Pre-print. The final version has been published in:

K.P. Lucht, J.L. Mendoza-Cortes, *The Journal of Physical Chemistry C*, **2015**, 119 (40), 22838-22846

Birnessite: A Layered Manganese Oxide to Capture Sunlight for Water-Splitting Catalysis.

Kevin P. Lucht^{†,§} and Jose L. Mendoza-Cortes^{*,†,‡,¶,§}

*Department of Chemical & Biomedical Engineering, FAMU-FSU College of Engineering,
Florida State University, Tallahassee FL, 32310, USA, University of California Berkeley,*

*Department of Chemistry, Berkeley, CA, 94720, U.S.A., and Scientific Computing
Department, Materials Science and Engineering Program, Condensed Matter Theory,
National High Magnetic Field Laboratory, Florida State University, Tallahassee FL, 32310,
USA*

E-mail: jmendozacortes@fsu.edu

*To whom correspondence should be addressed

†Department of Chemical & Biomedical Engineering, FAMU-FSU College of Engineering, Florida State University, Tallahassee FL, 32310, USA

‡University of California Berkeley, Department of Chemistry, Berkeley, CA, 94720, U.S.A.

¶Scientific Computing Department, Materials Science and Engineering Program, Condensed Matter Theory, National High Magnetic Field Laboratory, Florida State University, Tallahassee FL, 32310, USA

§Joint Center for Artificial Photosynthesis at Lawrence Berkeley National Laboratory, Materials Division, Berkeley, CA, 94720, U.S.A.

Abstract

We show a comprehensive study on the structure and electronic properties of a layered manganese oxide commonly known as Birnessite. We present the effects of substituting different intercalated cations (Li^+ , Na^+ , K^+ , Be^{2+} , Mg^{2+} , Ca^{2+} , Sr^{2+} , Zn^{2+} , B^{3+} , Al^{3+} , Ga^{3+} , Sc^{3+} , and Y^{3+}) and the role of waters in the intercalated layer. The importance of the Jahn-Teller effect and ordering of the Mn^{3+} centers due to cation intercalation are addressed to explain the ability to tune the indirect band gap (E_g^i) from 2.63 eV to \sim 2.20 eV and the direct band gap (E_g^d) from 3.09 eV to \sim 2.50 eV. By aligning the structures' bands, we noted that structures with Sr, Ca, B, and Al have potential for usage in water-splitting, and anhydrous B-Birnessite is predicted to have a suitable direct band gap for light capturing. Furthermore, we also demonstrate how the effects of cations in the bulk differ from the behavior on single layer surfaces. More specifically, we show that an indirect to direct band transition is observed when we separate the bulk into a single layer oxide. This study shows a new strategy for tuning the band gap of layered materials to capture light which may couple to its intrinsic water-splitting catalytic properties, thus resembling photosynthesis.

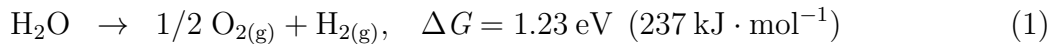
Keywords

water-splitting — oxygen evolution reaction — semi-conductor — light capture — band gap tuning

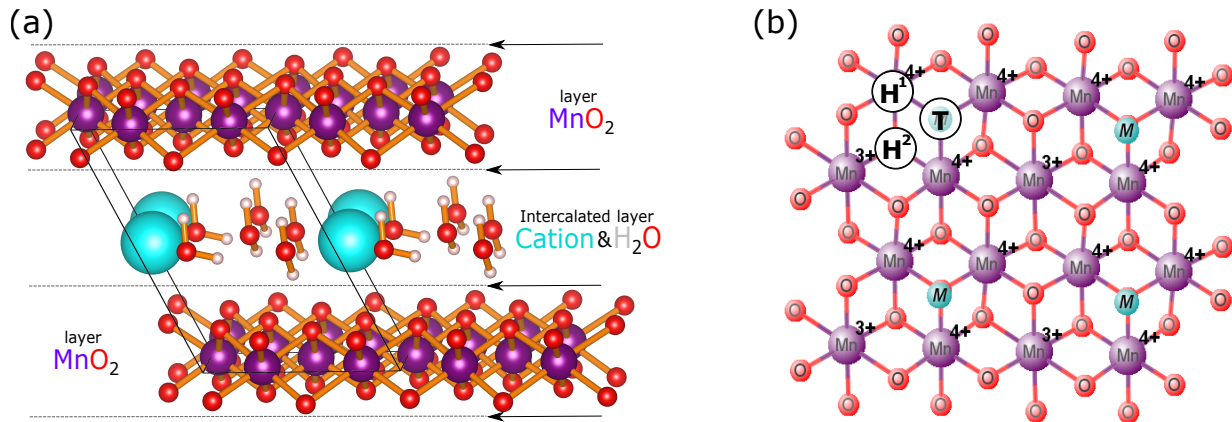
INTRODUCTION

The splitting of water is an attractive method to generate a renewable source of fuel through H_2 production and potentially reducing CO_2 into fuel such as methanol.¹ However, the oxidation of water comes at a price, requiring a substantial amount of energy to be a favorable

reaction:²



Fortunately, Nature has provided a successful method of water-splitting: photosystem II (PS-II), which stores energy by capturing solar energy to oxidize water. The core of this process is the oxygen evolution center (OEC) which is composed of $\text{Mn}_4\text{O}_8\text{Ca}$ in a cubane-like conformation coordinated to surrounding proteins and water.^{3,4} Although the process of water-splitting is not fully understood, it is known that the process occurs via five intermediate cycles known as S_i states (where i represents states 0 to 4). Throughout this process, Mn^{3+} ions in PS-II are oxidized to Mn^{4+} , allowing for photo-catalysis in the system to occur.⁵⁻⁸ Inspiration from the OEC have led to discussion and synthesis of various mimics to performing water-splitting and renewable fuel.⁹⁻¹¹ Some examples of this mimicking is found to some degrees in numerous natural mineral structures consist of manganese and oxygen content, for example: Ramsdellite ($\gamma\text{-MnO}_2$)¹², Pyrolusite ($\beta\text{-MnO}_2$)¹³, Hollandite ($\alpha\text{-MnO}_2$)¹⁴, Pyrochroite ($\text{Mn}[\text{OH}]_2$)¹⁵, Groutite ($\text{MnO}[\text{OH}]$)¹⁶, and Manganite ($\text{MnO}[\text{OH}]$)¹⁶, to name a few.



One of these natural geological forms of Mn_xO_y is a layered structure commonly known as Birnessite (see Figure 1). Birnessite is composed of layers of edge sharing MnO octahedra with an interlayer of hydrated cations and a general formula of $Na_{0.5}MnO_2 \cdot 1.5H_2O$.¹⁷⁻²⁰ Birnessite is known to catalyze water-splitting (also known as oxygen evolution reaction, OER) with a moderate overpotential.²¹ Regarding its application as a catalyst, Birnessite yields several similarities with the OEC in PS-II. For one, the octahedra structure of the MnO models the cubane-like conformation and contain manganese ions with oxidative states comparable to the S-states. It is also composed of mainly Mn^{3+} and Mn^{4+} , which are key intermediates in the OEC. However, an intercalated calcium ion in Birnessite assists by ensuring a neutral overall charge in the structure by modulating the oxidative state of the manganese rather than bonding to oxygens to form a cubane-like structure as in the OEC.^{22,23} Thus, our initial goal was to study the water-splitting mechanism by Birnessite, however during our study we found that Birnessite have promising properties as an effective light-capture material.

A major component needed for achieving artificial photosynthesis is to find water stable compounds with a direct band gap (E_g^d) ideally between 1.7 eV to 2.1 eV for O_2 generation and 1.1 eV for H_2 generation in a tandem cell. Sakai et al. suggest that synthetic Na-Birnessite has a band gap of 2.23 eV,²⁴ however, Pinaud et al. state that Na-Birnessite has a direct band gap of 2.7 eV with an indirect band gap around 2.1 eV.²⁵ Although these studies indicate Na-Birnessite is an inefficient material for light capture, the electronic structure and light capture capabilities have not been thoroughly studied. Manipulation of band transitions may be achieved through the insertion of various cations and studying the behavior of intercalated waters. Another study of interest are the properties of single-layer surfaces of Birnessite. Studies on ultra-thin surfaces of MoS_2 showed that as the number of layers are reduced, the indirect band transition decreases until it disappears with a single-layer surface,²⁶ and titanium oxides, a heavily studied photocatalyst, has shown anions and cations in the bulk and on surface structures alters their band gap energies by doping the

structures.²⁷⁻³⁰

To build an intuitive understanding of Birnessite's structural and electronic properties, it is worthwhile to investigate its behavior with the removal of water, cation exchange, and as an ultra-thin surface. In this paper, we present the effect on the band gap and electronic structure by substituting different cations (Li^+ , Na^+ , K^+ , Be^{2+} , Mg^{2+} , Ca^{2+} , Sr^{2+} , Zn^{2+} , B^{3+} , Al^{3+} , Ga^{3+} , Sc^{3+} , and Y^{3+}) between the layers and on single layer surfaces, the role of water in the interlayer, and changes in the arrangement of the oxidative pattern of managanese cations in the MnO layers. In this study we describe how some Birnessite structures can be promising light capture materials for the water-splitting reaction given their right band alignment and band gap. These predicted properties can be potentially combined with other Birnessites with intrinsic catalytic activity to build a large component of an artificial photosynthetic system.

MATERIALS AND METHODS

a. Structure Generation.

The structure of Birnessite was taken from experimental structures of Na-Birnessite: $\text{Na}_{0.5}\text{Mn}_2\text{O}_4 \cdot 1.5\text{H}_2\text{O}$ ^{19,20}. To generate a bulk model, the unit cell geometries were optimized on $\text{Mn}_4\text{O}_8 \cdot 3\text{H}_2\text{O}$ 1x2x1 supercells with Li, Na, K, Be, Mg, Ca, Sr, Zn, B, Al, Ga, Sc, and Y cations. DFT calculations were performed using B3PW91 hybrid density-functional^{31,32} implemented in the CRYSTAL09 code.³³ B3PW91 was chosen as it has shown to accurately predict band gaps for several semiconductors.³⁴ Optimization of the unit cell of the crystal structures were performed using TZVPP Gaussian basis sets for H, Li, Be, B, Na, K, Mg, Zn, Al, Sc, and Ga,³⁵, Hay-Walt VDZ effective core pseudopotentials for Sr, Y, and Mn³⁶⁻³⁸, and a modified 8-411d1 basis set for O.³⁸ A list of all the basis sets can be found in the supplementary information. The semi-empirical Grimme-D2 dispersion correction was used in order to estimate the van der Waal forces.³⁹ The reciprocal space for all the structures was sampled by

Γ -centered Monkhorst-Pack scheme with a resolution around $2\pi \times 1/40\text{\AA}^{-1}$. The threshold used for evaluating the convergence of the energy, forces, and electron density to optimize the structures was 10^{-7} au for each parameter. From the optimized structures, shifted cation, altered oxidative manganese patterned structures, two cation structures, and water removed structures were created. Shifting a cation's site occupation was done by manually shifting the cation to a new site and optimizing the structure. Two cation structures were constructed by manually adding a second cation into the interlayer and then optimizing the structures. To obtain the parallel Mn oxidative pattern, the spin distribution of the manganese ions was constrained from the alternative Mn oxidative pattern.

To determine the optimal structures for one, two, and three waters removed from the unit cell of the bulk structures, all possible combinations were considered. Since three waters are present in the unit cell, there are three possibilities each for removing one water and two waters. All of these possible structures were created, the electronic energy between the three structures for each water removed were compared, and the structure with the lowest energy for each water removed were chosen as the optimized structures.

Surfaces were initialized from the bulk structures from a slab cut along the (100) direction to generate a single layer MnO with the intercalated cation and waters. The $M_2^+Mn_4O_8 \cdot 6H_2O$ (using Li, Na, and K) surfaces were first optimized from $M^+Mn_2O_4 \cdot 3H_2O$ unit cells, and then expanded into $M_2^+Mn_4O_8 \cdot 6H_2O$ 1x2x1 supercells. Optimized water removal structures for the two cation surfaces were performed following the procedure for the bulk structures.

b. Electron Properties

The band pathway followed the symmetry points labeled in Table S7 with the pathways illustrated in Figure S5. Note that the N symmetry point for the surfaces was -1/2, 1/2, and 0 for b_1 , b_2 , and b_3 , respectively, the bulk structure followed the one labeled in Table S7. The density of states were plotted using the atomic orbitals of the manganese, oxygen, and intercalated cation while excluding oxygens from the intercalated waters as water did not

provide any energy states in either band. More comprehensive DOS diagrams can be found in the SI.

Band alignment was determined by taking the electrostatic potential energy from the MnO layer (the intercalated layer above the MnO layer) to the vacuum. The band energies were then set relative to this potential energy for both surfaces and bulk structures.

c. Calculating Relative Energies

The electronic energy of the optimized unit cells for each cation were compared to one another to determine their relative energy. Note that all reported relative energies are with respect to the unit cells (e.g. kcal mol⁻¹ per unit cell). The Gibbs' free energy of the systems was approximated using the electronic energy of the structure since vibrational contributions were negligible (shown in the SI for water removal in Na-Birnessite). The Gibbs' free energy including frequency calculations for water removed structures of Na-Birnessite were performed, and can be expressed as:

$$\Delta G = E_{\text{elec}} + E_0 + G_{\text{vib}} + PV - TS \quad (2)$$

where E_{elec} is the electronic energy, E_0 is the zero-point energy ($1/2 \hbar\omega$), G_{vib} is the thermal contribution to the vibrational energy, PV is pressure and volume, and TS is temperature and electronic entropy, respectively. The greatest vibrational contribution was the zero-point energy, which was still four orders of magnitude smaller than the electronic contribution alone (refer to the SI). Hence, the electronic energies for Birnessite structures were a fair approximate for the Gibbs' free energy for these cases. Thus, we refer to relative energies as ΔE unless otherwise indicated.

RESULTS AND DISCUSSION

Single Cation Bulk Structures

a. Structure

In the simplest Birnessite structure (no cation), the waters in the interlayer will situate themselves between an oxygen from each layer due to the hydrogens' affinity for the anionic oxygens. To achieve this conformation, the MnO layers will shift so that the oxygen facing into the interlayer will be on top of one another. When a cation is placed in the interlayer, it has the choice to situate itself between two oxygens, too, or wedge itself into two possible hollow sites in the layer, depicted in Figure 1b. For a majority of cations, there is a strong preference for the top site (**T**) in order to interact with the layer oxygens.

For Li, K, Na, and Sr the unit cell energy between the hollow site (**H²**) and **T** occupancy were nearly equivalent (Figure 1). Although the energy for B is also comparable, it is not due to occupancy but due to a difference in its coordination with water and an oxygen in the **T** location. Even though the location of the cations Li, K, Na, and Sr could shift, it was found that there were no significant differences in the electronic and structural properties due to site occupancy. Rather, the cations' charge act to modulate the oxidative state of the manganese while the size of the cation separates the layer. These two behaviors compete to determine a cation's affinity for the **T** site oxygen as greater Coulombic interaction promotes interaction while increasing a cation's size diminished it. Cations who interacted strongly were found to coordinate to one or both of the layers. The three possible interactions that were found are shown for selected structures in Figure 2. The ability to coordinate to the layers depended on the hardness (i.e. radial charge density) of the interlayer cation. In particular, the +2 cations demonstrate this dependence as the hardest cations (Be, Mg, and Zn) coordinate with water and the layers while the softest cations (Ca and Sr) have no interaction with oxygen on the layer and from water.

Beyond chemical interactions, as cations are intercalated, manganese ions are converted

from a stable d^3 (Mn^{4+}) state to an unstable high-spin d^4 state (Mn^{3+}). These Mn^{3+} cations will undergo a strong Jahn-Teller effect, elongating a pair of oxygens in order to split degenerate d orbitals to fill lower energy orbital shown in Figure 3.

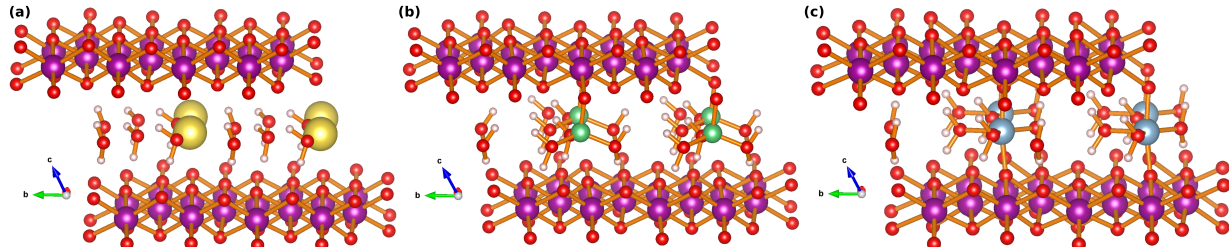


Figure 2: Representative Birnessite structures. (a) displays Na-Birnessite, an example where a cation has little interaction with the layers, (b) displays Be-Birnessite, where a cation coordinates to one layer, and (c) displays Al-Birnessite, where the cation coordinates to both layers.

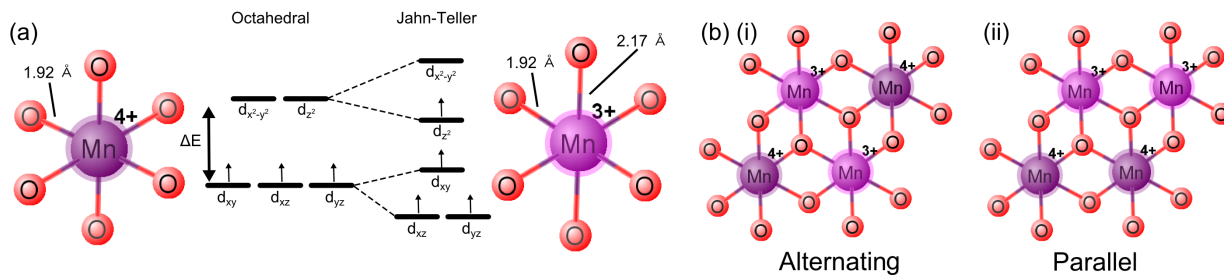


Figure 3: (a) illustrates the Jahn-Teller effect. For Mn^{3+} to the right, the Jahn-Teller effect causes elongation of the $\text{Mn}-\text{O}$ bond compared to Mn^{4+} to the left. Due to the loss of degeneracy, the orbitals for the Mn^{3+} are offset to lower the energy of the partially filled orbitals. (b) displays the two possible oxidative patterns of manganese when a +2 cation is present in the unit cell, (i) displays an alternating pattern of the manganese and (ii) displays a parallel pattern of the manganese.

Additionally, cations will induce a greater separation force which may be mitigated by enhancing the Jahn-Teller effect rather than increasing layer separation; alternatively, hard cations (i.e. Be, Mg, Zn, B, Al, and Ga) can induce local elongation of the Mn^{3+} -O bonds to allow oxygen to coordinate to the cation.⁴⁰ In both cases, layer expansion will occur as the Mn^{3+} -O bond weakens from the enhancing affects of the cations. Meanwhile, Mn^{4+} will not undergo distortion, and will stabilize elongated oxygens from Mn^{3+} centers it is coordinated

with. As the charge of the cation increases, and with it the number of Mn³⁺, the layers will be further destabilized as there are less Mn⁴⁺ to resist the elongation of the Mn³⁺ bonds. Thus, the MnO layers behave in two ways by varying the intercalated cation: either they separate by increasing the interlayer spacing or the layers spread out by expanding their average bonding distance. Generally, the separation of layers is more pronounced with decreasing hardness down a column on the periodic table since cations with a greater radial size induce a larger separation force. However, as cations increase in charge, the expansion of MnO layers becomes more pronounced as a greater number of Mn³⁺ centers are present, allowing the layers to relax by increasing bond lengths.

Another result of reducing the oxidative states of the manganese centers in the layer is rearrangement of the manganese oxidative pattern. Since the unit cell has four manganese arranged in a rhombus, two different oxidative state patterns are present for the MnO layer. These arrangements are both possible if two pairs of manganese cations with differing oxidative states are present in the unit cell, which are illustrated in Figure 3b. Comparison of their electronic energies shows the alternating oxidative pattern is slightly favorable (<3 kcal/mol), except for Sr (unfavorable by 6.26 kcal/mol) indicating the possibility of both structures being present. The main difference between the two manganese oxidative patterns is the strain on the Mn⁴⁺ cations which enforces or mitigates Jahn-Teller distortion. When the structure is arranged in the alternating Mn oxidative pattern, the MnO layers are destabilize as the oxygens effected by the Jahn-Teller effect are oriented such that three elongated bonds must be balanced by Mn⁴⁺, diminishing its resistance to the local elongation of the Mn³⁺-O bond to coordinating cations. With anisotropic ordering by aligning the oxidative states of manganese into the parallel patterning, the Jahn-Teller effect is diminished as two elongated oxygens along one axis must be controlled by Mn⁴⁺. Even in the example of the parallel Mn oxidative patterned structure for Be-Birnessite where one Mn³⁺-O bond breaks, this only allows Mn⁴⁺ to stabilize the oxygen coordinating to the Be²⁺ cation. By ordering the MnO layers in M²⁺-Birnessite structures, greater layer separation will occur

rather than relaxation through layer expansion.

For the bulk structures in general, their modification is due to Coulombic interactions between the layers and a separation force induced by the pressure a interlayer cation's size. However, a complete picture requires an understanding of cation interaction and structural changes due to the altered oxidative states of the manganese from the interlayer cations. The coordination of cations to layer oxygens can be explained in terms of hard-soft acid-base theory: as a cation increases in hardness (greater charge density) due to its charge and size, the smaller the layer separation can be expected due to greater cation interaction with the layers. Layers are further effected by the Jahn-Teller effect on Mn³⁺ centers. As more electrons are present in the surface, the easier it is for the layers to relax by elongating oxygens as Mn⁴⁺ centers are less able to stabilize the bonds. Cation coordination generally promotes layer expansion as coordination will cause local enhancement of the Jahn-Teller effect while large cations will induce greater Jahn-Teller distortion to mitigate the force their radial size induces on the MnO layers.

b. Single Cation Electronic Properties

For the simplest Birnessite structure (no cation) with three intercalated waters, a direct transition of 3.09 eV and a indirect transition of 2.63 eV are present. The bands of this structure are composed of mainly Mn⁴⁺ *d* orbitals in the conductive band and oxygen *s* and *sp* orbitals in the valence band. The band gaps for structures with a cation inserted in the interlayer are summarized in Table 1 and aligned band diagrams are shown in Figure 4.

Table 1: Band Gap for Bulk and Surface Birnessite Structures (eV)

Charge	Cation	Bulk $M^{n+}Mn_4O_8 \cdot 3H_2O$		Bulk $M_2^{n+}Mn_4O_8 \cdot 3H_2O$		Surface $M^{n+}Mn_4O_8 \cdot 3H_2O$		
		E_g^d	E_g^i	E_g^d	E_g^i	$E_g^d(\Gamma)$	E_g^i	$E_g^d(X)$
0	None	3.09	2.63	3.09	2.63			
+1	Li	2.56	2.25	3.01* (3.20) [†]	2.69* (2.63) [†]	2.71	2.33	
	Na	2.65	2.32	3.00* (3.05) [†]	2.64* (2.53) [†]	2.68	2.38	
	K	2.62	2.30	2.88* (3.11) [†]	2.59* (2.63) [†]	2.65	2.38	
+2	Be	2.95* (2.51) [†]	2.63* (2.23) [†]	2.76	2.42	2.82* (2.59) [†]	2.59* (2.39) [†]	
	Mg	2.92* (2.52) [†]	2.57* (2.19) [†]	2.91	2.54	2.78* (2.52) [†]	2.52* (2.19) [†]	
	Ca	3.02* (3.04) [†]	2.68* (2.47) [†]	3.31	2.99	2.93* (3.28) [†]	2.68* (2.93) [†]	
	Sr	2.94* (3.20) [†]	2.58* (2.67) [†]	3.60	3.44	2.84* (3.02) [†]	2.69* (2.69) [†]	
	Zn	2.94* (2.48) [†]	2.59* (2.21) [†]	3.01	2.60	3.00* (3.19) [†]	2.71* (2.89) [†]	
	B	2.65	2.49	2.72* (2.33) [†]	2.53* (2.17) [†]	2.86	2.73	
+3	Al	3.02	2.71	2.86* (2.80) [†]	2.43* (2.66) [†]	2.92	2.63	
	Ga	2.96	2.66	2.68	2.41	2.66	1.96	
	Sc	2.82	2.43	2.98* (2.69) [†]	2.72* (2.58) [†]	2.91	2.61	
	Y	2.92	2.51	2.67* (2.56) [†]	2.41* (2.24) [†]	2.94	2.58	

* Values for the alternating Mn oxidative pattern.

† Values for the parallel Mn oxidative pattern.

Inserting +1 cations into the interlayer resulted in a reduction in energy of the band transitions for all +1 cations. Although this reduction makes the cations immediate suspects, the valence band is composed primarily of Mn^{3+} d and the two Jahn-Teller distorted oxygens' s and sp orbitals while the conductive band is composed of mainly Mn^{4+} d orbitals (Figure 4a). Considering how soft the alkali metals are and how stable the structure is with three Mn^{4+} cations in the unit cell, they interact little with the layers. With the cations vindicated, the sudden reduction in the band gap can be attributed to the lowering of the energy of the valence band induced by Jahn-Teller distortion while the energy states for the conductive band are maintained by Mn^{4+} and its coordinated oxygens.

Once +2 cations are introduced, the band energies begin to shift to greater relative energies. For structures with the alternating Mn oxidative patterning, Be maintains a band gap similar to the alkali metals while the remaining +2 cations all have band gap energies similar to the simplest Birnessite structure. The difference in energies is a result of enhancing the Jahn-Teller effect due to cation size and oxidative patterning. For the harder coordinating +2 cations, enhancing of the Jahn-Teller effect occurs by elongating the coordinating layer oxygen. Furthermore, in the case of alternating oxidative patterning, the Mn^{4+} are forced to interact with three elongated oxygens. With larger Jahn-Teller distortion around one Mn^{3+} , the valence band energy shifts downward while the disruption on the Mn^{4+} shifts the conductive band higher in energy. Once the manganese oxidative pattern is adjusted to a parallel pattern, Be, Mg, and Zn reduce their band gap to ~ 2.50 eV direct and ~ 2.20 eV indirect, lower in energy than even the +1 cations. With anisotropic ordering by aligning the oxidative state of manganese into the parallel patterning, the Jahn-Teller effect is diminished for structures with Be, Mg, and Zn, allowing for both of the Mn^{3+} 's *d* orbitals to participate. Even in the case of Be which has a bond broken between a Jahn-Teller affected oxygen and Mn^{3+} , the square pyramidal geometry still lowers the valence band comparable to the remaining octahedral Mn^{3+} . Additionally, for these structures, Mn^{4+} ions now only interact with two opposing elongated oxygens as opposed to three in the alternating structure leaving four unaffected oxygens, lowering the energy of the conductive band. Comparing their DOS to their alternating Mn oxidative pattern counterparts, these effects result in the conductive band increasing slightly in energy and the valence band decreasing slightly in energy (Figure 4b and Figure 4c). However, Sr and Ca maintain band gap energies for either pattern as the Jahn-Teller effect for the parallel Mn oxidative patterned structures order the elongated oxygens differently than Be, Mg, and Zn. Rather than interfering with two Mn^{4+} -O bonds, their orientation disturbs four of the Mn^{4+} -O bonds, resulting in the conductive band shifting up while the Mn^{3+} orbitals remain unaffected. The difference in the orientation of the Jahn-Teller elongation is due to the coordination of the cation, as lowering the energy of

bonding orbitals promotes coordination of the cation metal with an elongated oxygen. However, Sr and Ca have no interaction with the layers but induce stress on the structure due to their size, therefore, the oxygens prefer to elongate away from these cations to relax the structure.

With the addition of +3 cations, the layers are highly distorted as the single Mn^{4+} interacts with four elongated oxygens, comparable to the Ca and Sr structures with parallel oxidative patterned layers. Since only a single Mn^{4+} is present to stabilize the structure, coordination offers little incentive to order the elongated oxygens as Mn^{4+} will always interact with at least four elongated oxygens regardless of orientation. Thus, it is no surprise that the band gap transitions (shown in Figure 4d) have similar energies for all +3 cations and near the values for the simplest Birnessite structure. Of all the structures, the energy of the valence band of Sr has the best alignment for the oxidation of oxygen in water, followed by structures containing B, Al, and Ca. To our knowledge, experiments have not been conducted on the catalytic properties of synthetic Birnessite structures with these cations. Experimental studies on these structures with a material suitable for the hydrogen evolution reaction could be excellent candidates for hydrogen production.

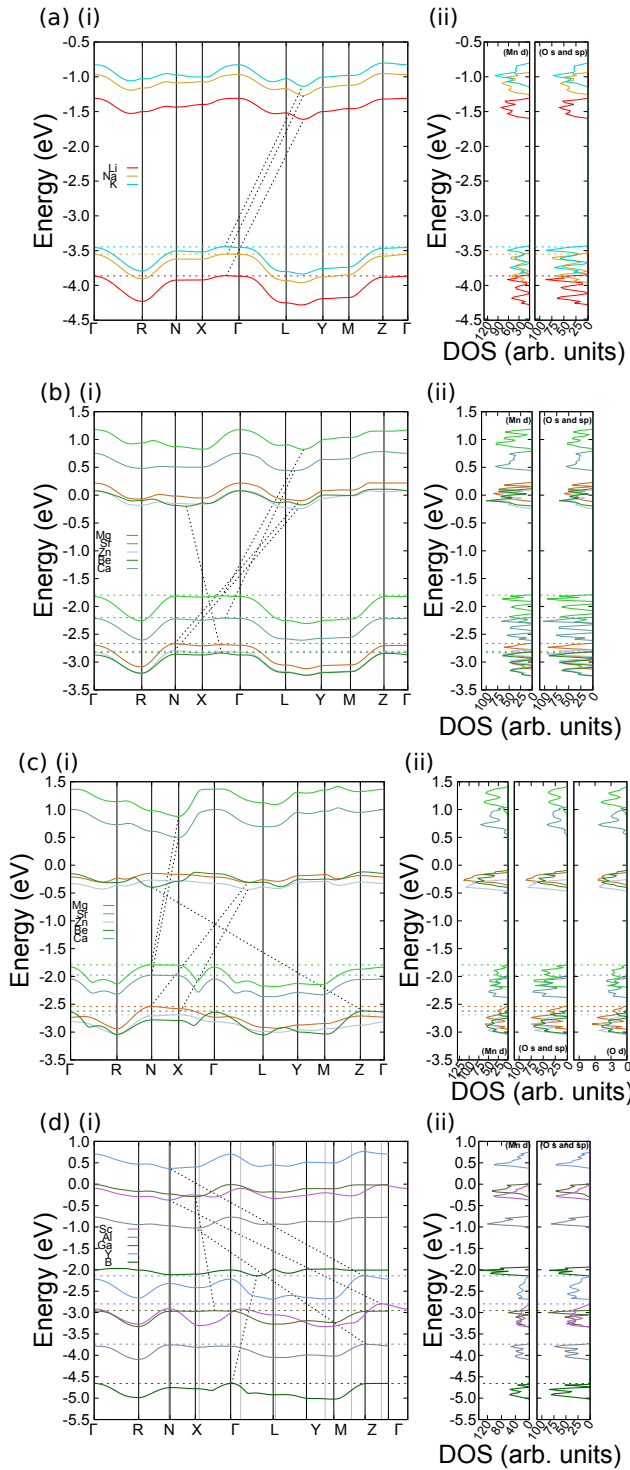


Figure 4: Electronic properties for (a) +1 cations, (b) +2 cations with an alternating Mn oxidative pattern, (c) +2 cations with a parallel Mn oxidative pattern, and (d) +3 cations. (i) displays the band structure and (ii) the total DOS for populated Mn and O orbitals.

c. Two Cation Structures and Electronic Properties

The addition of two cations of the same element were optimized in the bulk. A summary of the energy of formation from one cations structures is summarized in Table S1 in the SI. The lowest energies of formation were B⁺, Li, and Na, as these cations could either coordinate to the waters and layers rather favorable (in the case of B) or were small enough and interacted little with oxygen (Li and Na). For other cations, the disruption to their preferred coordination state due to two cations attempting to interact with oxygen resulted in large energies of formation.

For two cations and +3 cations, the formation energy for alternating and parallel oxidative patterning is very similar, thus, either pattern could be formed. For Li and Na, the shift was favorable by ~6.00 kcal/mol and unfavorable for B by 5.40 kcal/mol in energy. For the remaining structures, the energies were quite similar (<4 kcal/mol), indicating the possibility of either structure. With respect to their band structures (listed in Table 1), the addition of a cation resulted in increasing the band gap energy comparable to the single cation structure. For cations, the reduction of a manganese ion from Mn⁴⁺ to Mn³⁺ destabilizes the layers, causing an increase in band gap energy. The +2 cations also had rather large band energies as well since the oxidative state of all the manganese are 3+. The +3 cations provided the most interesting result as two of the manganese in the unit cell now have a 2+ oxidative state (except for Ga, where one Ga cation retains some electron density), which will act similarly to the 4+ oxidative state in terms of the degeneracy of their *d* orbitals. Hence, the structures with two +3 cations should have similar band gap energies as structures with one +2 cation. By orienting the structures in the parallel pattern, the band gap energies for B, Sc, and Y decrease as Be, Mg, and Zn did in the single cation structures. Although two cation structures provided interesting cation coordination and a different way to modulate the oxidative states of the manganese, the structures are largely unfavorable and as the band structures offer comparable behavior and no significant changes in energy to the single cation structures; these structures offer no additional properties of interest.

d. Water Removal Structures and Electron Properties

For all structures, the removal of water causes the α angle of the unit cell and layer spacing to decrease. As a result, the layer shifting brings the cation in closer proximity to the layers allowing for greater interaction. For several structures, the addition of the first water to the unit cell for a number of structures is not always preferred, but the addition of the remaining waters is unanimously favorable for all structures.

Table 2: Energy to Add Water to Bulk Unit Cell

Charge	Cation	Energy to Add a Water (kcalmol ⁻¹)		
		1 st	2 nd	3 rd
+1	Li	5.97	-25.7	-20.4
	Na	-9.85	-20.2	-18.1
	Na(freq)	-9.85	-20.2	-18.1
	K	-22.4	-17.3	-13.6
+2	Be	6.63	-52.6	-24.5
	Mg	13.6	-40.8	-29.5
	Ca	-16.4	-23.4	-28.5
	Sr	-31.5	-22.4	-19.1
	Zn	N/A	-28.2	-37.2
+3	B	-1.09	-62.1	-15.6
	Al	21.6	-51.3	-41.4
	Ga	4.92	-48.9	-38.0
	Sc	5.31	-41.5	-39.1
	Y	-25.0	-28.0	-29.4

As shown in Table 2 the cations of greater charge density have unfavorable energies for the addition of the first water: Li, Be, Mg, B (borderline), Al Ga, and Sc. These energies indicate that the opportunity to interact with layer oxygens for these structures is more favorable than the inclusion of water. For Zn with no waters, optimization of the structure was unsuccessful, however, the system should be expected to follow that of Mg. With the addition of water, the coordination geometry for cations are altered as they will lose their ability to strongly coordinate to layer oxygens. If water is added, the addition of a second water is largely favorable as it provides the cations with a preferred coordination geometry. Notably, Ga, Al, Sc, and Y shift from a tetrahedral geometry to a trigonal

pyramidal geometry, and B, switches from trigonal planar to tetrahedral geometry. These conformation changes are largely favorable, as indicated by the large decrease in relative energy for the addition of the second water. However, without waters, cations must solely coordinate with the layer oxygens, and those that do so readily display unfavorable energy for water addition. However, even with the possibility of forming these strongly coordinated bilayers, filling the structure with water is considerably favorable, which would mean hydrated structures should be expected to be filled with three interlayer waters at most.

Although the removal of water yielded changes for cations' coordination, there were generally few effects on the layers which consequently barely altered the band gap energies. The structures which caused considerable changes to the layers were B and Al structures with no waters. For boron in particular, the removal of all the waters yielded promising semiconducting behavior with band energies of 2.01 eV direct and 2.00 eV indirect. These energies emerge due to the severe structural changes coordination induce. The strength of boron's coordination causes two Mn³⁺ to alter themselves into a square pyramidal geometry and the third Mn³⁺ into square planar; even the Mn⁴⁺ is affected as several bonds are compressed in length. Although the ability to control the band gap by removing water could be a promising property for +3 cations, if hydration begins to occur, the structures would prefer to continue toward hydration until three waters per unit cell are reached. However, the anhydrous boron structure has promising semiconducting properties and has favorable stability relative to the hydration of water in the structure. A simple solution to avoid hydration would be to perform synthesis in inert or dry atmospheres until the structure is in the air-stable state.

Birnessite Surfaces

a. Single Cation Surfaces and Electronic Properties

A single MnO layer with the intercalated layer were generated from the bulk structures. The energy needed to separate the layers from their bulk counterparts is summarized in Table S1 of the SI. Separating Birnessite layers without a cation present is solely due to

attractive forces between them and to the waters, which was determined to be 22.8 kcal/mol. For structures with intercalated cations, only the alkali metals had layer separation energy comparable to the bare structure (20-30 kcal/mol). The only other structures with moderate separation energy were Be and B with 30.5 kcal/mol and 42.2 kcal/mol, respectively. For the remaining structures, the energy is considerably large, generally around 65.0 kcal/mol and in the most extreme case, for Ga, 118 kcal/mol. The two to three fold difference in energy is mainly due to disruption to the Mn-O bonds on the surface. For Be and B, which only coordinate to a single layer in the bulk, they more easily separate as they can maintain a favorable coordination arrangement while only enhancing their bonding to a single layer oxygen. However, for the softest +2 cations, Sr and Ca, their adsorption to the surface is mainly due to ionic contributions and stress on the layer due to their radial size. For Mg, Zn, Al, Sc, Y, and Ga, their separation energies mainly arise from a reduction in their coordination number. By losing interlayer coordination, these cations are forced into a less favorable conformation state. Ga is especially dissatisfied, and chooses to retain electron density in order to maintain its tetrahedral geometry. In either case, the physical stress induced from cation adsorption is the major component to structural changes on the MnO surface.

Compared to the bulk structures, the electronic properties of the surface structures in general vary only slightly due to the nuanced effects of Mn-O bonding and cation coordination, and can be found listed in Table 1 and their electronic properties are displayed in Figure 5. As these values show, the single layer surfaces are nearly equivalent to their bulk counterparts. The two structures with the most significant changes in the band structure are from B and Ga. For B, its strong coordination to oxygen from water causing proton transfer to the surface while its bonding to a surface oxygen results in breaking a Mn^{3+} -O bond at the coordination site. And, for Ga, the retention of electron density results in the alternating manganese oxidative pattern seen for +2 cations, yet Ga also contributes nearly all energy states in the valence band while also breaking a Mn^{3+} -O bond on each manganese.

The most interesting change resulted from shifting the +2 cations from their alternating Mn oxidative state to their parallel Mn oxidative pattern. In the anisotropic case, the conductive and valence bands bend along the X symmetry point which causes a direct transition for Mg and Sr rather than the usual indirect transition. This behavior is unique for these parallel oxidative patterned structures, and would be an interesting study for experimental investigation. These transitions manifest directly from the surface structure due to the forces exerted by the cation on the surface. For all +2 surface structures, the adsorption or coordination to the surface caused a Mn^{3+} -O bond to break, while adsorption of Be, Zn, and Ca caused significant Jahn-Teller distortion on the other Mn^{3+} center. For Mg and Sr, rather than inducing Jahn-Teller distortion, they broke a second Mn^{3+} -O bond. By breaking an additional bond, the surface loses a possible site for intraband transfer, removing the potential indirect transition, promoting the observed direct transition.

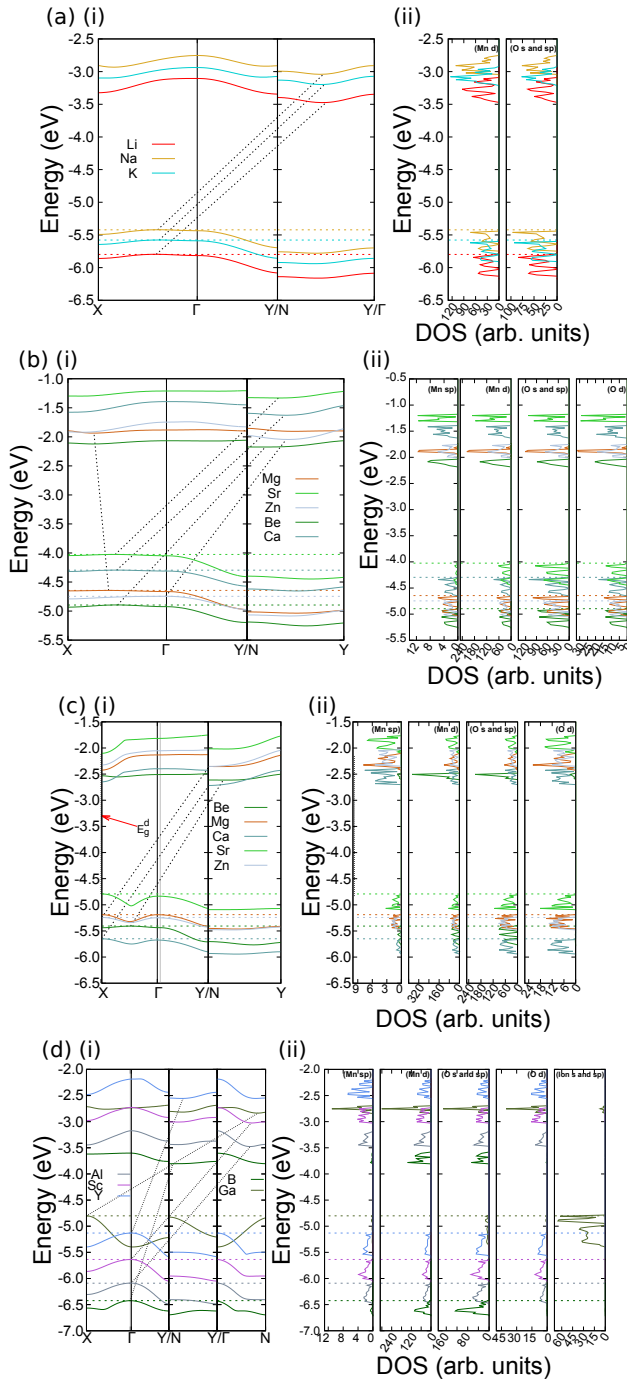


Figure 5: Electronic properties of surfaces with (a) +1 cations, (b) +2 cations with an alternating Mn oxidative pattern, (c) +2 cations with an alternating Mn oxidative pattern, and (d) +3 cations. (i) displays the band structures and (ii) displays the total DOS for manganese and oxygen in the layer.

CONCLUSION

In this paper, Birnessite is extensively studied to understand its electronic properties by examining its behavior due to cation substitution in bulk and surface structures as well as the removal of water from the interlayer. We found that cations play an important role in the structure by coordinating to surrounding oxygens from water and the layers and reducing the oxidative state of layer manganese. From the band aligned diagrams created of all the bulk structures, we predict structures with strontium, calcium, boron, or aluminum have valence bands with a band alignment suitable for water-splitting. These structures when placed in a tandem structure could be candidates for performing the OER. When all waters were removed in bulk structures, hard cations' affinity for layer oxygens made water uptake an unfavorable process, suggesting the possibility of studying hydrated and non-hydrated structures depending on their environment. In particular, intercalated boron in an anhydrous environment exhibits semiconducting behavior with a direct band transition for light capture of 2.01 eV.

From bulk structures, the separation of layers to form single layer surfaces was a low energy process of ~ 23.0 kcal/mol for the simplest Birnessite structure and +1 cations. For cations with a strong physical interaction with the layers or lost a favorable coordination number had an increase of separation energy by three to five fold. With respect to their electronic properties, cations modified the band transitions due to the Jahn-Teller effect on Mn^{3+} centers. Both bulk and surfaces structures had band transitions of similar energy. For surface structures, Mg and Sr surfaces with the layer manganese in a parallel oxidative pattern are predicted to have a direct transition of 2.19 eV for Mg and 2.69 eV for Sr along a direction other than the Γ -point. This unique behavior shows that an indirect band can become a direct band transition similar to chalcogenides. These predicted properties of bulk structures and surfaces suggest that Birnessite should be further investigated for its potential light capturing and catalytic properties.

ACKNOWLEDGMENTS

K.L. would like to acknowledge the initial support from the Workforce Development & Education-SULI (Science Undergraduate Laboratory Internship) program of the Department of Energys Lawrence Berkeley National Laboratory under U.S. Department of Energy Office of Science, Office of Basic Energy Sciences under Contract No. DE-AC02-05CH11231. J.L.M-C. would like to acknowledge initial support from the Joint Center for Artificial Photosynthesis (JCAP), a DOE Energy Innovation Hub, supported through the Office of Science of the U.S. Department of Energy under Award Number DE-SC0004993. We use the resource of National Energy Research Scientific Computing center (NERSC) located in the Lawrence Berkeley National Laboratory. J.L.M-C. would like to acknowledge the support from starting funds from Florida State University (FSU) and initial discussions with Manuel Soriaga and Jack Baricuatro. The initial project started at JCAP and was continued and finalized at FSU.

ASSOCIATED CONTENT

Supporting Information Available

Relative energy calculations and band transition energies for calculated structures (Li^+ , Na^+ , K^+ , Be^{2+} , Mg^{2+} , Ca^{2+} , Sr^{2+} , Zn^{2+} , B^{3+} , Al^{3+} , Ga^{3+} , Sc^{3+} , and Y^{3+}) as well as complete energy calculations for water removed structures of Na-Birnessite with vibrational contributions present; complete band and DOS diagrams are displayed as well as the pathway taken for the bulk structures and surfaces; a discussion on the structure and properties of two alkali metal cations in the unit cell of MnO surfaces. The Supporting Information is available free of charge on the ACS Publications website.

AUTHOR INFORMATION

Corresponding Authors

J.L.M.C. E-mail: jmendozacortes@fsu.edu.

Author Contributions

J.L.M.C. started and designed the tools for this project and also performed the electronic calculations for 8 ions (Li^+ , Na^+ , K^+ , Mg^{2+} , Ca^{2+} , Sr^{2+} , Zn^{2+} , and Y^{3+}) with different water contents as well as vibrational calculations. K.L. continued the project by using Be^{2+} , Zn^{2+} , B^{3+} , Al^{3+} , Ga^{3+} , and Sc^{3+} and exploring the different water contents. J.L.M.C. and K.L. analyzed the data and wrote the manuscript.

Notes

The authors declare no competing financial interests.

References

- (1) Lewis, N. S.; Nocera, D. G. Powering the planet: Chemical challenges in solar energy utilization. *Proc. Natl. Acad. Sci. U. S. A.* **2006**, *103*, 15729–15735.
- (2) Bard, A.; Fox, M. Artificial Photosynthesis - Solar Splitting of Water to Hydrogen and Oxygen. *Accounts Chem. Res.* **1995**, *28*, 141–145.
- (3) Umena, Y.; Kawakami, K.; Shen, J.-R.; Kamiya, N. Crystal Structure of Oxygen-Evolving Photosystem II at a Resolution of 1.9 Angstrom. *Nature* **2011**, *473*, 55–61.
- (4) Kanady, J.; Mendoza-Cortes, J.; Goddard III, W.; Agapie, T. *Oxygen-Evolving Complex of Photosystem II: Insights from Computation and Synthetic Models. Metalloproteins: Theory, Calculations, and Experiments*, 1st ed.; CRC Press: Boca Raton, FL, 2015; Vol. 1; Chapter 5, pp 165–203.
- (5) Haumann, M.; Muller, C.; Liebisch, P.; Iuzzolino, L.; Dittmer, J.; Grabolle, M.; Neissius, T.; Meyer-Klaucke, W.; Dau, H. Structural and Oxidation State Changes of the

Photosystem II Manganese Complex in Four Transitions of the Water Oxidation Cycle (S-0 -> S-1, S-1 -> S-2, S-2 -> S-3, and S-3,S-4 -> S-0) Characterized by X-ray Absorption Spectroscopy at 20 K and Room Temperature. *Biochemistry* **2005**, *44*, 1894–1908.

- (6) Kulik, L.; Epel, B.; Lubitz, W.; Messinger, J. Electronic Structure of the Mn₄OxCa Cluster in the S-0 and S-2 States of the Oxygen-Evolving Complex of Photosystem II Based on Pulse Mn-55-ENDOR and EPR Spectroscopy. *J. Am. Chem. Soc.* **2007**, *129*, 13421–13435.
- (7) Glatzel, P.; Schroeder, H.; Pushkar, Y.; Boron, T., III; Mukherjee, S.; Christou, G.; Pecoraro, V.; Messinger, J.; Yachandra, V.; Bergmann, U. et al. Electronic Structural Changes of Mn in the Oxygen-Evolving Complex of Photosystem II during the Catalytic Cycle. *Inorg. Chem.* **2013**, *52*, 5642–5644.
- (8) Yano, J.; Yachandra, V. Mn₄Ca Cluster in Photosynthesis: Where and How Water is Oxidized to Dioxygen. *Chem. Rev.* **2014**, *114*, 4175–4205.
- (9) Zaharieva, I.; Chernev, P.; Risch, M.; Klingan, K.; Kohlhoff, M.; Fischer, A.; Dau, H. Electrosynthesis, Functional, and Structural Characterization of a Water-Oxidizing Manganese Oxide. *Energy Environ. Sci.* **2012**, *5*, 7081–7089.
- (10) Iyer, A.; Del-Pilar, J.; King'ondu, C.; Kissel, E.; Garces, H.; Huang, H.; El-Sawy, A.; Dutta, P.; Suib, S. Water Oxidation Catalysis using Amorphous Manganese Oxides, Octahedral Molecular Sieves (OMS-2), and Octahedral Layered (OL-1) Manganese Oxide Structures. *J. Phys. Chem. C* **2012**, *116*, 6474–6483.
- (11) Najafpour, M.; Allakhverdiev, S. Manganese Compounds as Water Oxidizing Catalysts for Hydrogen Production via Water Splitting: from Manganese Complexes to Nano-sized Manganese Oxides. *Int. J. Hydrol. Energy* **2012**, *37*, 8753–8764.

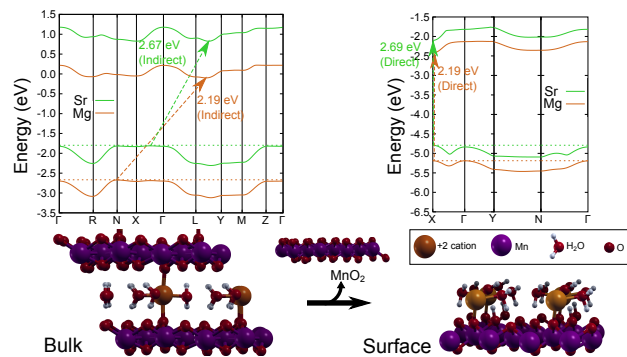
- (12) Fong, C.; Kennedy, B.; Elcombe, M. A Powder Neutron-Diffraction Study of Lambda-Manganese-Dioxide and Gamma-Manganese-Dioxide and of LiMn₂O₄. *Z. Kristall.* **1994**, *209*, 941–945.
- (13) Bolzan, A.; Fong, C.; Kennedy, B.; Howard, C. Powder Neutron-Diffraction Study of Pyrolusite, Beta-MnO₂. *Aust. J. Chem.* **1993**, *46*, 939–944.
- (14) Kijima, N.; Ikeda, T.; Oikawa, K.; Izumi, F.; Yoshimura, Y. Crystal Structure of an Open-tunnel Oxide Alpha-MnO₂ Analyzed by Rietveld Refinements and MEM-based Pattern Fitting. *J. Solid State Chem.* **2004**, *177*, 1258–1267.
- (15) Christen, A. A Single Crystal X-ray Diffraction Study of Mn(OH)₂. *Acta Chem. Scand.* **1965**, *19*, 1765–1766.
- (16) Kohler, T.; Armbruster, T.; Libowitzky, E. Hydrogen Bonding and Jahn-Teller Distortion in Groutite, Alpha-MnOOH, and Manganite, Gamma-MnOOH, and their Relations to the Manganese Dioxides Ramsdellite and Pyrolusite. *J. Solid State Chem.* **1997**, *133*, 486–500.
- (17) Lanson, B.; Drits, V.; Feng, Q.; Manceau, A. Structure of Synthetic Na-birnessite: Evidence for a Triclinic One-layer Unit Cell. *Am. Miner.* **2002**, *87*, 1662–1671.
- (18) Post, J.; Veblen, D. Crystal-Structure Determination of Synthetic Sodium, Magnesium, and Potassium Birnessite Using TEM and the Rietveld Method. *Am. Miner.* **1990**, *75*, 477–489.
- (19) Drits, V.; Silvester, E.; Gorshkov, A.; Manceau, A. Structure of Synthetic Monoclinic Na-rich Birnessite and Hexagonal Birnessite .1. Results from X-ray Diffraction and Selected-area Electron Diffraction. *Am. Miner.* **1997**, *82*, 946–961.
- (20) Golden, D.; Dixon, J.; Chen, C. Ion-Exchange, Thermal Transformations, and Oxidizing Properties of Birnessite. *Clay Clay Min.* **1986**, *34*, 511–520.

- (21) Robinson, D.; Go, Y. B.; Mui, M.; Gardner, G.; Zhang, Z.; Mastrogiovanni, D.; Garfunkel, E.; Li, J.; Greenblatt, M.; Dismukes, G. Photochemical Water Oxidation by Crystalline Polymorphs of Manganese Oxides: Structural Requirements for Catalysis. *J. Am. Chem. Soc.* **2013**, *135*, 3494–3501.
- (22) Lopano, C.; Heaney, P.; Post, J.; Hanson, J.; Komarneni, S. Time-resolved Structural Analysis of K- and Ba-exchange Reactions with Synthetic Na-birnessite Using Synchrotron X-ray Diffraction. *Am. Miner.* **2007**, *92*, 380–387.
- (23) Lopano, C.; Heaney, P.; Post, J. Cs-exchange in Birnessite: Reaction Mechanisms Inferred from Time-resolved X-ray Diffraction and Transmission Electron Microscopy. *Am. Miner.* **2009**, *94*, 816–826.
- (24) Sakai, N.; Ebina, Y.; Takada, K.; Sasaki, T. Photocurrent Generation from Semiconducting Manganese Oxide Nanosheets in Response to Visible Light. *J. Phys. Chem. B* **2005**, *109*, 9651–9655.
- (25) Pinaud, B.; Chen, Z.; Abram, D.; Jaramillo, T. Thin Films of Sodium Birnessite-Type MnO₂: Optical Properties, Electronic Band Structure, and Solar Photoelectrochemistry. *J. Phys. Chem. C* **2011**, *115*, 11830–11838.
- (26) Splendiani, A.; Sun, L.; Zhang, Y.; Li, T.; Kim, J.; Chim, C.-Y.; Galli, G.; Wang, F. Emerging Photoluminescence in Monolayer MoS₂. *Nano Lett.* **2010**, *10*, 1271–1275.
- (27) Beranek, R.; Kisch, H. Tuning the Optical and Photoelectrochemical Properties of Surface-modified TiO₂. *Photochem. Photobiol. Sci.* **2008**, *7*, 40–48.
- (28) Lee, J. Photocatalytic Water Splitting under Visible Light with Particulate Semiconductor Catalysts. *Catal. Surv. Asia* **2005**, *9*, 217–227.
- (29) Serpone, N. Is the Band Gap of Pristine TiO₂ Narrowed by Anion- and Cation-Doping

- of Titanium Dioxide in Second-Generation Photocatalysts? *J. Phys. Chem. B* **2006**, *110*, 24287–24293.
- (30) Kudo, A.; Niishiro, R.; Iwase, A.; Kato, H. Effects of Doping of Metal Cations on Morphology, Activity, and Visible Light Response of Photocatalysts. *Chem. Phys.* **2007**, *339*, 104–110.
- (31) Stephens, P.; Devlin, F.; Chabalowski, C.; Frisch, M. Ab-initio Calculations of Vibrational Absorption and Circular-Dichroism Spectra Using Density-Functional Force-Fields. *J. Phys. Chem.* **1994**, *98*, 11623–11627.
- (32) Kim, K.; J, K. Comparison of Density-Functional and MP2 Calculations on the Water Monomer and Dimer. *J. Phys. Chem.* **1994**, *98*, 10089–10094.
- (33) Dovesi, R.; Orlando, R.; Civalleri, B.; Roetti, C.; Saunders, V.; Zicovich-Wilson, C. Crystal: a Computational Tool for the Ab Initio Study of the Electronic Properties of Crystals. *Z. Kristall.* **2005**, *220*, 571–573.
- (34) Xiao, H.; Tahir-Kheli, J.; Goddard III, W. Accurate Band Gaps for Semiconductors from Density Functional Theory. *J. Phys. Chem. Lett.* **2011**, *2*, 212–217.
- (35) Peintinger, M.; Oliveira, D.; Bredow, T. Consistent Gaussian Basis Sets of Triple-Zeta Valence with Polarization Quality for Solid-State Calculations. *J. Comput. Chem.* **2013**, *34*, 451–459.
- (36) Erba, A.; El-Kelany, K.; Ferrero, M.; Baraille, I.; Rerat, M. Piezoelectricity of SrTiO₃: an Ab Initio Description. *Phys. Rev. B* **2013**, *88*.
- (37) Gennard, S.; Cora, F. *Unpublished*, http://www.crystal.unito.it/Basis_Sets/yttrium.html#buljan_1999.
- (38) Bredow, T.; Jug, K.; Evarestov, R. Electronic and Magnetic Structure of ScMnO₃. *Phys. Status Solidi B-Basic Solid State Phys.* **2006**, *243*, R10–R12.

-
- (39) Grimme, S. Semiempirical Gga-type Density Functional Constructed with a Long-range Dispersion Correction. *J. Comput. Chem.* **2006**, *27*, 1787–1799.
- (40) Alonso, J.; Martinez-Lope, M.; Casais, M.; Fernandez-Diaz, M. Evolution of the Jahn-Teller Distortion of MnO₆ Octahedra in RMnO₃ Perovskites (R = Pr, Nd, Dy, Tb, Ho, Er, Y): A Neutron Diffraction Study. *Inorg. Chem.* **2000**, *39*, 917–923.

TABLE OF CONTENTS GRAPHIC



This is a Pre-print. The final version has been published in:

K.P. Lucht, J.L. Mendoza-Cortes, *The Journal of Physical Chemistry C*, **2015**, 119 (40), 22838-22846

Supporting Information

Birnessite: A Layered Manganese Oxide to Capture Sunlight for Water-Splitting Catalysis.

Kevin Lucht^{1,2}, Jose L. Mendoza-Cortes^{1,2,3,4}

¹ Joint Center for Artificial Photosynthesis at Lawrence Berkeley National Laboratory, Materials Division, Berkeley, CA, 94720, U.S.A.

² Department of Chemical & Biomedical Engineering, FAMU-FSU College of Engineering, Florida State University, Tallahassee FL, 32310, USA

³ University of California Berkeley, Department of Chemistry, Berkeley, CA, 94720, U.S.A.

⁴ Scientific Computing Department, Materials Science and Engineering Program, Condensed Matter Theory, National High Magnetic Field Laboratory, Florida State University, Tallahassee FL, 32310, USA

E-mail: jmendozacortes@fsu.edu

Contents

	Page
Title	S1
List of Contents	S3
List of Figures	S5
List of Tables	S6
1 Bulk Birnessite	S1
1.1 $M^{n+}Mn_4O_8 \cdot H_3O$	S1
1.2 $M_2^{n+}Mn_4O_8 \cdot H_3O$	S3
2 Birnessite Surfaces	S4
2.0.1 a. $M^{n+}Mn_4O_8 \cdot 3H_2O$ Structure and Electronic Properties	S4
2.0.2 b. Two Cation Surfaces Structure and Electron Properties	S5
2.0.3 c. Two Cation Surfaces with Water Removal	S9
3 Materials and Methods	S12
3.1 Band Diagrams	S12
3.2 Relative Energies	S13
3.3 Relative Energies for Mn Oxidative Pattern	S15
3.4 Basis Sets	S17
4 Bulk Birnessite Structures	S21
4.1 $M^{n+}Mn_4O_8 \cdot 3H_2O$ Bulk	S21
4.2 $M^{n+}Mn_4O_8 \cdot 3H_2O$ Shifted Cation Site	S25
4.3 $M^{n+}Mn_4O_8 \cdot 3H_2O$ Parallel Oxidative Pattern	S29
4.4 $M_2^{n+}Mn_4O_8 \cdot 3H_2O$ Structures	S31
4.5 $M_2^{n+}Mn_4O_8 \cdot 3H_2O$ Parallel Oxidative Pattern	S35
4.6 $M^{n+}Mn_4O_8 \cdot 3H_2O$ Bulk Water Removal	S37
5 Surface Birnessite Structures	S48
5.1 $M^{n+}Mn_4O_8 \cdot 3H_2O$ Surfaces	S48
5.2 $M^{n+}Mn_4O_8 \cdot 3H_2O$ Parallel Oxidative Pattern	S52
6 Two Cation Surface Structures	S54
6.1 $M_2^{n+}Mn_4O_8 \cdot 6H_2O$ Parallel Pattern, Manganese Hollow Sites	S54

6.2	$M_2^{n+}Mn_4O_8 \cdot 6H_2O$ Parallel Pattern, Oxygen Hollow Sites	S54
6.3	$M_2^{n+}Mn_4O_8 \cdot 6H_2O$ Alternating Pattern, Oxygen Hollow Sites	S56

List of Figures

	Page
1	+1 cation bulk structures band and DOS diagrams S2
2	+2 cation bulk structures band and DOS diagrams, alternating Mn oxidative pattern S2
3	+2 cation bulk structures band and DOS diagrams, parallel Mn oxidative pattern S2
4	+3 cation bulk structures band and DOS diagrams S3
5	Electronic properties of surfaces with +1 cations. (a) displays the band structures and (b) displays the total DOS for manganese and oxygen in the layer. S5
6	Electronic properties of surfaces with +2 metal cations in the alternating Mn oxidative pattern. (a) displays the band structures and (b) displays the total DOS for manganese and oxygen in the layer. S6
7	Electronic properties of surfaces with +2 cations in the parallel Mn oxidative arrangement. (a) displays the band structures and (b) displays the total DOS for manganese and oxygen in the layer. S6
8	Electronic properties of surfaces with +3 cations. (a) displays the band structures and (b) displays the total DOS for manganese and oxygen in the layer. S7
9	Structure of the two cation surface with the manganese in the parallel oxidative pattern and the cations over H¹ sites. (a) Displays the surface while (b) displays an overview of the Mn oxidative pattern and cation site location (waters removed for clarity). S8
10	Structure of the two cation surface with the manganese in the parallel oxidative pattern where a cation occupies a H² site. (a) Displays the surface while (b) displays an overview of the Mn oxidative pattern and cation site location (waters removed for clarity). S8
11	Structure of the two cation surface with the manganese in the alternating oxidative pattern. (a) Displays the surface while (b) displays an overview of the Mn oxidative pattern and cation site location (waters removed for clarity). S8
12	Electronic properties for two cation surfaces in the parallel state with both metals over Mn ³⁺ H¹ sites. (a) displays the band structures and (b) displays the total DOS for manganese and oxygen in the layer. S9
13	Electronic properties for two cation surfaces in the parallel state with the metals over a H² site and a Mn ⁴⁺ H¹ site. (a) displays the band structures and (b) displays the total DOS for manganese and oxygen in the layer. S10

14	Electronic properties for two cation surfaces in the alternating state. (a) displays the band structures and (b) displays the total DOS for manganese and oxygen in the layer.	S11
15	Symmetry point pathway for bulk structures	S12
16	Symmetry point pathway for surface structures	S12
17	Layer Separation versus Charge Density	S16

List of Tables

	Page	
1	Relative Energy to Shift Cation Site and Structure Band Gap Energies	S1
2	Band Gaps for Water Addition in Bulk Structures	S1
3	Energy to Add Cation in Bulk Structures	S3
4	Energy for Separating Layers	S4
5	Band Gaps for Surface Structures ($M^{n+}Mn_4O_8 \cdot 3H_2O$)	S5
6	Energy for Second Cation Addition to the Surfaces	S6
7	Band Transitions for Two Cation Surfaces	S9
8	Band Gap for Surface Water Removed Structures	S10
9	Band Transitions for Two Cation Surfaces with Water Addition	S10
10	Symmetry Points in Reciprocal Space for Bulk Structures	S12
11	Symmetry Points in Reciprocal Space for Surface Structures	S12
12	Relative Energies for Mn Oxidative Pattern.	S15
13	Layer Separation Distance with respect to different cations and alternating and parallel pattern. . .	S16

1 Bulk Birnessite: Relative Energies and Band Diagrams

1.1 $M^{n+}Mn_4O_8 \cdot H_3O$

Table S1: Relative Energy to Shift Cation Site and Structure Band Gap Energies

Charge	Cation	ΔE (kcalmol ⁻¹)	E_g^d	E_g^i
+1	Li ^a	1.62	2.56	2.25
	Na ^a	5.66	2.77	2.36
	K ^a	0.05	2.69	2.39
+2	Be	9.40	3.15	2.74
	Mg ^b	17.7	2.77	2.34
	Ca ^a	10.5	2.85	2.52
	Sr ^a	5.93	2.58	2.27
	Zn ^b	19.7	3.07	2.62
+3	B	-2.21	3.21	2.94
	Al ^b	50.8	2.69	2.40
	Ga ^b	24.3	3.10	2.88
	Sc ^b	35.8	2.92	2.62
	Y ^b	13.3	2.97	2.65

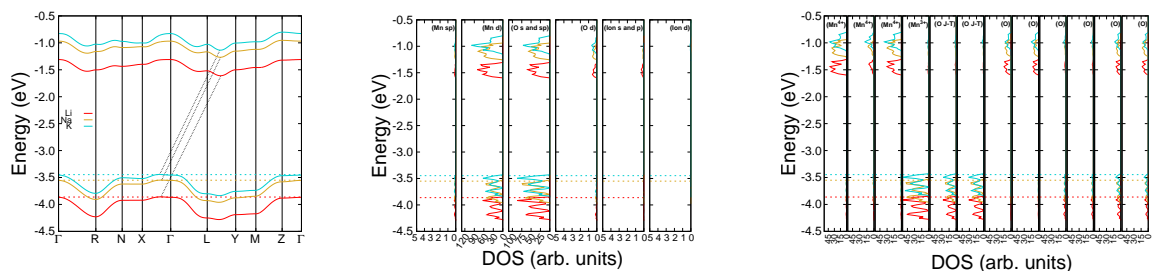
a. Cation shifted their occupation site in the structure

b. Cation had an altered coordination state, no shifting

Table S2: Band Gaps for Water Addition in Bulk Structures

Charge	Cation	Waters in Structure					
		Two		One		Zero	
		E_g^d	E_g^i	E_g^d	E_g^i	E_g^d	E_g^i
0	None	N/A	N/A	N/A	N/A	4.02	3.21
	Li	2.57	2.26	2.71	2.37	2.62	2.23
	Na	3.04	2.92	2.92	2.72	2.73	2.41
	Na(freq)	2.85	2.62	2.63	2.30	2.84	2.56
+1	K	2.64	2.31	2.77	2.59	2.69	2.29
	Be ^a	3.11	2.72	2.92	2.71	3.01	2.75
	Mg ^a	2.93	2.57	2.87	2.46	3.04	2.60
	Ca ^a	3.00	2.55	3.02	2.55	3.01	2.67
	Sr ^a	2.97	2.63	3.03	2.63	2.90	2.50
+2	Zn ^a	2.90	2.49	2.78	2.63		
	B	2.83	2.65	3.23	2.88	2.01	2.00
	Al	2.88	2.75	3.10	2.85	3.04	2.62
	Ga	2.85	2.73	2.77	2.67	3.08	2.33
	Sc	3.04	2.84	2.92	2.73	2.72	2.41
+3	Y	3.14	2.82	3.16	2.83	3.07	2.52

a. Values for the structures with an alternating Mn oxidative pattern

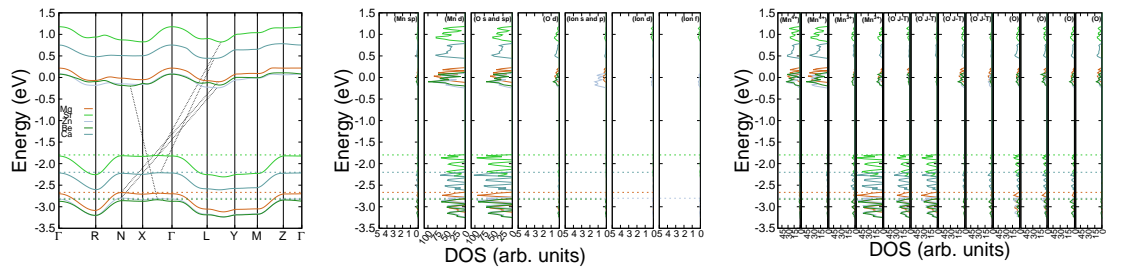


1.1: Band structure

1.2: Density of state for (i) Mn *sp*, (ii) Mn *d*, (iii) O *s* and *sp*, (iv) Mn *d*, (v) *d* orbitals and Oxygen *s* and *sp* orbitals. Ion *s* and *sp*, and (vi) Ion *d* orbitals.

1.3: Density of states for individual Mn

Figure S1: +1 cation bulk structures band and DOS diagrams

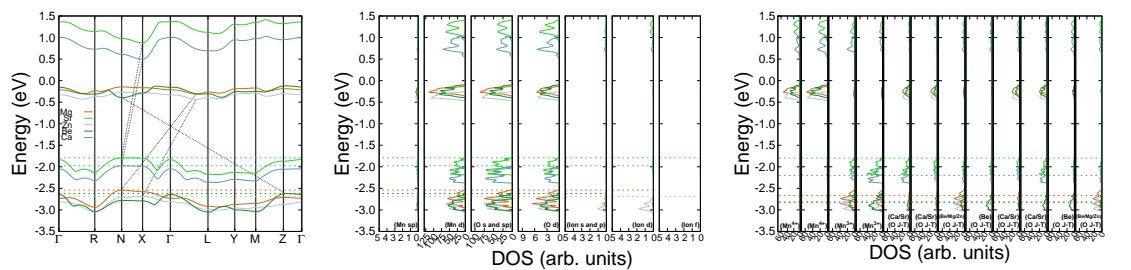


2.1: Band structure

2.2: Density of state for (i) Mn *sp*, (ii) Mn *d*, (iii) O *s* and *sp*, (iv) Mn *d*, (v) *d* orbitals and Oxygen *s* and *sp* orbitals. Ion *s* and *sp*, (vi) Ion *d* orbitals, and (vii) Ion *f* orbitals.

2.3: Density of states for individual Mn

Figure S2: +2 cation bulk structures band and DOS diagrams, alternating Mn oxidative pattern

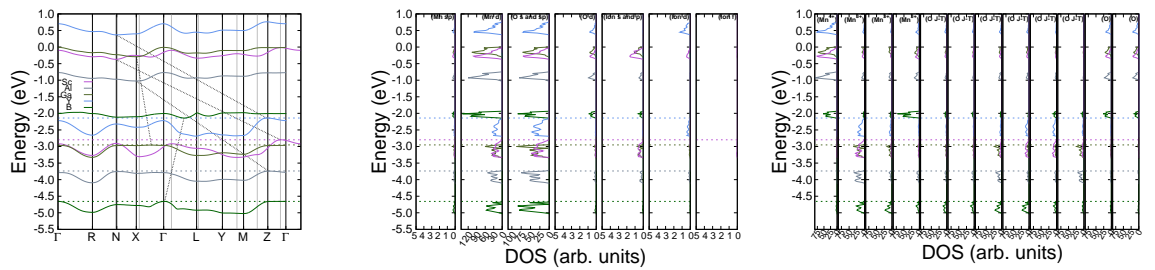


3.1: Band structures

3.2: Density of state for (i) Mn *sp*, (ii) Mn *d*, (iii) O *s* and *sp*, (iv) Mn *d*, (v) *d* orbitals and Oxygen *s* and *sp* orbitals. Ion *s* and *sp*, (vi) Ion *d* orbitals, and (vii) Ion *f* orbitals.

3.3: Density of states for individual Mn

Figure S3: +2 cation bulk structures band and DOS diagrams, parallel Mn oxidative pattern



4.1: Band structures

4.2: Density of state for (i) Mn *sp*, (ii) 4.3: Density of states for individual Mn *d*, (iii) O *s* and *sp*, (iv) Mn *d*, (v) *d* orbitals and Oxygen *s* and *sp* orbitals. Ion *s* and *sp*, (vi) Ion *d* orbitals, and (vii) Ion *f* orbitals.

Figure S4: +3 cation bulk structures band and DOS diagrams

1.2 $\text{M}_2^{n+}\text{Mn}_4\text{O}_8 \cdot \text{H}_3\text{O}$

Table S3: Energy to Add Cation in Bulk Structures

Charge	Cation	ΔE (kcalmol $^{-1}$)
+1	Li	15.8 ^a (9.45) ^b
	Na	27.5 ^a (22.5) ^b
	K	47.3 ^a (41.4) ^b
+2	Be	90.3
	Mg	62.8
	Ca	57.7
	Sr	86.5
	Zn	53.9
+3	B	30.6 ^a (36.0) ^b
	Al	94.3 ^a (93.2) ^b
	Ga	138
	Sc	105 ^a (108) ^b
	Y	109 ^a (105) ^b

a. Values for the alternating oxidative pattern

b. Values for the parallel oxidative pattern

2 Birnessite Surfaces: Surface Band Diagrams and Structures

2.0.1 a. $M^{n+}Mn_4O_8 \cdot 3H_2O$ Structure and Electronic Properties

A single MnO layer with the intercalated layer were generated from the bulk structures. The energy needed to separate the layers from their bulk counterparts is summarized in Table S4. Separating Birnessite layers without

Table S4: Energy for Separating Layers
 Charge Cation | ΔE (kcal/mol⁻¹)

0	None	22.8
1	Li	22.6
	Na	29.2
	K	26.3
+2	Be	42.2
	Mg	68.2
	Ca	67.8
	Sr	67.1
	Zn	67.0
+3	B	30.5
	Al	63.4
	Ga	118
	Sc	73.6
	Y	78.4

a cation present is solely due to attractive forces between them and to the waters, which was determined to be 22.8 kcal/mol. For structures with intercalated cations, only the alkali metals had layer separation energy comparable to the bare structure (20-30 kcal/mol). The only other structures with moderate separation energy were Be and B with 30.5 kcal/mol and 42.2 kcal/mol, respectively. For the remaining structures, the energy is considerably large, generally around 65.0 kcal/mol and in the most extreme case for Ga, 118 kcal/mol. The two to three fold difference in energy is mainly due to disruption to the Mn-O bonds on the surface. For Be and B, which only coordinate to a single layer in the bulk, they more easily separate as they can maintain a favorable coordination arrangement while only enhancing their bonding to a single layer oxygen. However, for the softest +2 cations, Sr and Ca, their adsorption to the surface is mainly due to ionic contributions and stress on the layer due to their radial size. For Mg, Zn, Al, Sc, Y, and Ga, their separation energies mainly arise from a reduction in their coordination number. By losing interlayer coordination, these cations are forced into a less favorable conformation state. Ga is especially dissatisfied, and chooses to retain electron density in order to maintain its tetrahedral geometry. In either case, the physical stress induced from cation adsorption is the major component to structural changes on the MnO surface.

Compared to the bulk structures, the electronic properties of the surface structures in general vary only slightly due to the nuanced effects of Mn-O bonding and cation coordination, and can be found listed in Table S5. As these values show, the single layer surfaces are nearly equivalent to their bulk counterparts. The two structures with the most significant changes in the band structure are from B and Ga. For B, its strong coordination to oxygen from water causing proton transfer to the surface while its bonding to a surface oxygen results in breaking a Mn^{3+} -O bond at the coordination site. And, for Ga, the retention of electron density results in the alternating manganese oxidative pattern seen for +2 cations, yet Ga also contributes nearly all energy states in the valence band while also breaking a Mn^{3+} -O bond on each manganese.

The most interesting change resulted from shifting the +2 cations from their alternating Mn oxidative state to their parallel Mn oxidative pattern. In the anisotropic case, the conductive and valence bands bend along the X symmetry point which causes a direct transition for Mg and Sr rather than the usual indirect transition. These transitions manifest directly from the surface structure due to the forces exerted by the cation on the surface. For all +2 surface structures, the adsorption or coordination to the surface caused a Mn^{3+} -O bond to break, while adsorption of Be, Zn, and Ca caused significant Jahn-Teller distortion on the other Mn^{3+} center. For Mg and Sr, rather than inducing Jahn-Teller distortion, they broke a second Mn^{3+} -O bond. By breaking an additional bond, the surface loses a possible site for intraband transfer, removing the potential indirect transition which promotes

Table S5: Band Gaps for Surface Structures ($M^{n+}Mn_4O_8 \cdot 3H_2O$)
 Bandgap (eV)

Charge	Cation	$E_g^d(\Gamma)$	E_g^i	$E_g^d(X)$
+1	Li	2.71	2.33	
	Na	2.68	2.38	
	K	2.65	2.38	
+2	Be	2.82* (2.59) [†]	2.59* (2.39) [†]	
	Mg	2.78* (2.52) [†]	2.52*	2.19 [†]
	Ca	2.93* (3.28) [†]	2.68* (2.93) [†]	
	Sr	2.84* (3.02) [†]	2.69*	2.69 [†]
	Zn	3.00* (3.19) [†]	2.71* (2.89) [†]	
+3	B	2.86	2.73	
	Al	2.92	2.63	
	Ga	2.66	1.96	
	Sc	2.91	2.61	
	Y	2.94	2.58	

the direct transition.

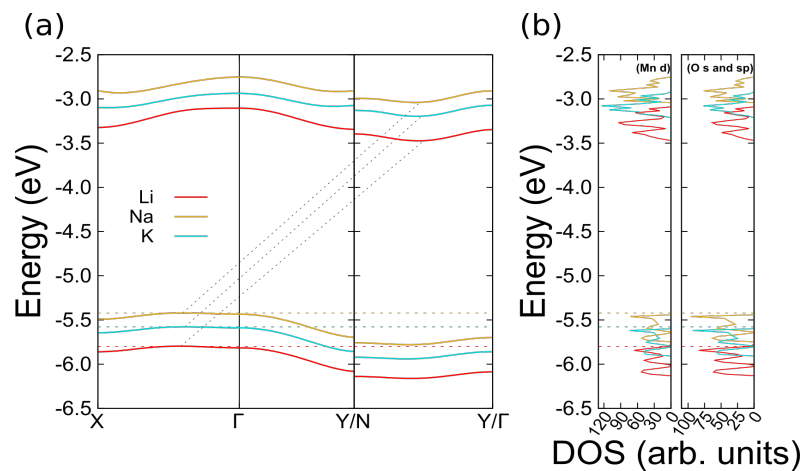


Figure S5: Electronic properties of surfaces with +1 cations. (a) displays the band structures and (b) displays the total DOS for manganese and oxygen in the layer.

2.0.2 b. Two Cation Surfaces Structure and Electron Properties

As anisotropic ordering of the MnO layers appears to promote semiconducting behavior, alkali metal structures were optimized with double the concentration of cations and waters to generate $M_2^+Mn_4O_8 \cdot 6H_2O$ surfaces. With this supercell, the layers mimic the oxidative patterning of the +2 cation surfaces as two Mn^{4+} are reduced to Mn^{3+} . Three different structures were found: two structures with parallel Mn oxidative pattern and one alternating Mn oxidative patterned structure. The relative energy to add a cation to these structures from their one cation surface counterparts is summarized in Table S6. For one of the parallel patterned structures, the cations protruding above the surface with four of the waters residing between the MnO layer and the cation, and two waters between the cations. Both cations rest in H^1 sites, where both cations were on top of Mn^{3+} ions shown in Figure S9. For the other parallel structure, the cations shift their adsorption site: one of the cations shifts to a H^1 site over Mn^{4+} while the other cation shifts into a H^2 site (Figure S10). Compared to the H^1 surfaces, the H^2 were considerably favorable for Na and Li, and slightly favorable for K.

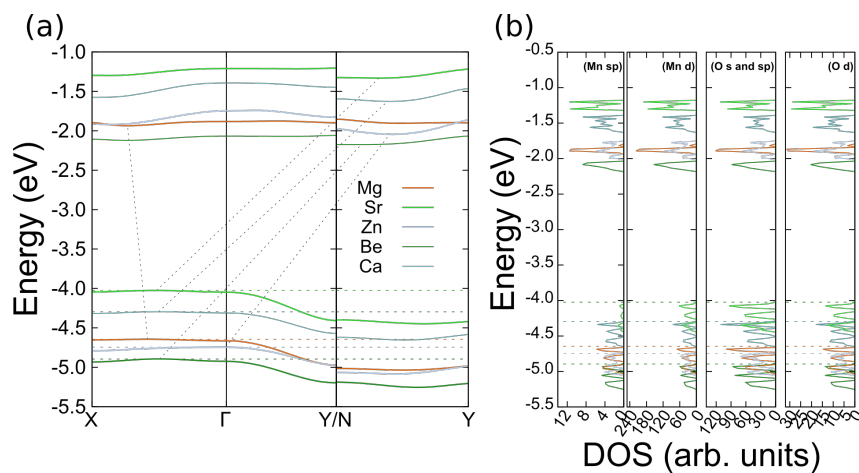


Figure S6: Electronic properties of surfaces with +2 metal cations in the alternating Mn oxidative pattern. (a) displays the band structures and (b) displays the total DOS for manganese and oxygen in the layer.

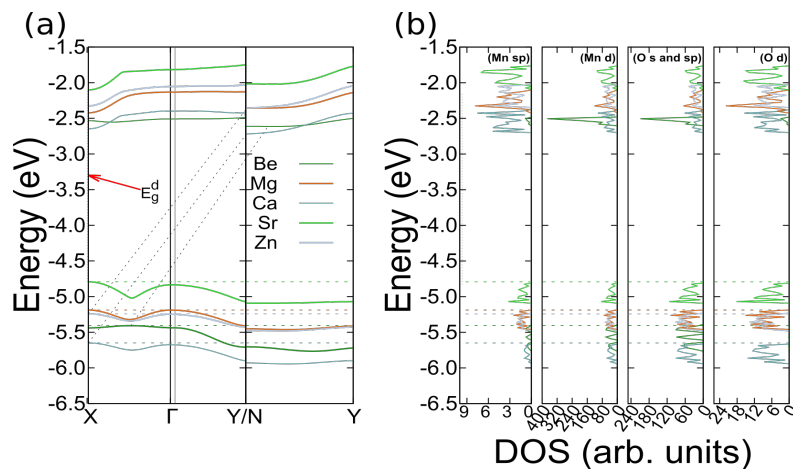


Figure S7: Electronic properties of surfaces with +2 cations in the parallel Mn oxidative arrangement. (a) displays the band structures and (b) displays the total DOS for manganese and oxygen in the layer.

Table S6: Energy for Second Cation Addition to the Surfaces

Cation	Parallel (\mathbf{H}^1)	Parallel (\mathbf{H}^2)	Alternating
Li	56.0	0.910	1.26
Na	39.3	15.4	11.2
K	44.4	43.3	34.8

Additionally, these structures can become an alternative Mn oxidative pattern, which maintains the cations' occupation on the layer as the structure with a cation in a \mathbf{H}^2 site (Figure S11). Compared to the favorable parallel structure (with cations shifted off the Mn^{3+} ions), the alternating patterning was favorable for Na by 4.17 kcal/mol and K for 8.50 kcal/mol. and nearly equivalent possibility of these structures for Li with 0.350 kcal/mol added to become alternating.

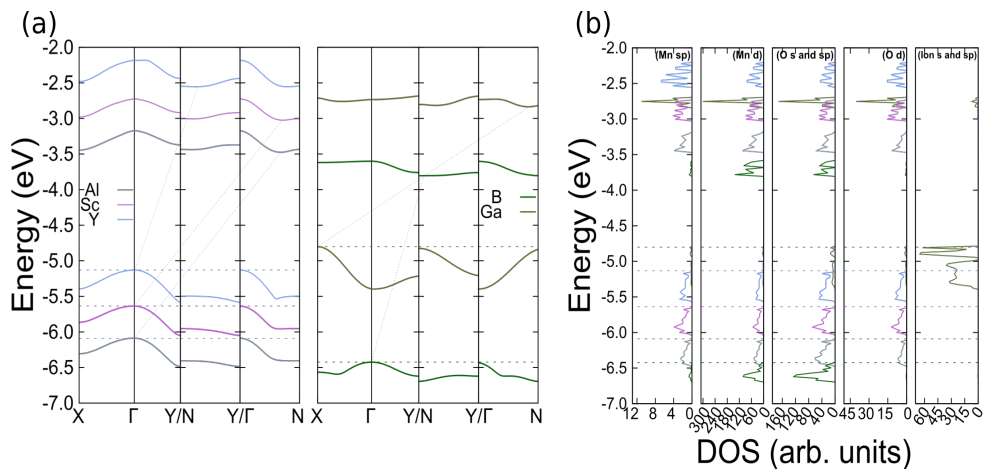


Figure S8: Electronic properties of surfaces with +3 cations. (a) displays the band structures and (b) displays the total DOS for manganese and oxygen in the layer.

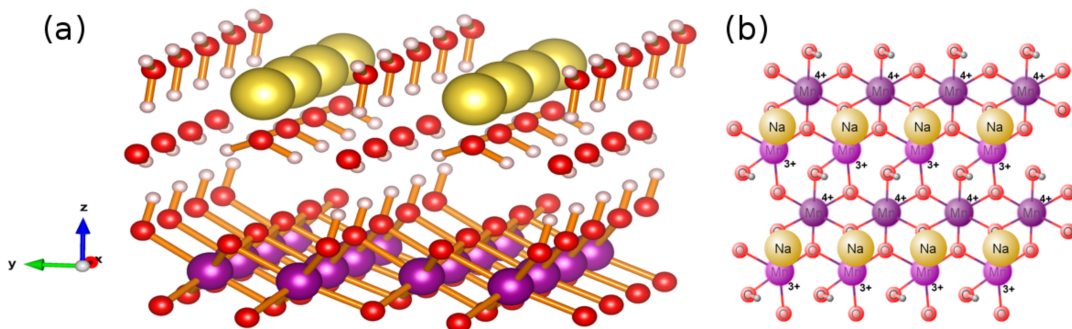


Figure S9: Structure of the two cation surface with the manganese in the parallel oxidative pattern and the cations over \mathbf{H}^1 sites. (a) Displays the surface while (b) displays an overview of the Mn oxidative pattern and cation site location (waters removed for clarity).

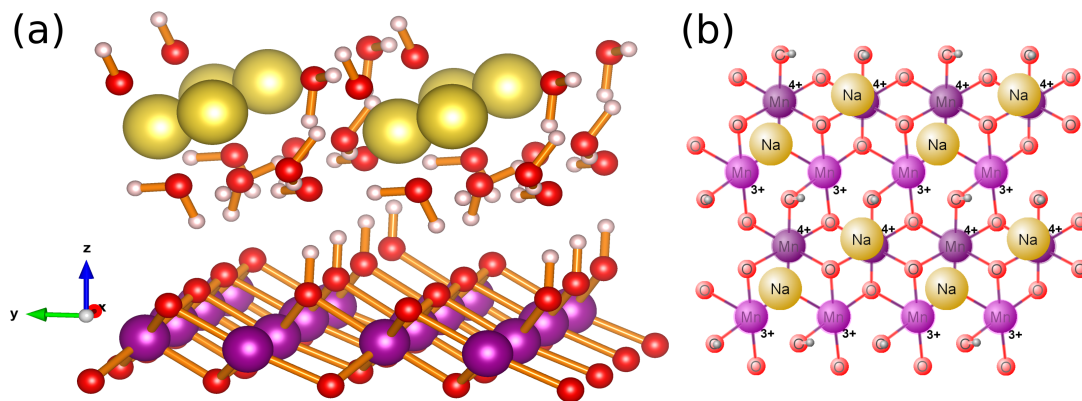


Figure S10: Structure of the two cation surface with the manganese in the parallel oxidative pattern where a cation occupies a \mathbf{H}^2 site. (a) Displays the surface while (b) displays an overview of the Mn oxidative pattern and cation site location (waters removed for clarity).

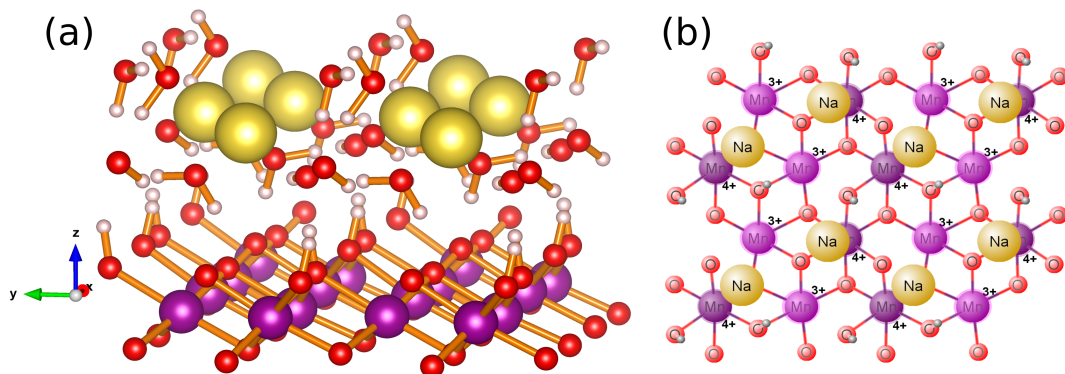


Figure S11: Structure of the two cation surface with the manganese in the alternating oxidative pattern. (a) Displays the surface while (b) displays an overview of the Mn oxidative pattern and cation site location (waters removed for clarity).

Band gap transition energies can be found listed in Table S7 and their properties in Figures 12, 13, and 14. For the \mathbf{H}^1 parallel patterned structure, Li and Na only had a direct band transition while K had both direct and indirect transitions. For the other two types of Mn oxidative patterning, all structures had direct and indirect band transitions, with the indirect band gap lower in energy. These energies can be understood based upon the

Table S7: Band Transitions for Two Cation Surfaces

Cation	Parallel (\mathbf{H}^1)		Parallel (\mathbf{H}^2)		Alternating	
	E_g^d	E_g^i	E_g^d	E_g^i	E_g^d	E_g^i
Li	1.88	N/A	2.59	2.32	2.38	2.37
Na	1.84	N/A	2.52	2.33	2.61	2.52
K	2.47	2.28	2.45	2.33	2.74	2.60

hardness of the cation affecting cation adsorption. Considering the greater electron density Li has over Na or K, its ionic interaction will be greatest. If Li is occupied over the manganese ion as for the \mathbf{H}^1 site structure, the Li will be repealed by the manganese ion and relocate to a more favorable adsorption site, which was shown to be the \mathbf{H}^2 site. But, if Li is situated over Mn^{3+} , it still has a strong affinity for the surface oxygens in that \mathbf{H}^2 site. To diminish the physical adsorption of Li, the Mn^{3+} may couple with Li to promote electron transfer in order to be oxidized to the more stable Mn^{4+} state. However, once the cation is shifted off of the manganese, this direct transition to the cation is lost, resulting in band gap transitions expected for a parallel patterned +2 cation. For K, its softness causes little ionic interaction, which allows the cation to be highly flexible in its adsorption site on the surface (reflected by the similar energies of formation). The only interaction the surface must accommodate is the large ionic radius of K, which is best mitigated in the alternating structure. Meanwhile, Na is situated in a Goldilock zone, not too hard and not too soft—just right—allowing Na to exhibit properties of Li (ionic behavior and electron affinity) and K (force due to ion size).

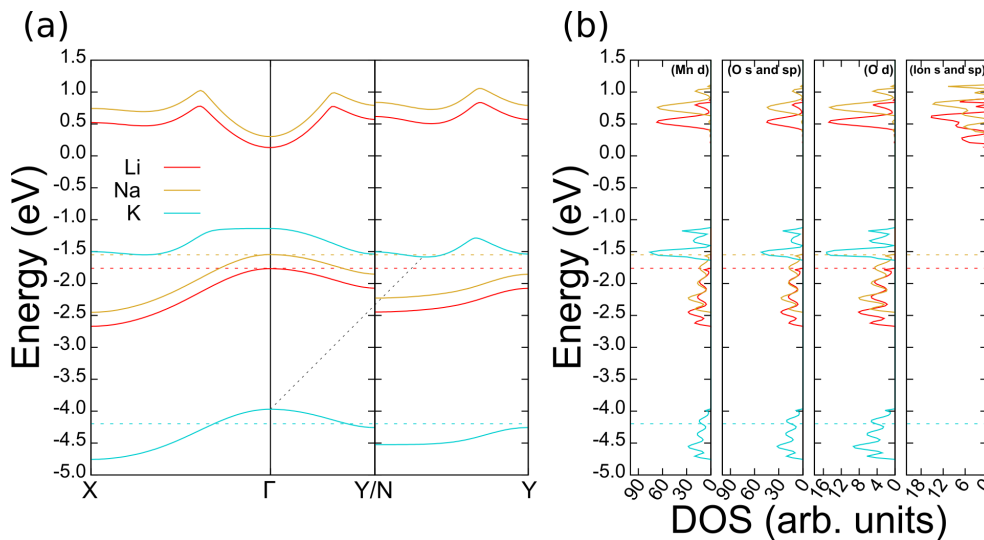


Figure S12: Electronic properties for two cation surfaces in the parallel state with both metals over Mn^{3+} \mathbf{H}^1 sites. (a) displays the band structures and (b) displays the total DOS for manganese and oxygen in the layer.

2.0.3 c. Two Cation Surfaces with Water Removal

With the interesting properties of the two cation surfaces, it is worth considering the effects of hydration of the surfaces. If a cation is added to a single cation surface, the unit cell must be hydrated with three additional waters to become supercells with six waters. The energies of water addition to the structure with cations over the Mn^{3+} ions are displayed in Table S8. Beginning with no waters in the structure, only sodium is expected to fully hydrate whereas lithium and potassium only accept four and five waters into the structure, respectively.

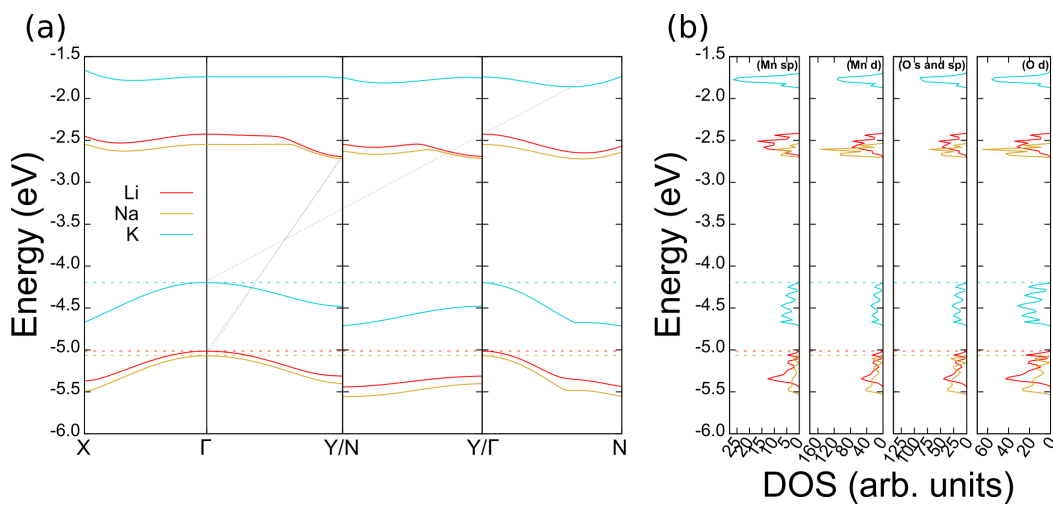


Figure S13: Electronic properties for two cation surfaces in the parallel state with the metals over a \mathbf{H}^2 site and a \mathbf{Mn}^{4+} \mathbf{H}^1 site. (a) displays the band structures and (b) displays the total DOS for manganese and oxygen in the layer.

Table S8: Band Gap for Surface Water Removed Structures

Cation	Water Added ΔE (kcalmol $^{-1}$)					
	1 st	2 nd	3 rd	4 th	5 th	6 th
Li	-72.5	-119	-44.7	-18.1	1.56	7.45
Na	-83.9	-1.87	-30.0	-15.8	-21.8	-15.7
K	-48.9	-44.3	-25.4	-21.7	-21.5	9.83

For all structures, the removal of waters allows for stronger adsorption of the cation with the surface as waters under the cations can no longer block them. Once waters beneath a cation are removed, the cation will begin to fall to the surface and interact with the layers. When all waters are removed, K resembles the structure present in Figure S10 while Na and Li follow their original structure shown in Figure S9. However, for the Na and Li structures, electron density is retained on the cations, resulting in the oxidative state of the manganese in the unit cell shifting from $2\text{Mn}^{3+}2\text{Mn}^{4+}$ to $\text{Mn}^{3+}3\text{Mn}^{4+}$. Several reasons for the structure to alter its oxidative state are, for one, a strong interaction of these harder alkali metals with the electrons on the manganese ion. Secondly, the ionic interaction of the metals with the oxygens is disruptive to the layers and by reducing its oxidative state, the manganese can maintain its interaction with oxygen. With the addition of water, the layer can further prevent structural deformation by allowing waters to interact with layer oxygens, forcing the cations away. Therefore, water not only provides the manganese with a comfortable interaction with its oxygens, but also to serve as a buffer for the layer by preventing cations from interacting with its precious oxygens. For the intermediate water

Table S9: Band Transitions for Two Cation Surfaces with Water Addition
 Waters in the Unit Cell / Band Gap (eV)

Cation	0		1 st		2 nd		3 rd		4 th		5 th	
	E_g^d	E_g^i	E_g^d	E_d^i	E_g^d	E_g^i	E_g^d	E_g^i	E_g^d	E_g^i	E_g^d	E_g^i
Li	1.08 [†]		2.49 [†]		2.14*		2.86*		2.45		1.97	
		0.142 [†]										1.73
Na	1.54 [†]		2.85*		2.64*		2.53*		2.34		2.05	
		0.429 [†]		2.64*								1.76
K	1.81*	1.79*	1.93	1.88			2.12	2.03	2.29	2.18	2.47	2.28
					2.69*	2.58*						

* Values for the alternating Mn oxidative pattern.

† Values for the parallel Mn oxidative pattern.

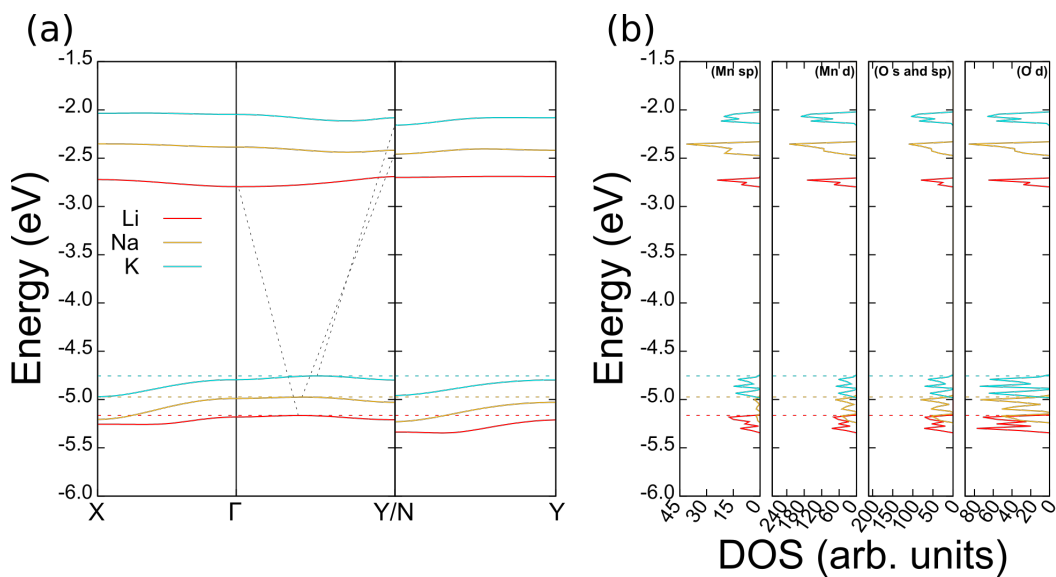


Figure S14: Electronic properties for two cation surfaces in the alternating state. (a) displays the band structures and (b) displays the total DOS for manganese and oxygen in the layer.

removed structures (2^{nd} and 3^{rd}), as waters are removed from the surface, the manganese can only attempt to reduce the strain the harder cations place on them as they begin to adsorb. To do so, the structures shift between parallel and alternating oxidative states until the manganese must donate an electron in order to preserve its bonds to oxygen. These oxidative changes are represented by the band transition of the water added structures in Table S9. As waters are removed, the alternating patterning and electron density retention become present sooner for the harder cations as they induce the greatest strain onto the structure. For the alternating pattern, the band gaps generally increase in energy as usual, yet, once strong cation adsorption occurs when all waters are removed, the bands nearly transition to becoming metallic. Although the generation of these two metal surfaces and the uptake of water is a steep uphill process, their properties highlight the importance of oxidative patterning, cation to layer interactions, and the role of water in producing electronic properties.

3 Materials and Methods

3.1 Band Diagrams

For bulk and surface structures, the alternating oxidative patterned structures were first optimized and then forcing the Mn spin into the parallel pattern.

For two alkali metal surfaces, only single-point energies were calculated for each possible water removed structures. These structures were then compared, those with the lowest electronic energy were chosen as the water removed structures.

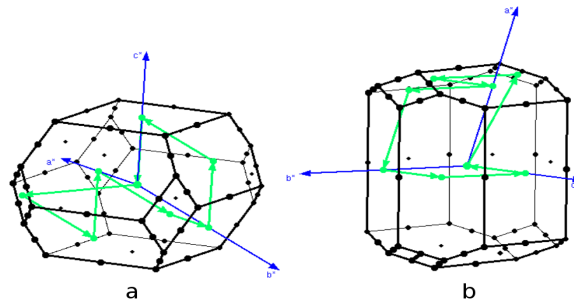


Figure S15: A single symmetry point pathway was chosen for bulk Birnessite structures. The pathway follows: Γ -R-N-X- Γ -L-Y-M-Z- Γ . Both (a) and (b) display this pathway, but from a different point-of-view.

Table S10: Symmetry Points in Reciprocal Space for Bulk Structures

Symmetry Point	$\times b_1$	$\times b_2$	$\times b_3$	Symmetry Point	$\times b_1$	$\times b_2$	$\times b_3$
Γ	0	0	0	R	-1/2	-1/2	-1/2
N	1/2	0	-1/2	X	1/2	0	0
L	1/2	1/2	0	Y	1/2	1/2	0
M	0	1/2	1/2	Z	0	0	1/2

Table S11: Symmetry Points in Reciprocal Space for Surface Structures

Symmetry Point	$\times b_1$	$\times b_2$	$\times b_3$
Γ	0	0	0
X	1/2	0	0
Y	0	1/2	0
N	-1/2	1/2	0

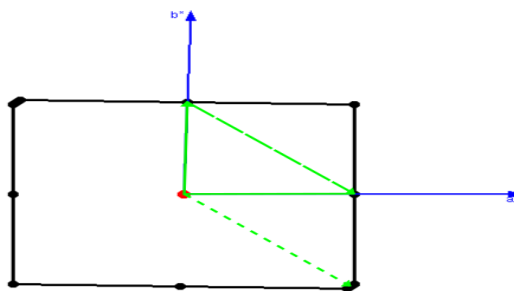


Figure S16: Symmetry point pathways chosen for surface structures. Three different pathways were chosen, X- Γ -Y, N-Y, and Γ -N.

3.2 Relative Energies

The formulas used to calculate the relative energies for the structures are shown below. (i) *Relative energies for bulk structures:*

- Cation to oxygen hollow site: the energy to shift a cation were determined by taking

$$\Delta E = E_{\text{elec,T}} - E_{\text{elec,H}_2} \quad (1)$$

where $E_{\text{elec,T}}$ is the electronic energy of the bulk structures with cations on an oxygen top site and $E_{\text{elec,H}_2}$ is the electronic energy of the bulk structures with cations in an oxygen hollow site.

- Mn oxidative pattern: The energy to compare the structures between a parallel pattern were found by subtracting the electronic energy of the parallel patterned structures from the bulk structures in the alternating pattern,

$$\Delta E = E_{\text{elec,para}} - E_{\text{elec,alt}} \quad (2)$$

where $E_{\text{elec,para}}$ is the electronic energy of the bulk structures with the parallel pattern and $E_{\text{elec,alt}}$ is the electronic energy of the bulk structures with the alternating pattern.

- Energy of water removal: the energy of water addition was approximated for the Birnessite structures from the calculated electronic energy of the structure using the following formula:

$$\Delta E_n = E_{\text{elec,n}} - (E_{\text{elec,n-1}} + E_{\text{elec,H}_2\text{O}}) \quad (3)$$

where ΔE_n is the relative energy, n is an integer used to index the number of waters in the structure; it cannot be greater than the number of waters in the structure or less than 1, $E_{\text{elec},n}$ is the electronic energy of a structure with n waters, $E_{\text{elec},n-1}$ is the electronic energy of a structure with $n-1$ waters, and $E_{\text{elec,H}_2\text{O}}$ is the electronic energy of water.

- Energy to add a second cation: the energy to add a cation was calculated by taking the electronic energy of the two cations

$$\begin{aligned} \Delta E = & E_{\text{elec,Bulk,M}_2^{n+}} \\ & - (2E_{\text{elec,Bulk}} - E_{\text{elec,Bulk,0}}) \end{aligned} \quad (4)$$

where $E_{\text{elec,Bulk,M}_2^{n+}}$ is the energy of the two cation bulk structures and $E_{\text{elec,Bulk,0}}$ is the energy of the optimized Birnessite structure with only waters, no cation. For example, to add a second cation structure to $\text{NaMn}_4\text{O}_8 \cdot 3\text{H}_2\text{O}$ is:

$$\begin{aligned} \Delta E = & E(\text{Na}_2\text{Mn}_4\text{O}_8 \cdot 3\text{H}_2\text{O}) \\ & - [2E(\text{NaMn}_4\text{O}_8 \cdot 3\text{H}_2\text{O}) - E(\text{Mn}_4\text{O}_8 \cdot 3\text{H}_2\text{O})] \end{aligned} \quad (5)$$

Note that by doubling the electronic energy of the one cation bulk structures, the formula will be $\text{Na}_2\text{Mn}_8\text{O}_{16} \cdot 6\text{H}_2\text{O}$ which can match the formula of a two cation bulk structure by then subtracting the energy of a Birnessite structure with only waters.

- (ii) *Relative energies for surface structures:*

- Energy to separate layers: subtracting the electronic energy of the surface structured by its bulk counterpart was done to determine the minimum energy required to separate layers:

$$\Delta E = E_{\text{elec,Sur}} - E_{\text{elec,Bulk}} \quad (6)$$

where $E_{\text{elec,Sur}}$ is the electronic energy of the surface.

- Energy to alter the Mn oxidative pattern: the energy of altering the oxidative pattern follows Equation (2), but using the surface electronic energy instead of the bulk.

- Energy to add cation: the energy to add a cation to the surface structures was performed for the cations. The formula follows Equation (4) using energies with respect to the surface structures. This calculation was performed between parallel Mn oxidative patterns and alternating Mn oxidative patterns for two cation and single cation surface unit cells. The corresponding $E_{\text{elec,Bulk},0}$ energy for surfaces was the M_4O_8 surface (no cation and no waters as these are structures with six waters).
- Energy to add water in $\text{M}_2^+\text{Mn}_4\text{O}_8 \cdot 6\text{H}_2\text{O}$ surfaces: unsurprisingly, the energy of water addition follows Equation (3) from the bulk structures. In this case, n will span from 6 to 0 rather than 3 to 0.

3.3 Relative Energies for Mn Oxidative Pattern

The Table S12 contains the relative energy to go from an alternating pattern to the parallel pattern (i.e. negative is favorable to shift to, positive unfavorable). Notice that only alternating vs parallel pattern occurs only when we have a structure with two different pair of Manganese, each pair with a different oxidation state. For example:

- $\text{Al}_2\text{-Mn}_4\text{O}_8$ BULK; contains two Mn^{2+} and two Mn^{3+} . The same goes for other +3 ions.
- $\text{Be}\text{-Mn}_4\text{O}_8$ BULK; contains two Mn^{3+} and two Mn^{4+} . The same goes for other +2 ions.
- $\text{K}_2\text{-Mn}_4\text{O}_8$ BULK; contains two Mn^{3+} and two Mn^{4+} . The same goes for other +1 ions.
- Unlike the other +3 cations, the Ga's retained some electron density, leading to 3 Mn_{3+} and 1 Mn_{2+} in the unit cell. That made it unable to alter its patterning. The other +3 cations had 2Mn^{2+} and 2Mn^{3+} allowing them to have an alternative oxidative pattern.

Table S12: Relative Energies for Mn Oxidative Pattern.

CATION	STRUCTURE		
	M-Mn ₄ O ₈ BULK	M ₂ -Mn ₄ O ₈ BULK	M-Mn ₄ O ₈ SURFACE
Al			-1.06
Be	1.42		-4.04
B		5.4	
Ca	0.803		-10.2
K		-5.93	
Li		-6.3	
Mg	2.41		-2.41
Na		-5.06	
Sc		2.55	
Sr	-6.26		-5.36
Y		-3.83	
Zn	2.21		-11.1

In general, when the structures are in the parallel pattern, they have greater separation distance between layers (along the z-axis) whereas in the alternating pattern there is greater layer expansion (separation in the x-y plane). This can be better in Table S13 and Figure S17.

In Figure S17, we have calculated the correlation between layer separation (Table S13) and charge density (ρ). Ionic radii were used to calculate the charge density of each cations.

The values used for this plot are (in Å):

Li=7.04, Na=7.14, K=7.24;

Be=6.59, Mg=6.72, Zn=6.70, Ca=6.99, Sr=7.10;

B=6.77, Al=6.50, Ga=6.56, Sc=6.66, Y=6.82.

There is some correlation +1 cations, +2 cation in the parallel pattern and +3 cations. However, a correlation for +2 cation in the alternating pattern is not clear. In the +3 cations, Boron is a large outlier. The reason is that this is the only bulk structure with proton transfer onto the surface. Deviation from the correlation occur because some chemistry is happening, i.e. the ions chemically binds to the layers and affects the assumption of pure electrostatics.

Table S13: Layer Separation Distance with respect to different cations and alternating and parallel pattern.

Cation	Layer Separation Distance (\AA)
+1 Charge	
Li	7.04
Na	7.14
K	7.24
+2 Charge Alternating Pattern	
Be	6.59
Mg	6.72
Zn	6.70
Ca	6.99
Sr	7.1
+2 Charge Parallel Pattern	
Be	6.55
Mg	6.82
Zn	6.79
Ca	6.91
Sr	6.82
+3 Charge	
B	6.77
Al	6.50
Ga	6.56
Sc	6.66
Y	6.82

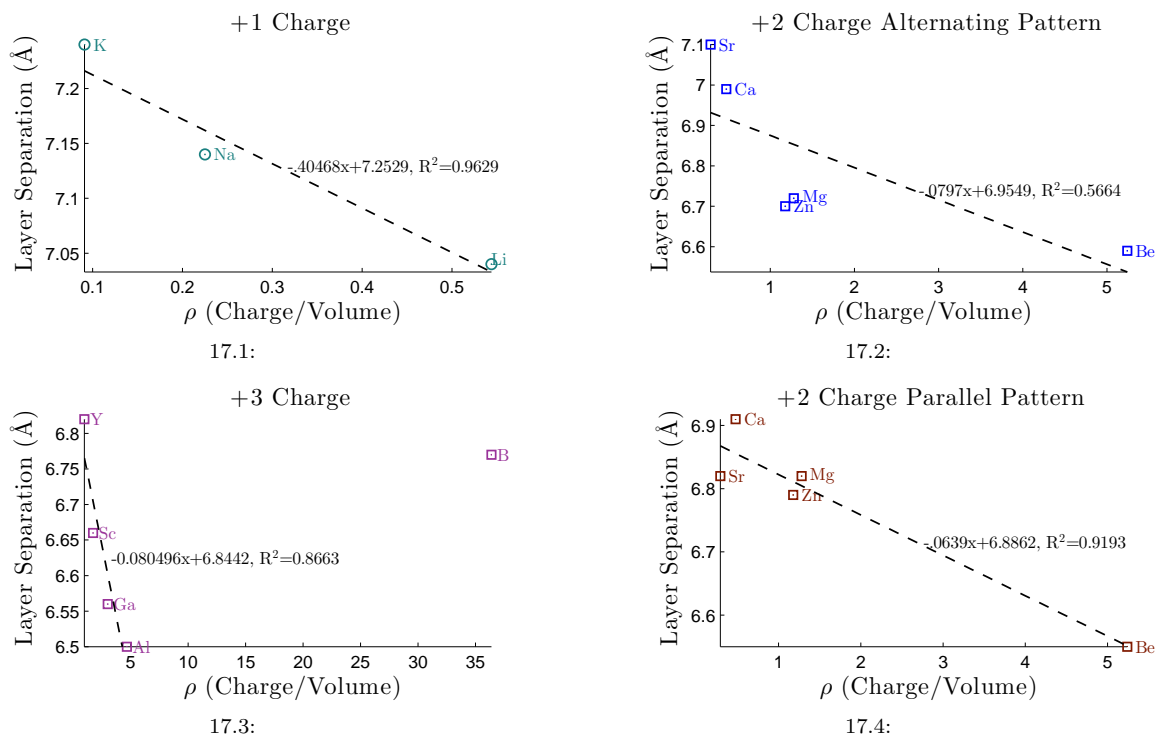


Figure S17: Layer Separation versus Charge Density

3.4 Basis Sets

Aluminum	0.75005942000 1.000000000000000
Al_pob_TZVP_2012	
13 10	
0 0 7 2.0 1.0	
37792.5507720 0.00057047888709	
5668.06821650 0.00440930165380	
1289.85828410 0.02263096741100	
364.865960280 0.08802564429500	
118.576315150 0.25223701612000	
42.0248676050 0.45960547169000	
15.4995016290 0.33277886014000	
0 0 3 2.0 1.0	
75.2080265980 0.01925056019000	
23.0314089720 0.08790674395200	
3.63487976490 -0.34246704535000	
0 0 2 2.0 1.0	
1.60650499570 1.51062660580000	
0.76103394581 0.58071016470000	
0 0 1 0.0 1.0	
0.69881874000 1.000000000000000	
0 0 1 0.0 1.0	
0.34940937000 1.000000000000000	
0 2 5 6.0 1.0	
452.523031920 0.00231108124660	
107.081950490 0.01856864182300	
34.1310212550 0.08721623703500	
12.5870374280 0.26902101523000	
4.98119197040 0.52128324272000	
0 2 1 1.0 1.0	
1.93791887000 1.000000000000000	
0 2 1 0.0 1.0	
0.72047185000 1.000000000000000	
0 2 1 0.0 1.0	
0.18328583000 1.000000000000000	
0 3 1 0.0 1.0	
0.57798580000 1.000000000000000	
Boron	
B_pob_TZVP_2012	
5 8	
0 0 6 2.0 1.0	
8564.86606870 0.00022837198155	
1284.15162630 0.00176825764470	
292.278716040 0.00914070805160	
82.7754691760 0.03634263898900	
27.0179392690 0.11063458441000	
9.81496196600 0.23367344321000	
0 0 2 2.0 1.0	
3.93185590590 0.41818777978000	
1.65955997120 0.22325473798000	
0 0 1 0.0 1.0	
0.53318702000 1.000000000000000	
0 0 1 0.0 1.0	
0.26659351000 1.000000000000000	
0 2 4 1.0 1.0	
22.4538758030 0.00502655751790	
5.10450583300 0.03280173896500	
1.49860813440 0.13151230768000	
0.50927831315 0.33197167769000	
0 2 1 0.0 1.0	
0.53857716000 1.000000000000000	
0 2 1 0.0 1.0	
0.26928858000 1.000000000000000	
0 3 1 0.0 1.0	
Beryllium	
Be_pob_TZVP_2012	
4 5	
0 0 6 2.0 1.0	
4700.2365626 0.00023584389316	
704.82845622 0.00182437910190	
160.43110478 0.00939661482240	
45.425347336 0.03690892415900	
14.798334125 0.10897561281000	
5.3512452537 0.21694284551000	
0 0 2 2.0 1.0	
2.1542044819 0.44695408857000	
0.9336374440 0.20866985771000	
0 0 1 0.0 1.0	
0.24174508 1.000000000000000	
0 0 1 0.0 1.0	
0.12111452 1.000000000000000	
0 2 1 0.0 1.0	
0.79262157 1.000000000000000	
Calcium	
Ca_pob_TZVP_2012	
20 11	
0 0 8 2.0 1.0	
172517.326850 0.00023317502546	
25861.5192750 0.00180765219800	
5885.66186680 0.00939438442550	
1665.97300310 0.03810840900900	
542.367181480 0.12331203853000	
194.578034920 0.29004470954000	
75.3035976360 0.40587151157000	
29.5740625890 0.20398410743000	
0 0 4 2.0 1.0	
191.200746600 -0.02441975975900	
58.8402998830 -0.11547027448000	
8.96425408450 0.56356636717000	
3.68569605410 0.56709682704000	
0 0 2 2.0 1.0	
5.24642897260 -0.22825334325000	
0.84862621528 0.72625219172000	
0 0 1 2.0 1.0	
1.30710626000 1.000000000000000	
0 0 1 0.0 1.0	
0.38027232000 1.000000000000000	
0 0 1 0.0 1.0	
0.16014616000 1.000000000000000	
0 2 6 6.0 1.0	
836.972620580 0.00252583460920	
197.930401420 0.02007650668600	
63.1355580540 0.09130298736600	
23.2826871700 0.25247029915000	
9.11764449320 0.39426326344000	
3.63361201390 0.23011559492000	
0 2 3 6.0 1.0	
13.4941631200 -0.02649502195100	
1.81392597900 0.55088108210000	
0.71981826006 1.02806166200000	
0 2 1 0.0 1.0	
0.36108303000 1.000000000000000	
0 2 1 0.0 1.0	
0.16029529000 1.000000000000000	
0 3 1 0.0 1.0	
0.78864471000 1.000000000000000	

Gallium	0.1795111000 1.000000000000	
Ga_pob_TZVP_2012	0 2 1 0.0 1.0 0.8000000000 1.000000000000	
Potassium		
K_pob_TZVP_2012	19 11 0 0 8 2.0 1.0 153976.183250 0.00023662636107 23082.4976720 0.00183429291370 5253.23447450 0.00953105277690 1486.95501330 0.03863840698000 484.063337260 0.12480768502000 173.566539800 0.29278861009000 67.1163814640 0.40633425860000 26.3395020540 0.20077215860000 0 0 4 2.0 1.0 172.876935670 -0.02420096093600 53.0586490630 -0.11553095040000 7.92127539640 0.57455545175000 3.2108804720 0.57023185107000 0 0 2 2.0 1.0 172.876935670 -0.02420096093600 53.0586490630 -0.11553095040000 7.92127539640 0.57455545175000 3.2108804720 0.57023185107000 0 0 1 0.0 1.0 1.1590064400 1.0000000000000000 0 0 1 2.0 1.0 0.5763081300 1.0000000000000000 0 0 1 0.0 1.0 0.2433825700 1.0000000000000000 0 2 6 6.0 1.0 0.2432.0171070 0.00224340659280 576.12049582 0.01834226533600 185.11584354 0.08727969716700 69.246572556 0.25684868351000 27.818107777 0.42398378107000 11.420229938 0.25701340043000 0 2 3 6.0 1.0 42.819661530 -0.01932651911900 6.3885901000 0.31571386917000 2.6698993326 0.57617792822000 0 2 1 1.0 1.0 1.0663932200 1.0000000000000000 0 2 1 0.0 1.0 0.3641398200 1.0000000000000000 0 2 1 0.0 1.0 0.1148217200 1.0000000000000000 0 3 5 10 1.0 103.92331829 0.01146461365200 30.371094389 0.07362574738300 10.872078097 0.23505107382000 4.1549137954 0.40318563513000 1.5345659145 0.40824748152000 0 3 1 0.0 1.0 1.7915711500 1.0000000000000000 0 3 1 0.0 1.0 0.7852028800 1.0000000000000000 0 3 1 0.0 1.0 0.2830723400 1.0000000000000000 Hydrogen H_pob_TZVP_2012	3 5 0 0 6 2.0 1.0 6269.2628010 0.00020540968826 940.31612431 0.00159165540890 214.22107528 0.00828698297070 60.759840184 0.03385637424900 19.915152032 0.11103225876000 7.3171509797 0.27449383329000 0 0 2 1.0 1.0 2.9724674216 0.23792456411000 1.2639852314 0.30765411924000 0 0 1 0.0 1.0 0.5025516200 1.0000000000000000 0 0 1 0.0 1.0 0.1000746200 1.0000000000000000 0 2 1 0.0 1.0 0.1450713300 1.0000000000000000

Magnesium

Mg_pob_TZVP_2012

12 9	53.7694101790	0.01952773187200
0 0 7 2.0 1.0	16.3082430250	0.09264801079400
31438.3495550 0.00060912311326	2.37303841250	-0.39938670172000
4715.51533540 0.00470661964650	0 0 2 1.0 1.0	
1073.16292470 0.02413582065700	0.95730772603	1.64285953910000
303.572387680 0.09362895983400	0.40806460959	0.55692596966000
98.6262510420 0.26646742093000	0 0 1 0.0 1.0	
34.9438084170 0.47890929917000	0.67460191000	1.0000000000000000
12.8597851990 0.33698490286000	0 0 1 0.0 1.0	
0 0 3 2.0 1.0	0.10055549000	1.0000000000000000
64.8769130040 0.01918088930700	0 2 5 6.0 1.0	
19.7255207770 0.09091370439200	138.079799890	0.00579518919290
2.89518043390 -0.39563756125000	32.2327003930	0.04162084625100
0 0 2 2.0 1.0	9.98160753600	0.16281916885000
1.19604547100 1.68276033730000	3.48220339280	0.36011784647000
0.54329451156 0.52141091954000	1.22991346200	0.44858979889000
0 0 1 0.0 1.0	0 2 1 0.0 1.0	
1.34711883000 1.0000000000000000	0.40094322000	1.0000000000000000
0 0 1 0.0 1.0	0 2 1 0.0 1.0	
0.34506887000 1.0000000000000000	0.10067345000	1.0000000000000000
0 2 5 6.0 1.0	0 3 1 0.0 1.0	
179.871896120 0.00537995490180	1.046300000000	1.0000000000000000

Oxygen

Modified_O_8-411d1_bredow_2006

42.1200693760 0.03931801409800	8 5	
13.1205030320 0.15740129476000	0 0 8 2.0 1.0	
4.62575036090 0.35919094128000	8020.0000000	0.0010800
1.66952110160 0.45533379310000	1338.0000000	0.0080400
0 2 1 0.0 1.0	255.4000000	0.0532400
0.56631001000 1.0000000000000000	69.2200000	0.1681000
0 2 1 0.0 1.0	23.9000000	0.3581000
0.18813966000 1.0000000000000000	9.2640000	0.3855000
0 3 1 0.0 1.0	3.8510000	0.1468000
0.69355357000 1.0000000000000000	1.2120000	0.0728000
0 1 4 6.0 1.0	0 1 4 6.0 1.0	
49.4300000	49.4300000	-0.0088300
10.4700000	10.4700000	-0.0915000
3.2350000	3.2350000	-0.0402000
1.2170000	1.2170000	0.3790000
0 1 1 0.0 1.0	0 1 1 0.0 1.0	
0.4591770	0.4591770	1.0000000
0 1 1 0.0 1.0	0 1 1 0.0 1.0	
0.1508470	0.1508470	1.0000000
0 3 1 0.0 1.0	0 3 1 0.0 1.0	
0.4684940	0.4684940	1.0000000

Scandium

Sc_pob_TZVP_2012

35.3511 0.02748	21 14	
9.6888 0.14835	0 0 8 2.0 1.0	
3.2186 0.36932	191612.918740	0.00023076475942
1.09526 0.47933	28723.8503630	0.00178903299460
0 3 1 0.0 1.0	6537.01164900	0.00929904011400
0.3562 1.0	1850.30971710	0.03773943801100
Sodium	602.388551560	0.12227148359000
Na_pob_TZVP_2012	216.173247660	0.28814821470000
11 9	83.7125178800	0.40517543099000
0 0 7 2.0 1.0	32.9087071890	0.20566019623000
26041.1099270 0.00061806342811	0 0 4 2.0 1.0	
3906.12685480 0.00477486044140	211.343932340	-0.02452799146200
888.974549930 0.02447168482900	65.1289201390	-0.11570158142000
251.454979610 0.09475539497700	10.0343115350	0.55995283317000
81.6501435120 0.26867496920000	4.1596845970	0.56087765073000
28.9041584010 0.47925475440000	0 0 2 2.0 1.0	
10.6257829320 0.33248591469000	6.00090416130	-0.22840494325000
0 0 3 2.0 1.0	0.98255784150	0.71948970378000
	0 0 1 2.0 1.0	

1.42204508000	1.000000000000000	0 1 1 0.0 1.0	
0 0 1 0.0 1.0		0.338 1.0 1.0	
0.41466167000	1.000000000000000	0 3 2 0.0 1.0	
0 0 1 0.0 1.0		0.996242225138 0.903211811619	
0.14961565000	1.000000000000000	0.331873211212 1.80273382161	
0 2 6 6.0 1.0			
947.341228230	0.00247372087440	Zinc	
224.096997320	0.01974296706000	Zn_pob_TZVP_2012	
71.5603348820	0.09035714754900		
26.4448244900	0.25201602503000	30 14	
10.3937982850	0.39675535929000	0 0 8 2.0 1.0	
4.16063045590	0.23208624517000	405924.31028 0.00022442017483	
0 2 3 6.0 1.0		60846.955735 0.00174020866260	
15.5657371350	-0.02712942397400	13847.343092 0.00905133395650	
2.11215448650	0.55109256629000	3919.6158551 0.03681734144500	
0.84184709021	1.00906358060000	1276.3594167 0.12004850256000	
0 2 1 0.0 1.0		458.67254435 0.28576057621000	
0.63537059000	1.000000000000000	178.28725246 0.41087462062000	
0 2 1 0.0 1.0		70.612192837 0.21816962456000	
0.31768530000	1.000000000000000	0 0 4 2.0 1.0	
0 3 4 1.0 1.0		443.88077950 -0.02493427498400	
30.9893909930	0.01190283743100	137.55875267 -0.11817955766000	
8.69054650690	0.06765585685000	22.268083479 0.55367318468000	
2.95202563370	0.21332539722000	9.5217310606 0.52628934936000	
1.07619107450	0.38391075578000	0 0 2 2.0 1.0	
0 3 1 0.0 1.0		14.874114065 -0.22929955254000	
0.35567614000	1.000000000000000	2.4647517612 0.71135484742000	
0 3 1 0.0 1.0		0 0 1 2.0 1.0	
0.12383645000	1.000000000000000	1.0113272200 1.000000000000000	
0 4 1 0.0 1.0		0 0 1 0.0 1.0	
0.34500000000	1.000000000000000	0.322980200 1.000000000000000	
0 0 1 0.0 1.0		0 0 1 0.0 1.0	
0.1016731100	1.000000000000000	0 2 6 6.0 1.0	
HAYWSC		2205.3508534 0.00233562404480	
0 1 2 8.0 1.0		522.35300699 0.01903102263400	
3.2429	0.23210	-0.12996	167.73055542 0.08995575867500
2.4027	-0.70898	0.050457	62.670045373 0.26113248631000
0 1 1 2. 1.		25.109749456 0.42348448173000	
0.694	1. 1.		10.225142681 0.24618926885000
0 1 1 0. 1.		0 2 3 6.0 1.0	
0.258	1. 1.		40.713442521 -0.03002966759200
0 3 1 0. 1.		5.6247090696 0.55575254864000	
1.2 1.		2.2279949116 0.95581013442000	
0 3 1 0. 1.		0 2 1 0.0 1.0	
0.4 1.		1.1601141800 1.000000000000000	
0 4 1 0. 1.		0 2 1 0.0 1.0	
0.9 1.		0.2624550000 1.000000000000000	
0 3 4 10.0 1.0		0 3 4 10.0 1.0	
Yttrium		88.554315311 0.01272817001500	
ECP HAYWSC		25.721525557 0.07939449984300	
239 3		9.1278367624 0.24491506805000	
HAYWSC		3.4312364064 0.40390526479000	
0 1 3 8.0 1.0		0 3 1 0.0 1.0	
3.87710632535	0.240698694374	-0.110990397203	
2.67832616053	-0.81743893727	-0.0447243390536	
0.861411547924	0.843241417526	0.905500379629	
		0 3 1 0.0 1.0	
		0.4308920600 1.000000000000000	
		0 4 1 0.0 1.0	
		2.6140000000 1.000000000000000	

4 Bulk Structures

4.1 $M^{n+}Mn_4O_8 \cdot 3H_2O$ Bulk

Aluminum

data_BG_AlMn408_3H20.D1.TZVP2012.121.out

```

_cell_length_a          5.071742
_cell_length_b          6.098278
_cell_length_c          7.187646
_cell_angle_alpha        64.770712
_cell_angle_beta         104.883858
_cell_angle_gamma        88.014086
_symmetry_space_group_name_H-M   'P 1'
_symmetry_Int_Tables_number      1

loop_
_symmetry_equiv_pos_as_xyz
'x, y, z'

loop_
_atom_site_label
_atom_site_type_symbol
_atom_site_fract_x
_atom_site_fract_y
_atom_site_fract_z
MN001 MN -0.169352  0.062782  0.001454
0002 O  0.199994  0.454096  0.160948
0003 O  0.473506  0.135414 -0.481004
0004 O  0.453209  0.172797 -0.150113
MN005 MN  0.329074  0.298102  0.016417
0006 O -0.306339  0.206933  0.203549
AL007 AL -0.172222  0.083677 -0.496890
0008 O -0.057029  0.383060 -0.149917
H009 H  0.449017  0.167737 -0.358660
H010 H  0.341493  0.274102  0.378172
MN011 MN -0.175868 -0.437481 -0.013505
0012 O  0.221373 -0.021372  0.152839
0013 O  0.427374 -0.385513 -0.143563
0014 O  0.065240 -0.155252  0.499418
MN015 MN  0.330960 -0.190292 -0.006353
0016 O -0.275560 -0.264384  0.135720
0017 O -0.042506 -0.088489 -0.195609
0018 O -0.058114  0.369446  0.498290
H019 H -0.054398  0.393360 -0.370647
H020 H -0.142906 -0.469602  0.363047
H021 H  0.220073 -0.256809 -0.360334
H022 H  0.148613 -0.111101  0.378429

```

Boron

data_BG_BMn408_3H20.D1.TZVP2012.SPLOCK4.01.out

```

_cell_length_a          5.104838
_cell_length_b          6.086771
_cell_length_c          7.631700
_cell_angle_alpha        62.517132
_cell_angle_beta         103.822621
_cell_angle_gamma        85.246771
_symmetry_space_group_name_H-M   'P 1'
_symmetry_Int_Tables_number      1

loop_
_symmetry_equiv_pos_as_xyz
'x, y, z'

loop_
_atom_site_label
_atom_site_type_symbol
_atom_site_fract_x
_atom_site_fract_y
_atom_site_fract_z
MN001 MN -0.130245  0.062954  0.001678
0002 O  0.202747  0.444842  0.150973
0003 O  0.319077  0.165528 -0.465970
0004 O -0.473683  0.181669 -0.147884
MN005 MN  0.370075  0.313177  0.002017
0006 O -0.289989  0.252325  0.152881
BE007 BE  0.025032  0.059062 -0.410600
0008 O  0.010347  0.403018 -0.151679
H009 H  0.427531  0.214233 -0.372940
H010 H  0.307980  0.292406  0.385278
MN011 MN -0.138732 -0.444039 -0.006825
0012 O  0.228926 -0.023343  0.142250
0013 O -0.495669 -0.357337 -0.146249
0014 O  0.012434 -0.144673  0.492079
MN015 MN  0.372395 -0.195097  0.000122

```

0016 O -0.263835 -0.284242 0.139792
 0017 O 0.020310 -0.115111 -0.166491
 0018 O -0.172353 0.326188 -0.489450
 H019 H -0.141201 0.395814 -0.394869
 H020 H -0.202582 0.473515 0.367716
 H021 H 0.101507 -0.301394 -0.394283
 H022 H 0.115558 -0.098286 0.374145

Calcium

data_BG_CaMn408_3H20.D1.121.511d21G.FMIX90.out

_cell_length_a 4.962067
 _cell_length_b 6.067112
 _cell_length_c 7.752213
 _cell_angle_alpha 64.358134
 _cell_angle_beta 104.806667
 _cell_angle_gamma 89.501013
 _symmetry_space_group_name_H-M 'P 1'
 _symmetry_Int_Tables_number 1

loop_
 _atom_site_label
 _atom_site_type_symbol
 _atom_site_fract_x
 _atom_site_fract_y
 _atom_site_fract_z

MN001 MN -0.134818 0.075550 -0.002544
 0002 O 0.241444 0.455964 0.157841
 0003 O 0.311855 0.144174 -0.478056
 0004 O 0.483396 0.186200 -0.144986
 MN005 MN 0.365348 0.317871 0.006287
 0006 O -0.256477 0.255139 0.162737
 CA007 CA -0.169888 0.033467 -0.491906
 0008 O -0.025032 0.404369 -0.137627
 H009 H 0.372535 0.210804 -0.380195
 H010 H 0.282528 0.284889 0.385283
 MN011 MN -0.133708 -0.439071 0.007895
 0012 O 0.261254 -0.006922 0.140397
 0013 O 0.474064 -0.364553 -0.137776
 0014 O 0.139160 -0.268970 0.496737
 MN015 MN 0.366159 -0.184090 -0.002735
 0016 O -0.241559 -0.259339 0.136075
 0017 O -0.021161 -0.134560 -0.147996
 0018 O -0.254113 0.420994 0.498834
 H019 H -0.143703 0.441713 -0.386348
 H020 H -0.217303 -0.451098 0.378079
 H021 H 0.291657 -0.309724 -0.380134
 H022 H 0.213994 -0.191600 0.381829

Gallium

data_BG_GaMn408_3H20.D1.TZVP2012.121.out

_cell_length_a 5.074451
 _cell_length_b 6.111125
 _cell_length_c 7.258368
 _cell_angle_alpha 64.629462
 _cell_angle_beta 104.767190
 _cell_angle_gamma 88.349771
 _symmetry_space_group_name_H-M 'P 1'
 _symmetry_Int_Tables_number 1

loop_
 _atom_site_label
 _atom_site_type_symbol
 _atom_site_fract_x
 _atom_site_fract_y
 _atom_site_fract_z

MN001 MN -0.105745 0.031638 0.005263
 0002 O 0.251475 0.405887 0.152386
 0003 O 0.210926 0.228122 -0.480426
 0004 O -0.455580 0.150965 -0.134148
 MN005 MN 0.397211 0.275785 0.008318
 0006 O -0.233275 0.186471 0.144593
 K007 K -0.276423 0.029487 -0.477916
 0008 O 0.025619 0.366931 -0.125222
 H009 H 0.273540 0.358948 -0.446742
 H010 H 0.210360 0.302975 0.384975
 MN011 MN -0.102182 -0.478753 0.012820
 0012 O 0.270888 -0.057202 0.136786
 0013 O -0.476199 -0.389031 -0.124447
 0014 O 0.179387 -0.268528 -0.479529
 MN015 MN 0.393116 -0.215759 -0.000158
 0016 O -0.226881 -0.304891 0.139607
 0017 O 0.011454 -0.142751 -0.122955
 0018 O -0.316124 -0.455930 0.492446

H019 H -0.139327 -0.483182 -0.427959
H020 H -0.272816 -0.392039 0.367365
H021 H 0.326071 -0.309810 -0.373456
H022 H 0.260133 -0.218124 0.410090

Lithium

data_BG_LiMn408_3H20.D1.121.LiTZVPP.out

_cell_length_a 4.973608
_cell_length_b 5.865353
_cell_length_c 7.779916
_cell_angle_alpha 64.735228
_cell_angle_beta 99.451330
_cell_angle_gamma 88.156140
_symmetry_space_group_name_H-M 'P 1'
_symmetry_Int_Tables_number 1

loop_
_symmetry_equiv_pos_as_xyz
'x, y, z'

loop_
_atom_site_label
_atom_site_type_symbol
_atom_site_fract_x
_atom_site_fract_y
_atom_site_fract_z

MN001 MN -0.148923 0.070560 -0.000369
0002 O 0.207252 0.456719 0.152737
0003 O 0.334454 0.139226 -0.472331
0004 O 0.498559 0.179308 -0.140187
MN005 MN 0.354804 0.310517 0.010080
0006 O -0.270585 0.232070 0.148188
LI007 LI -0.066828 0.055120 -0.452352
0008 O -0.015292 0.391017 -0.129849
H009 H 0.429063 0.224588 -0.401073
H010 H 0.293986 0.263999 0.390734
MN011 MN -0.147111 -0.440675 0.006551
0012 O 0.225106 -0.013533 0.138594
0013 O 0.477259 -0.368137 -0.129273
0014 O 0.111229 -0.259719 -0.484205
MN015 MN 0.349599 -0.180507 -0.004219
0016 O -0.271821 -0.256038 0.134896
0017 O -0.031455 -0.112137 -0.137498
0018 O -0.218430 0.396988 -0.495763
H019 H -0.082044 0.485691 -0.449195
H020 H -0.268261 -0.485118 0.366931
H021 H 0.271201 -0.286962 -0.383484
H022 H 0.173866 -0.181766 0.392776

Mn₄O₈·3H₂O (no cation)

data_BG_Mn408_3_H20.D1.121.LiTZVPP.01.out

_cell_length_a 4.928875
_cell_length_b 5.774115
_cell_length_c 9.113848
_cell_angle_alpha 51.985903
_cell_angle_beta 101.639810
_cell_angle_gamma 90.363513
_symmetry_space_group_name_H-M 'P 1'
_symmetry_Int_Tables_number 1

loop_
_symmetry_equiv_pos_as_xyz
'x, y, z'

loop_
_atom_site_label
_atom_site_type_symbol
_atom_site_fract_x
_atom_site_fract_y
_atom_site_fract_z

MN001 MN -0.142652 0.024959 0.001249
0002 O 0.242793 0.393839 0.138097
0003 O 0.224821 0.238719 -0.495717
0004 O 0.473763 0.154949 -0.133367
MN005 MN 0.357887 0.274437 0.000759
0006 O -0.260969 0.143062 0.136355
0007 O -0.026345 0.405201 -0.131542
H008 H 0.377695 0.290105 -0.439641
H009 H 0.235515 0.345144 0.372784
MN010 MN -0.142611 -0.477085 0.002621
0011 O 0.240160 -0.107446 0.135944
0012 O 0.475932 -0.345239 -0.132471
0013 O 0.186320 -0.242496 -0.485215
MN014 MN 0.357091 -0.223774 0.000059
0015 O -0.258554 -0.358097 0.137598
0016 O -0.026049 -0.095917 -0.133191
0017 O -0.287505 -0.484176 -0.490164
H018 H -0.131644 -0.384624 -0.477575
H019 H -0.201745 0.406555 0.478113
H020 H 0.226746 -0.100250 -0.461824
H021 H 0.351810 -0.291775 0.491171

Calcium

data_BG_CaMn408_3H20.D1.121.wat1wat2wat3.Ca.01.out

_cell_length_a 4.994407
 _cell_length_b 5.738092
 _cell_length_c 6.177423
 _cell_angle_alpha 62.146339
 _cell_angle_beta 123.923002
 _cell_angle_gamma 90.877919
 _symmetry_space_group_name_H-M 'P 1'
 _symmetry_Int_Tables_number 1

0012 0 0.231391 -0.012023 0.138486
 0013 0 0.483685 -0.370940 -0.124969
 0014 0 0.161781 -0.299417 -0.482493
 MN015 MN 0.353667 -0.180266 -0.003292
 0016 0 -0.266868 -0.253829 0.136739
 0017 0 -0.029250 -0.117571 -0.130878
 0018 0 -0.261555 0.449878 -0.495285
 H019 H -0.090459 -0.495658 -0.450234
 H020 H -0.292608 -0.443180 0.367626
 H021 H 0.311229 -0.306785 -0.382375
 H022 H 0.219576 -0.212859 0.396024

Strontium

loop_
 _symmetry_equiv_pos_as_xyz
 'x, y, z'

data_BG_SrMn408_3H20.D1.121.511d21G.out
 _cell_length_a 4.966521
 _cell_length_b 6.010950
 _cell_length_c 7.936687
 _cell_angle_alpha 63.516690
 _cell_angle_beta 107.062011
 _cell_angle_gamma 89.985487
 _symmetry_space_group_name_H-M 'P 1'
 _symmetry_Int_Tables_number 1

loop_
 _atom_site_label
 _atom_site_type_symbol
 _atom_site_fract_x
 _atom_site_fract_y
 _atom_site_fract_z
 MN001 MN -0.130027 0.074062 0.002208
 0002 0 0.352568 0.465305 0.221073
 0003 0 0.388499 0.182378 -0.215206
 MN004 MN 0.370202 0.324390 0.002393
 0005 0 -0.148093 0.215310 0.220783
 0006 0 -0.111533 0.432607 -0.215202
 MN007 MN -0.129210 -0.426625 0.003430
 0008 0 0.351695 -0.033964 0.220212
 0009 0 0.389085 -0.317565 -0.215064
 MN010 MN 0.370748 -0.176181 0.003252
 0011 0 -0.147716 -0.284399 0.220833
 0012 0 -0.110990 -0.068210 -0.214739

loop_
 _symmetry_equiv_pos_as_xyz
 'x, y, z'

loop_
 _atom_site_label
 _atom_site_type_symbol
 _atom_site_fract_x
 _atom_site_fract_y
 _atom_site_fract_z
 MN001 MN -0.123149 0.081584 -0.002406
 0002 0 0.264743 0.453956 0.157937
 0003 0 0.262478 0.157077 -0.478489
 0004 0 0.485970 0.194447 -0.145815
 MN005 MN 0.376617 0.325894 0.002552
 0006 0 -0.237304 0.257031 0.159247
 SR007 SR -0.227095 -0.006771 -0.496486
 0008 0 -0.023713 0.418475 -0.142021
 H009 H 0.335243 0.221937 -0.381910
 H010 H 0.250552 0.293861 0.388732
 MN011 MN -0.119973 -0.433970 0.008981
 0012 0 0.283562 -0.004258 0.142984
 0013 0 0.479679 -0.351364 -0.140903
 0014 0 0.160930 -0.289572 0.497728
 MN015 MN 0.379520 -0.179232 -0.000707
 0016 0 -0.220090 -0.260416 0.138562
 0017 0 -0.014751 -0.123547 -0.144318
 0018 0 -0.285263 0.436157 0.493261
 H019 H -0.153030 0.430025 -0.385710
 H020 H -0.212598 -0.461785 0.384121
 H021 H 0.311000 -0.319105 -0.378804
 H022 H 0.232303 -0.219212 0.385155

Sodium

data_BG_NaMn408_3H20.D1.121.k14.SPLK4.FMIX90.out

_cell_length_a 4.977447
 _cell_length_b 5.847388
 _cell_length_c 7.838952
 _cell_angle_alpha 65.532174
 _cell_angle_beta 99.631780
 _cell_angle_gamma 88.034051
 _symmetry_space_group_name_H-M 'P 1'
 _symmetry_Int_Tables_number 1

Yttrium

data_BG_YMn408_3H20.D1.121.SPLOCK4.out

loop_
 _atom_site_label
 _atom_site_type_symbol
 _atom_site_fract_x
 _atom_site_fract_y
 _atom_site_fract_z
 MN001 MN -0.144702 0.068632 0.002322
 0002 0 0.213261 0.457492 0.154046
 0003 0 0.335610 0.136982 -0.476609
 0004 0 -0.497237 0.175044 -0.136838
 MN005 MN 0.358544 0.310454 0.010817
 0006 0 -0.267263 0.232113 0.149594
 NA007 NA -0.153108 0.041679 -0.480640
 0008 0 -0.011447 0.388760 -0.125660
 H009 H 0.405392 0.232159 -0.405232
 H010 H 0.287766 0.262923 0.389238
 MN011 MN -0.141775 -0.442378 0.011304

_cell_length_a 5.003355
 _cell_length_b 6.194088
 _cell_length_c 7.409866
 _cell_angle_alpha 66.963571
 _cell_angle_beta 104.338092
 _cell_angle_gamma 85.746233
 _symmetry_space_group_name_H-M 'P 1'
 _symmetry_Int_Tables_number 1

```

loop_
_symmetry_equiv_pos_as_xyz
'x, y, z'

loop_
_atom_site_label
_atom_site_type_symbol
_atom_site_fract_x
_atom_site_fract_y
_atom_site_fract_z
MN001 MN -0.153665 0.080695 -0.002341
0002 O 0.234886 0.465818 0.163839
0003 O 0.354081 0.131152 -0.486873
0004 O 0.464129 0.181170 -0.155743
MN005 MN 0.343140 0.323842 0.001104
0006 O -0.270773 0.213912 0.169913
Y007 Y -0.157989 0.034719 -0.491552
0008 O -0.031264 0.433360 -0.158281
H009 H 0.389520 0.183180 -0.369535
H010 H 0.295212 0.284047 0.374682
MN011 MN -0.151750 -0.433222 0.007215
0012 O 0.244173 0.013432 0.143897
0013 O 0.450175 -0.372881 -0.135805
0014 O 0.141860 -0.256416 0.494239
MN015 MN 0.352284 -0.181047 0.007305
0016 O -0.266405 -0.269347 0.153826
0017 O -0.035115 -0.078388 -0.158476
0018 O -0.188308 0.394677 -0.499300
H019 H -0.112614 0.422209 -0.373308
H020 H -0.207262 -0.458556 0.368725
H021 H 0.293676 -0.315823 -0.370535
H022 H 0.217638 -0.175322 0.378696

Scandium
data_ScMn408_3H2O.D1.TZVP2012.121.freq.out

_cell_length_a 5.053785
_cell_length_b 6.210935
_cell_length_c 7.236825
_cell_angle_alpha 66.983324
_cell_angle_beta 103.340047
_cell_angle_gamma 85.873073
_symmetry_space_group_name_H-M 'P 1'
_symmetry_Int_Tables_number 1

loop_
_symmetry_equiv_pos_as_xyz
'x, y, z'

loop_
_atom_site_label
_atom_site_type_symbol
_atom_site_fract_x
_atom_site_fract_y
_atom_site_fract_z
MN001 MN -0.164865 0.066799 0.000760
0002 O 0.210068 0.461339 0.160514
0003 O 0.425572 0.138573 -0.488290
0004 O 0.461296 0.166802 -0.151840
MN005 MN 0.332386 0.308286 0.006377
0006 O -0.290694 0.201077 0.182026
SC007 SC -0.166594 0.072141 -0.496174
0008 O -0.036891 0.407257 -0.154582
H009 H 0.421639 0.175708 -0.362592
H010 H 0.318989 0.284340 0.374097
MN011 MN -0.167292 -0.439860 -0.002738
0012 O 0.223102 -0.000828 0.143826
0013 O 0.439909 -0.389768 -0.137219
0014 O 0.100077 -0.202204 -0.499446
MN015 MN 0.336680 -0.190921 0.001178
0016 O -0.284305 -0.274914 0.145656
0017 O -0.042170 -0.083950 -0.174219
0018 O -0.100195 0.389267 0.499155
H019 H -0.072693 0.417827 -0.369128
H020 H -0.173427 -0.457039 0.364961
H021 H 0.251478 -0.286347 -0.362536
H022 H 0.183559 -0.142379 0.381902

Zinc
data_BG_ZnMn408_3H2O.D1.121.511d21G.FMIX90.out

_cell_length_a 4.982341
_cell_length_b 6.089927
_cell_length_c 7.505374
_cell_angle_alpha 63.266268
_cell_angle_beta 104.825638
_cell_angle_gamma 89.938137
_symmetry_space_group_name_H-M 'P 1'
_symmetry_Int_Tables_number 1

loop_
_symmetry_equiv_pos_as_xyz
'x, y, z'

loop_
_atom_site_label
_atom_site_type_symbol
_atom_site_fract_x
_atom_site_fract_y
_atom_site_fract_z
MN001 MN -0.136243 0.067855 -0.000637
0002 O 0.235355 0.459738 0.156277
0003 O 0.317023 0.149120 -0.474074
0004 O 0.483829 0.184557 -0.142724
MN005 MN 0.366180 0.307018 0.015549
0006 O -0.253716 0.248426 0.177893
ZN007 ZN -0.085383 0.071668 -0.490655
0008 O -0.024106 0.393342 -0.137698
H009 H 0.391589 0.210442 -0.371556
H010 H 0.305824 0.287039 0.383780
MN011 MN -0.138949 -0.441159 -0.000088
0012 O 0.254919 -0.019904 0.145520
0013 O 0.469750 -0.373860 -0.142312
0014 O 0.088124 -0.231004 0.497344

Aluminum
4.2  $M^{n+} \cdot Mn_4O_8 \cdot 3H_2O$  Shifted Cation Site
data_BG_AlMn408_3H2O.D1.TZVP2012.SPLOCK4.Na.OXO.01.out

_cell_length_a 5.056157
_cell_length_b 6.221589
_cell_length_c 7.006644
_cell_angle_alpha 68.059080
_cell_angle_beta 102.712782
_cell_angle_gamma 86.140663
_symmetry_space_group_name_H-M 'P 1'
_symmetry_Int_Tables_number 1

```

```

loop_
_symmetry_equiv_pos_as_xyz
'x, y, z'

loop_
_atom_site_label
_atom_site_type_symbol
_atom_site_fract_x
_atom_site_fract_y
_atom_site_fract_z
MN001 MN -0.162598 0.086474 0.010793
0002 O 0.207873 0.494203 0.170508
0003 O 0.188166 0.181213 -0.498495
0004 O 0.471855 0.183699 -0.144253
MN005 MN 0.340133 0.317862 0.023622
0006 O -0.275096 0.223007 0.191887
AL007 AL -0.120093 0.060164 -0.466041
0008 O -0.047783 0.375338 -0.123100
H009 H 0.290601 0.209001 -0.373709
H010 H 0.201338 0.370049 0.323689
MN011 MN -0.170221 -0.414379 -0.001935
0012 O 0.211046 -0.027530 0.172120
0013 O 0.455724 -0.337210 -0.143812
0014 O 0.255669 -0.354107 -0.487617
MN015 MN 0.340917 -0.158087 -0.002537
0016 O -0.271852 -0.219370 0.142261
0017 O -0.051797 -0.040147 -0.180047
0018 O -0.219361 -0.196279 -0.476933
H019 H 0.065307 -0.337634 -0.468154
H020 H -0.292844 -0.196271 0.381809
H021 H 0.375419 -0.335475 -0.355441
H022 H 0.246336 -0.207318 0.367076

Beryllium
data_BG_BeMn408_3H20.D1.121.BeTZVPP.Na.OX0.01.out
_cell_length_a 4.986811
_cell_length_b 5.995163
_cell_length_c 7.619996
_cell_angle_alpha 64.831556
_cell_angle_beta 98.603534
_cell_angle_gamma 87.659864
_symmetry_space_group_name_H-M 'P 1'
_symmetry_IntTables_number 1

loop_
_symmetry_equiv_pos_as_xyz
'x, y, z'

loop_
_atom_site_label
_atom_site_type_symbol
_atom_site_fract_x
_atom_site_fract_y
_atom_site_fract_z
MN001 MN -0.122810 0.067097 0.025448
0002 O 0.212264 0.473010 0.158346
0003 O 0.197197 0.210970 -0.487744
0004 O -0.465304 0.168239 -0.139589
MN005 MN 0.371735 0.318348 0.011485
0006 O -0.287367 0.277586 0.173555
CA007 CA -0.281907 0.147907 -0.443153
0008 O 0.008197 0.377215 -0.128343
H009 H 0.220292 0.356260 -0.451285
H010 H 0.182882 0.295139 0.361793
MN011 MN -0.133311 -0.435439 0.008070
0012 O 0.250123 0.000554 0.151476
0013 O -0.497149 -0.373587 -0.135330
0014 O 0.241562 -0.358564 -0.478820
MN015 MN 0.367054 -0.176250 -0.005949
0016 O -0.268324 -0.250184 0.147141
0017 O 0.003319 -0.143253 -0.144813
0018 O -0.251162 -0.208399 -0.499321
H019 H -0.060123 -0.277113 -0.452896
H020 H -0.289215 -0.216541 0.367378
H021 H 0.372409 -0.343884 -0.369718
H022 H 0.268378 -0.231903 0.393960

Pottassium
data_BG_KMn408_3H20.D1.121.TZVPP.Na.OX0.out
_cell_length_a 5.044146
_cell_length_b 5.788419
_cell_length_c 7.927584
_cell_angle_alpha 64.751554
_cell_angle_beta 101.253894
_cell_angle_gamma 88.896862
_symmetry_space_group_name_H-M 'P 1'
_symmetry_IntTables_number 1

loop_
_symmetry_equiv_pos_as_xyz

```

```

'x, y, z'

loop_
_atom_site_label
_atom_site_type_symbol
_atom_site_fract_x
_atom_site_fract_y
_atom_site_fract_z
MN001 MN -0.126621 0.048071 0.010902
0002 O 0.232777 0.439525 0.153912
0003 O 0.215850 0.145854 -0.475650
0004 O -0.481203 0.159624 -0.132505
MN005 MN 0.373857 0.298502 0.010077
0006 O -0.251266 0.217860 0.150029
K007 K -0.280207 0.331332 -0.481775
0008 O -0.001083 0.374993 -0.125806
H009 H 0.235594 0.293810 -0.446741
H010 H 0.204849 0.220104 0.386430
MN011 MN -0.127166 -0.452247 0.010223
0012 O 0.253926 -0.031896 0.143084
0013 O 0.494893 -0.378757 -0.122603
0014 O 0.229094 -0.372883 -0.480278
MN015 MN 0.370675 -0.194769 0.000570
0016 O -0.240088 -0.279430 0.146166
0017 O -0.019275 -0.124797 -0.125731
0018 O -0.275671 -0.163396 -0.488608
H019 H -0.082143 -0.225962 -0.443043
H020 H -0.290532 -0.051291 0.376854
H021 H 0.361371 -0.327222 -0.394991
H022 H 0.241106 -0.249817 0.391175

Lithium
data_BG_LiMn408_3H20.D1.121.k14.SPLK4.FMIX90.Na.OX0.out

_cell_length_a 4.971805
_cell_length_b 5.818346
_cell_length_c 8.163002
_cell_angle_alpha 61.702530
_cell_angle_beta 96.383636
_cell_angle_gamma 88.513782
_symmetry_space_group_name_H-M 'P 1'
_symmetry_Int_Tables_number 1

loop_
_symmetry_equiv_pos_as_xyz
'x, y, z'

loop_
_atom_site_label
_atom_site_type_symbol
_atom_site_fract_x
_atom_site_fract_y
_atom_site_fract_z
MN001 MN -0.139713 0.033471 0.012885
0002 O 0.217453 0.415378 0.147068
0003 O 0.315378 0.243000 0.499372
0004 O -0.478129 0.149618 -0.144514
MN005 MN 0.353892 0.280335 0.004214
0006 O -0.299589 0.163435 0.153370
MG007 MG -0.342486 0.051808 -0.341436
0008 O -0.008213 0.361143 -0.122859
H009 H 0.262099 0.391604 -0.482635
H010 H 0.275006 0.299754 0.360306
MN011 MN -0.143597 -0.477678 0.014992
0012 O 0.229711 -0.047614 0.141215
0013 O 0.488307 -0.382580 -0.127774
0014 O 0.221512 -0.333218 -0.480144
MN015 MN 0.357213 -0.215567 0.007357
0016 O -0.271746 -0.291744 0.137893
0017 O -0.009560 -0.091480 -0.141604
0018 O -0.253184 -0.106434 -0.492213
H019 H -0.077035 -0.213113 -0.461654
H020 H -0.283605 -0.002233 0.365865
H021 H 0.361718 -0.337031 -0.383236
H022 H 0.263303 -0.213647 0.395222

Sodium
data_BG_NaMn408_3H20.D1.121.k14.SPLK4.FMIX90.OX0.out

_cell_length_a 4.997232
_cell_length_b 5.803953
_cell_length_c 7.659038
_cell_angle_alpha 66.866801
_cell_angle_beta 100.081800
_cell_angle_gamma 88.775452
_symmetry_space_group_name_H-M 'P 1'
_symmetry_Int_Tables_number 1

loop_
_symmetry_equiv_pos_as_xyz
'x, y, z'

loop_

```

_atom_site_label
 _atom_site_type_symbol
 _atom_site_fract_x
 _atom_site_fract_y
 _atom_site_fract_z

MN001	MN	-0.122842	0.064067	0.010124	H020	H	-0.305483	-0.205027	0.359898
0002	O	0.230390	0.461951	0.154266	H021	H	0.349651	-0.350821	-0.367052
0003	O	0.230658	0.155529	-0.479371	H022	H	0.257998	-0.200526	0.390197
0004	O	-0.471944	0.168608	-0.138636	Strontium				
MN005	MN	0.377500	0.314149	0.008433	data_BG_SrMn408_3H20.D1.121.MgTVZZP.Ca.OX0.out				
0006	O	-0.252168	0.242320	0.150821	_cell_length_a		5.043949		
NA007	NA	-0.274094	0.225752	-0.450141	_cell_length_b		5.935974		
0008	O	0.006007	0.381134	-0.128920	_cell_length_c		7.434199		
H009	H	0.258497	0.281560	-0.425677	_cell_angle_alpha		67.400505		
H010	H	0.208399	0.253430	0.380225	_cell_angle_beta		101.053673		
MN011	MN	-0.125471	-0.438685	0.008698	_cell_angle_gamma		89.985454		
0012	O	0.254447	-0.008310	0.144034	_symmetry_space_group_name_H-M		'P 1'		
0013	O	-0.498566	-0.371104	-0.125614	_symmetry_Int_Tables_number		1		
0014	O	0.214563	-0.352529	-0.483582	loop_				
MN015	MN	0.374716	-0.181280	0.000501	_symmetry_equiv_pos_as_xyz				
0016	O	-0.244230	-0.255992	0.146684	'x, y, z'				
0017	O	-0.010543	-0.116427	-0.128998	loop_				
0018	O	-0.279187	-0.196458	-0.482938	_atom_site_label				
H019	H	-0.082961	-0.251775	-0.461695	_atom_site_type_symbol				
H020	H	-0.342849	-0.147398	0.379881	_atom_site_fract_x				
H021	H	0.363126	-0.313053	-0.401467	_atom_site_fract_y				
H022	H	0.225290	-0.238282	0.385064	_atom_site_fract_z				

Scandium

data_BG_ScMn408_3H20.D1.TZVP2012.SPLOCK4.Na.OX0.01.out

_cell_length_a		5.024565			MN001	MN	-0.125257	0.053357	0.022188
_cell_length_b		6.123648			0002	O	0.233541	0.451131	0.152827
_cell_length_c		6.686317			0003	O	0.182677	0.220500	-0.497253
_cell_angle_alpha		72.428677			0004	O	-0.470624	0.154638	-0.141124
_cell_angle_beta		97.076394			MN005	MN	0.369702	0.304252	0.003557
_cell_angle_gamma		87.089973			0006	O	-0.257436	0.240852	0.154614
_symmetry_space_group_name_H-M		'P 1'			SR007	SR	-0.293815	0.207758	-0.463037
_symmetry_Int_Tables_number		1			0008	O	0.015534	0.340706	-0.143673
loop_					H009	H	0.208978	0.371255	-0.467659
_symmetry_equiv_pos_as_xyz					H010	H	0.174200	0.289309	0.354586
'x, y, z'					MN011	MN	-0.135217	-0.445678	0.002439
loop_					0012	O	0.252502	-0.010121	0.157955
_atom_site_label					0013	O	0.487585	-0.376611	-0.129262
_atom_site_type_symbol					0014	O	0.249160	-0.355844	-0.479310
_atom_site_fract_x					MN015	MN	0.368860	-0.189694	0.012241
_atom_site_fract_y					0016	O	-0.270336	-0.240935	0.168268
_atom_site_fract_z					0017	O	-0.014458	-0.123722	-0.122756
					0018	O	-0.244053	-0.198984	-0.485403
					H019	H	-0.051520	-0.261840	-0.443843
					H020	H	-0.285964	-0.189811	0.376197
					H021	H	0.375884	-0.341004	-0.365525
					H022	H	0.268798	-0.222305	0.395662

Yttrium

data_BG_YMn408_3H20.D1.TZVP2012.SPLOCK4.Na.OX0.out

_cell_length_a		5.127872							
_cell_length_b		5.996303							
_cell_length_c		6.747330							
_cell_angle_alpha		74.462710							
_cell_angle_beta		96.403031							
_cell_angle_gamma		86.060817							
_symmetry_space_group_name_H-M		'P 1'							
_symmetry_Int_Tables_number		1							
loop_									
_symmetry_equiv_pos_as_xyz									
'x, y, z'									
loop_									
_atom_site_label									
_atom_site_type_symbol									
_atom_site_fract_x									

```

._atom_site_fract_y
._atom_site_fract_z
MN001 MN -0.126187 0.052129 0.032034
0002 O 0.201545 0.486704 0.144846
0003 O 0.203971 0.240963 0.497800
0004 O -0.454552 0.127315 -0.147996
MN005 MN 0.366967 0.304726 0.002034
0006 O -0.260779 0.218346 0.205892
Y007 Y -0.229539 0.155479 -0.437627
0008 O -0.032381 0.331293 -0.148513
H009 H 0.224261 0.381380 -0.451924
H010 H 0.189150 0.327220 0.340299
MN011 MN -0.141706 -0.445701 -0.005529
0012 O 0.229228 -0.002757 0.162942
0013 O -0.496625 -0.398844 -0.134089
0014 O 0.235282 -0.335178 -0.478896
MN015 MN 0.364897 -0.187839 0.002341
0016 O -0.269744 -0.237099 0.152215
0017 O 0.006681 -0.106870 -0.153659
0018 O -0.247411 -0.206568 -0.479713
H019 H -0.056787 -0.275620 -0.447613
H020 H -0.289462 -0.208941 0.371796
H021 H 0.367752 -0.331303 -0.358954
H022 H 0.254179 -0.211625 0.394006

```

Boron

data_BMn408_3H20.D1.TZVP2012.SPLOCK4.Na.OX0.02.out

```

._cell_length_a 5.105276
._cell_length_b 6.126386
._cell_length_c 7.749249
._cell_angle_alpha 62.693034
._cell_angle_beta 100.390505
._cell_angle_gamma 89.145172
._symmetry_space_group_name_H-M 'P 1'
._symmetry_Int_Tables_number 1

```

```

loop_
._symmetry_equiv_pos_as_xyz
'x, y, z'

```

```

loop_
._atom_site_label
._atom_site_type_symbol
._atom_site_fract_x
._atom_site_fract_y
._atom_site_fract_z
MN001 MN -0.161042 0.070691 -0.016202
0002 O 0.188581 0.437392 0.156613
0003 O 0.153905 0.167223 -0.459118
0004 O 0.461159 0.193444 -0.160478
MN005 MN 0.316082 0.306244 0.008502
0006 O -0.328691 0.201811 0.163094
B007 B -0.009620 -0.008193 -0.377233
0008 O -0.040564 0.387244 -0.134344
H009 H 0.358942 0.239609 -0.296966
H010 H 0.156544 0.251836 0.397413
MN011 MN -0.168743 -0.449874 0.004067
0012 O 0.213797 -0.022359 0.128942
0013 O 0.453511 -0.381580 -0.122446
0014 O 0.239174 -0.341849 -0.495900
MN015 MN 0.352591 -0.204417 0.008963
0016 O -0.274793 -0.249057 0.118472
0017 O -0.002938 -0.095583 -0.177332
0018 O -0.170975 -0.112615 -0.477158
H019 H -0.041299 -0.233104 -0.486743
H020 H -0.293670 0.067595 0.306396
H021 H 0.375818 -0.326718 -0.397623
H022 H 0.260972 -0.220533 0.370775

```

4.3 $M^{n+}Mn_4O_8 \cdot 3H_2O$ Parallel Oxidative Pattern**Beryllium**

data_BG_BeMn408_3H20.D1.121.BeTZVPP.para.14.relax.out

```

._cell_length_a 5.115890
._cell_length_b 5.874085
._cell_length_c 7.572269
._cell_angle_alpha 59.855511
._cell_angle_beta 95.876123
._cell_angle_gamma 92.861338
._symmetry_space_group_name_H-M 'P 1'
._symmetry_Int_Tables_number 1

```

```

loop_
._symmetry_equiv_pos_as_xyz
'x, y, z'

```

```

loop_
._atom_site_label
._atom_site_type_symbol
._atom_site_fract_x
._atom_site_fract_y
._atom_site_fract_z

```

```

MN001 MN -0.130662 0.059103 0.007714
0002 O 0.228605 0.466416 0.140731
0003 O 0.323972 0.184785 -0.480888
0004 O -0.484233 0.158402 -0.142915
MN005 MN 0.370805 0.316193 -0.003725
0006 O -0.301382 0.249732 0.144206
BE007 BE 0.041661 0.060708 -0.410907
0008 O 0.032153 0.390894 -0.160090
H009 H 0.442089 0.221602 -0.387505
H010 H 0.324034 0.316607 0.369361
MN011 MN -0.139572 -0.433510 -0.013327
0012 O 0.223953 -0.037308 0.147432
0013 O 0.499229 -0.332188 -0.152518
0014 O -0.004132 -0.149387 -0.496098
MN015 MN 0.373844 -0.190693 0.001682
0016 O -0.295960 -0.272775 0.152645
0017 O 0.039088 -0.103037 -0.164429
0018 O -0.158894 0.314498 -0.488546
H019 H -0.114973 0.380860 -0.393552
H020 H -0.210255 0.466969 0.371306
H021 H 0.039106 -0.326495 -0.374061
H022 H 0.107153 -0.120167 0.395174

```

Calcium

data_BG_CaMn408_3H20.D1.121.511d21G.FMIX90.para.relax.14.out

```

._cell_length_a 5.217677
._cell_length_b 5.736330
._cell_length_c 7.456631
._cell_angle_alpha 67.933308
._cell_angle_beta 104.939223
._cell_angle_gamma 89.603851
._symmetry_space_group_name_H-M 'P 1'
._symmetry_Int_Tables_number 1

```

```

loop_
._symmetry_equiv_pos_as_xyz
'x, y, z'

```

```

loop_
._atom_site_label
._atom_site_type_symbol
._atom_site_fract_x
._atom_site_fract_y

```

_atom_site_fract_z

MN001	MN	-0.124070	0.072929	0.001988	data_BG_SrMn408_3H20.D1.121.511d21G.para.14.relax.out
0002	O	0.304896	0.499058	0.157544	_cell_length_a 5.242834
0003	O	0.269774	0.158829	0.495162	_cell_length_b 5.697088
0004	O	0.452174	0.148636	-0.149395	_cell_length_c 7.335957
MN005	MN	0.377431	0.321863	0.004804	_cell_angle_alpha 68.378004
0006	O	-0.246683	0.250421	0.146112	_cell_angle_beta 103.962624
CA007	CA	-0.197028	0.016328	0.492652	_cell_angle_gamma 90.636160
0008	O	0.004081	0.388136	-0.129079	_symmetry_space_group_name_H-M 'P 1'
H009	H	0.334418	0.192925	-0.380255	_symmetry_Int_Tables_number 1
H010	H	0.281434	0.314454	0.381775	
MN011	MN	-0.119359	-0.430136	0.008351	loop_
0012	O	0.313889	-0.008664	0.166407	_symmetry_equiv_pos_as_xyz
0013	O	0.454472	-0.352931	-0.153080	'x, y, z'
0014	O	0.131337	-0.289820	0.495935	
MN015	MN	0.378824	-0.176834	0.002952	loop_
0016	O	-0.248421	-0.244171	0.139284	_atom_site_label
0017	O	-0.001847	-0.108043	-0.139578	_atom_site_type_symbol
0018	O	-0.269451	0.415694	-0.493140	_atom_site_fract_x
H019	H	-0.128010	0.424299	-0.380745	_atom_site_fract_y
H020	H	-0.240819	-0.460234	0.382426	_atom_site_fract_z
H021	H	0.266839	-0.311166	-0.375878	MN001 MN -0.123189 0.100934 -0.003954
H022	H	0.211747	-0.200364	0.387449	0002 O 0.317508 -0.484138 0.171294

Magnesium

data_BG_MgMn408_3H20.D1.121.MgTZVPP.para.14.relax.01.out

_cell_length_a	5.073187	SR007 SR -0.232662 -0.054119 -0.494933
_cell_length_b	5.945564	0008 O 0.020253 0.411907 -0.121002
_cell_length_c	7.449180	H009 H 0.321867 0.183839 -0.375848
_cell_angle_alpha	66.147541	H010 H 0.262666 0.296626 0.385941
_cell_angle_beta	105.903334	MN011 MN -0.105544 -0.413899 0.024878
_cell_angle_gamma	89.621306	0012 O 0.315176 0.009822 0.172707
_symmetry_space_group_name_H-M	'P 1'	0013 O 0.468524 -0.334032 -0.151360
_symmetry_Int_Tables_number	1	0014 O 0.161405 -0.333219 -0.499303

loop_	MN015 MN 0.386313 -0.155636 0.006608
_symmetry_equiv_pos_as_xyz	0016 O -0.248238 -0.212841 0.144250
'x, y, z'	0017 O 0.013922 -0.098305 -0.129143

loop_	0018 O -0.260530 0.394398 -0.485012
_atom_site_label	H019 H -0.082384 0.451862 -0.480767
_atom_site_type_symbol	H020 H -0.361626 0.478021 0.374417
_atom_site_fract_x	H021 H 0.282485 -0.328488 -0.373875
_atom_site_fract_y	H022 H 0.215541 -0.214760 0.383287
_atom_site_fract_z	

Zinc

data_BG_ZnMn408_3H20.D1.121.511d21G.FMIX90.para.relax.out

_cell_length_a	5.082552	_cell_length_a 5.082552
_cell_length_b	5.938406	_cell_length_b 5.938406
_cell_length_c	7.429328	_cell_length_c 7.429328
_cell_angle_alpha	66.027478	_cell_angle_alpha 66.027478
_cell_angle_beta	105.988228	_cell_angle_beta 105.988228
_cell_angle_gamma	89.601316	_cell_angle_gamma 89.601316
_symmetry_space_group_name_H-M	'P 1'	_symmetry_space_group_name_H-M 'P 1'
_symmetry_Int_Tables_number	1	_symmetry_Int_Tables_number 1

loop_	loop_
_symmetry_equiv_pos_as_xyz	_symmetry_equiv_pos_as_xyz
'x, y, z'	'x, y, z'

loop_	MN001 MN -0.134343 0.057929 0.004940
_atom_site_label	0002 O 0.259984 -0.497809 0.142629
_atom_site_type_symbol	0003 O 0.299234 0.174459 -0.499664
_atom_site_fract_x	0004 O 0.468787 0.144188 -0.135627
_atom_site_fract_y	
_atom_site_fract_z	

Strontium

MN005	MN	0.369968	0.299652	0.021145	
0006	O	-0.270193	0.217118	0.186826	
ZN007	ZN	-0.086340	0.080723	0.498212	
0008	O	-0.024329	0.374811	-0.129826	
H009	H	0.381494	0.204167	-0.375499	
H010	H	0.313284	0.321515	0.378705	
MN011	MN	-0.138854	-0.436031	-0.005500	
0012	O	0.263139	-0.029347	0.150194	
0013	O	0.462247	-0.381694	-0.141561	
0014	O	0.097065	-0.242513	-0.499143	
MN015	MN	0.359814	-0.183515	-0.010481	
0016	O	-0.245563	-0.260145	0.132158	
0017	O	0.000719	-0.095474	-0.183154	
0018	O	-0.241538	0.398660	0.498053	
H019	H	-0.143843	0.420310	-0.376530	
H020	H	-0.223500	-0.455494	0.377787	
H021	H	0.248471	-0.304410	-0.365508	
H022	H	0.189930	-0.185888	0.393535	

4.4 $\text{M}_2^{n+}\text{Mn}_4\text{O}_8\cdot3\text{H}_2\text{O}$ Structures

Potassium

data_BG_K2Mn408_3H20.121.SPLOCK4.2.02.out

_cell_length_a		5.055886
_cell_length_b		5.980736
_cell_length_c		9.754688
_cell_angle_alpha		75.597833
_cell_angle_beta		116.578701
_cell_angle_gamma		90.409399
_symmetry_space_group_name_H-M		'P 1'
_symmetry_Int_Tables_number		1

loop_
_symmetry_equiv_pos_as_xyz
'x, y, z'

loop_
_atom_site_label
_atom_site_type_symbol
_atom_site_fract_x
_atom_site_fract_y
_atom_site_fract_z

MN001	MN	-0.162227	0.011498	-0.014590
0002	O	0.263261	0.420897	0.102926
0003	O	0.452448	0.147634	-0.413040
0004	O	0.420980	0.081322	-0.142534
MN005	MN	0.328076	0.256828	-0.024925
0006	O	-0.235228	0.206906	0.097124
K007	K	-0.348852	0.124018	0.358756
0008	O	-0.083230	0.275018	-0.142361
H009	H	0.392003	0.118036	-0.325448
H010	H	-0.333675	0.143770	-0.348355
MN011	MN	-0.154622	-0.499268	-0.000759
0012	O	0.269570	-0.028754	0.098202
0013	O	0.403461	-0.446615	-0.124294
0014	O	0.002708	-0.234450	-0.417597
MN015	MN	0.338460	-0.242535	-0.005224
0016	O	-0.237586	-0.257793	0.110784
0017	O	-0.092228	-0.204270	-0.116280
0018	O	-0.027319	-0.496779	0.397685
H019	H	0.141335	0.389222	0.430639
H020	H	-0.099255	-0.396603	0.282273
H021	H	0.137613	-0.313459	-0.303283
H022	H	-0.012405	-0.344523	-0.481347
K023	K	-0.455064	-0.368891	-0.384577

Lithium

				data_BG_Li2Mn408_3H20.121.LiTZVPP.out	
				_cell_length_a	4.980953
				_cell_length_b	6.062084
				_cell_length_c	7.712836
				_cell_angle_alpha	61.818035
				_cell_angle_beta	102.495917
				_cell_angle_gamma	90.157762
				_symmetry_space_group_name_H-M	'P 1'
				_symmetry_Int_Tables_number	1

loop_
_symmetry_equiv_pos_as_xyz
'x, y, z'

loop_
_atom_site_label
_atom_site_type_symbol
_atom_site_fract_x
_atom_site_fract_y
_atom_site_fract_z

MN001	MN	-0.134096	0.070391	0.005574
-------	----	-----------	----------	----------

0002	O	0.226819	0.458060	0.154556
------	---	----------	----------	----------

0003	O	0.298174	0.170303	-0.480879
------	---	----------	----------	-----------

0004	O	0.491650	0.192971	-0.138481
------	---	----------	----------	-----------

MN005	MN	0.371522	0.311112	0.019146
-------	----	----------	----------	----------

0006	O	-0.263510	0.249285	0.173299
------	---	-----------	----------	----------

LI007	LI	-0.075381	0.042996	-0.485142
-------	----	-----------	----------	-----------

0008	O	-0.014463	0.400639	-0.136485
------	---	-----------	----------	-----------

H009	H	0.484375	0.203217	-0.434780
------	---	----------	----------	-----------

H010	H	0.261405	0.284378	0.366472
------	---	----------	----------	----------

MN011	MN	-0.138239	-0.436151	0.001389
-------	----	-----------	-----------	----------

0012	O	0.248859	-0.018542	0.145305
------	---	----------	-----------	----------

0013	O	0.480573	-0.362303	-0.140400
------	---	----------	-----------	-----------

0014	O	0.146082	-0.257308	-0.493921
------	---	----------	-----------	-----------

MN015	MN	0.358767	-0.177632	-0.013484
-------	----	----------	-----------	-----------

0016	O	-0.256801	-0.267072	0.134486
------	---	-----------	-----------	----------

0017	O	-0.014890	-0.122373	-0.158850
------	---	-----------	-----------	-----------

0018	O	-0.237750	0.390667	-0.494539
------	---	-----------	----------	-----------

H019	H	-0.237238	0.459936	-0.403303
------	---	-----------	----------	-----------

H020	H	-0.253595	-0.467085	0.364624
------	---	-----------	-----------	----------

H021	H	0.287451	-0.260872	-0.380417
------	---	----------	-----------	-----------

H022	H	0.211476	-0.165511	0.380052
------	---	----------	-----------	----------

LI023	LI	0.171691	0.378823	-0.374885
-------	----	----------	----------	-----------

Sodium

data_BG_Na2Mn408_3H20.121.NaTZVPP.Li.01.out

				_cell_length_a	4.966791
--	--	--	--	----------------	----------

				_cell_length_b	6.089490
--	--	--	--	----------------	----------

				_cell_length_c	8.360066
--	--	--	--	----------------	----------

				_cell_angle_alpha	57.159433
--	--	--	--	-------------------	-----------

				_cell_angle_beta	97.032653
--	--	--	--	------------------	-----------

				_cell_angle_gamma	90.262595
--	--	--	--	-------------------	-----------

				_symmetry_space_group_name_H-M	'P 1'
--	--	--	--	--------------------------------	-------

				_symmetry_Int_Tables_number	1
--	--	--	--	-----------------------------	---

loop_
_symmetry_equiv_pos_as_xyz
'x, y, z'

loop_
_atom_site_label

				_atom_site_type_symbol
--	--	--	--	------------------------

				_atom_site_fract_x
--	--	--	--	--------------------

				_atom_site_fract_y
--	--	--	--	--------------------

				_atom_site_fract_z
--	--	--	--	--------------------

MN001	MN	-0.134394	0.072860	0.011264
-------	----	-----------	----------	----------

0002	O	0.214043	0.428844	0.162418
------	---	----------	----------	----------

0003 0 0.331506 0.139633 -0.484273
 0004 0 -0.483261 0.206080 -0.127544
 MN005 MN 0.372939 0.314602 0.018783
 0006 0 -0.286309 0.225115 0.172868
 NA007 NA -0.136030 -0.078595 -0.432719
 0008 0 0.004371 0.424237 -0.121468
 H009 H 0.493853 0.222344 -0.465046
 H010 H 0.275905 0.257791 0.369231
 MN011 MN -0.133277 -0.445853 0.020567
 0012 0 0.231508 -0.028636 0.139045
 0013 0 -0.488574 -0.347223 -0.120969
 0014 0 0.273474 -0.266711 -0.497546
 MN015 MN 0.367190 -0.186307 0.003416
 0016 0 -0.269335 -0.283775 0.142809
 0017 0 0.012706 -0.113443 -0.133352
 0018 0 -0.282268 0.434797 -0.497824
 H019 H -0.392249 -0.476356 -0.457293
 H020 H -0.282123 -0.446140 0.357951
 H021 H 0.329858 -0.141764 -0.461227
 H022 H 0.255338 -0.167922 0.358313
 NA023 NA 0.138011 0.334351 -0.348064

Beryllium

data_BG_Be2Mn408_3H20.121.BeTZVPP.05.out

_cell_length_a 5.058203
 _cell_length_b 6.482883
 _cell_length_c 7.884199
 _cell_angle_alpha 52.022798
 _cell_angle_beta 91.999531
 _cell_angle_gamma 93.336348
 _symmetry_space_group_name_H-M 'P 1'
 _symmetry_Int_Tables_number 1

loop_
 _atom_site_label
 _atom_site_type_symbol
 _atom_site_fract_x
 _atom_site_fract_y
 _atom_site_fract_z

MN001 MN -0.172861 0.046766 -0.008263
 0002 0 0.139939 0.414337 0.123020
 0003 0 0.378532 0.183988 -0.478305
 0004 0 -0.491759 0.218154 -0.174151
 MN005 MN 0.315915 0.310712 -0.010764
 0006 0 -0.387084 0.231155 0.154525
 BE007 BE 0.062544 0.084178 -0.415579
 0008 0 -0.029896 0.408959 -0.207724
 H009 H 0.485735 0.176869 -0.368368
 H010 H 0.477502 0.163427 0.429381
 MN011 MN -0.192108 -0.437217 -0.008303
 0012 0 0.139863 -0.026132 0.156818
 0013 0 -0.481882 -0.367386 -0.212277
 0014 0 -0.004742 -0.085591 0.495642
 MN015 MN 0.292958 -0.268797 0.096479
 0016 0 -0.319580 -0.299727 0.161865
 0017 0 -0.001710 -0.102727 -0.164194
 0018 0 -0.078691 0.362807 0.480511
 H019 H -0.019372 0.410223 -0.426533
 H020 H -0.190932 -0.487192 0.344406
 H021 H 0.064935 -0.259837 -0.395842
 H022 H 0.050550 -0.033797 0.351519
 BE023 BE -0.332225 0.484237 -0.272770

Strontium

data_BG_Sr2Mn408_3H20.121.511d21G.out

_cell_length_a 5.129031
 _cell_length_b 6.760394
 _cell_length_c 8.024265
 _cell_angle_alpha 57.663747
 _cell_angle_beta 110.470480
 _cell_angle_gamma 98.997242
 _symmetry_space_group_name_H-M 'P 1'
 _symmetry_Int_Tables_number 1

loop_
 _atom_site_label
 _atom_site_type_symbol
 _atom_site_fract_x
 _atom_site_fract_y
 _atom_site_fract_z

MN001 MN -0.084545 0.040918 0.010813
 0002 0 0.291541 0.487292 0.161155

Calcium

0003 0 0.238255 0.165537 -0.499921
 0004 0 -0.474485 0.109730 -0.153735
 MN005 MN 0.410974 0.293842 -0.006198
 0006 0 -0.214948 0.244287 0.153369
 SR007 SR -0.273836 0.061476 0.497534
 0008 0 0.027757 0.349835 -0.151212
 H009 H 0.370285 0.143646 -0.360323
 H010 H 0.263195 0.293474 0.359603
 MN011 MN -0.096302 -0.450286 -0.007215
 0012 0 0.302591 -0.017685 0.188023
 0013 0 -0.478753 -0.390299 -0.190730
 0014 0 0.027258 -0.214326 -0.490365
 MN015 MN 0.409830 -0.204410 0.000236
 0016 0 -0.203967 -0.271984 0.156898
 0017 0 0.028421 -0.138776 -0.149885
 0018 0 -0.227274 0.412638 -0.494288
 H019 H -0.103456 0.401960 -0.353572
 H020 H -0.209750 -0.446579 0.367759
 H021 H 0.170624 -0.247876 -0.357620
 H022 H 0.084772 -0.071313 0.403534
 SR023 SR 0.347443 -0.429892 0.481344

Zinc

data_BG_Zn2Mn408_3H20.D1.121.511d21G.FMIX90.01.out

_cell_length_a 5.117573
 _cell_length_b 6.376886
 _cell_length_c 7.475926
 _cell_angle_alpha 63.245066
 _cell_angle_beta 105.108651
 _cell_angle_gamma 87.322465
 _symmetry_space_group_name_H-M 'P 1'
 _symmetry_Int_Tables_number 1

loop_
 _atom_site_label
 _atom_site_type_symbol
 _atom_site_fract_x
 _atom_site_fract_y
 _atom_site_fract_z

MN001 MN -0.137373 0.066484 0.018425
 0002 0 0.231336 0.480144 0.157444
 0003 0 0.283264 0.160855 -0.498040
 0004 0 0.483657 0.190262 -0.133911
 MN005 MN 0.361595 0.304852 0.031636
 0006 0 -0.269156 0.220967 0.207902
 ZN007 ZN -0.100875 0.113518 -0.496058
 0008 0 -0.036246 0.387082 -0.127727
 H009 H 0.428738 0.025444 -0.395825
 H010 H 0.264421 0.333981 0.305002
 MN011 MN -0.156050 -0.417003 -0.010419
 0012 0 0.240890 -0.048341 0.157595
 0013 0 0.466218 -0.325230 -0.155513
 0014 0 0.185764 -0.286098 -0.491426
 MN015 MN 0.348186 -0.163855 -0.017057
 0016 0 -0.253277 -0.252551 0.139392
 0017 0 -0.031804 -0.075842 -0.193548
 0018 0 -0.235663 0.444276 -0.499808
 H019 H -0.118730 0.448472 -0.367898
 H020 H -0.231174 -0.412676 0.354552
 H021 H 0.295819 -0.277700 -0.357687
 H022 H 0.222186 -0.168105 0.371923
 ZN023 ZN 0.413903 0.422274 -0.427920

Aluminum

data_BG_Al2Mn408_3H20.D1.TZVP2012.121.Ga.SPINLOCK500.01.relax.out

_cell_length_a 5.498769
 _cell_length_b 6.366665
 _cell_length_c 7.263967
 _cell_angle_alpha 60.687590
 _cell_angle_beta 108.042849
 _cell_angle_gamma 93.452362
 _symmetry_space_group_name_H-M 'P 1'
 _symmetry_Int_Tables_number 1

loop_
 _atom_site_label
 _atom_site_type_symbol
 _atom_site_fract_x
 _atom_site_fract_y
 _atom_site_fract_z

MN001 MN -0.212966 0.079657 -0.012252
 0002 0 0.162935 -0.499453 0.144056

Magnesium

0003 O 0.493020 0.162104 0.499861
 0004 O 0.397927 0.106248 -0.134960
 MN005 MN 0.308672 0.310803 0.013698
 0006 O -0.296234 0.291373 0.190898
 AL007 AL -0.165260 0.095004 0.498507
 0008 O -0.144463 0.427207 -0.205417
 H009 H 0.464686 0.119358 -0.357293
 H010 H 0.353941 0.298474 0.374189
 MN011 MN -0.190582 -0.421926 -0.025882
 0012 O 0.173868 -0.025570 0.177971
 0013 O 0.435656 -0.329008 -0.158925
 0014 O -0.022123 -0.143593 0.490911
 MN015 MN 0.274698 -0.191792 0.017582
 0016 O -0.370499 -0.335899 0.257732
 0017 O -0.098374 -0.094788 -0.182121
 0018 O 0.021275 0.334651 -0.470207
 H019 H 0.181230 0.249034 -0.330896
 H020 H -0.362133 -0.483433 0.244457
 H021 H 0.332943 -0.230483 -0.315457
 H022 H 0.151255 -0.079208 0.323976
 AL023 AL -0.133839 -0.417552 -0.475796

Boron

data_BG_B2Mn408_3H20.D1.TZVP2012.SPLOCK500.1.relax.out

_cell_length_a 5.099646
 _cell_length_b 6.543042
 _cell_length_c 8.429988
 _cell_angle_alpha 57.410976
 _cell_angle_beta 109.426583
 _cell_angle_gamma 90.108880
 _symmetry_space_group_name_H-M 'P 1'
 _symmetry_Int_Tables_number 1

loop_
 _atom_site_label
 _atom_site_type_symbol
 _atom_site_fract_x
 _atom_site_fract_y
 _atom_site_fract_z

MN001 MN -0.086360 0.056060 0.009023
 0002 O 0.329877 0.431402 0.173160
 0003 O -0.441168 0.232109 -0.449118
 0004 O 0.471341 0.160553 -0.163244
 MN005 MN 0.397006 0.316933 -0.003844
 0006 O -0.202666 0.194654 0.162128
 B007 B -0.133353 0.079387 -0.371867
 0008 O 0.008159 0.439128 -0.140059
 H009 H 0.447936 -0.244806 -0.299706
 H010 H 0.410767 0.333958 0.329220
 MN011 MN -0.073535 -0.454564 0.011148
 0012 O 0.357144 -0.036945 0.180723
 0013 O -0.495270 -0.349044 -0.152735
 0014 O -0.194015 -0.060315 -0.467573
 MN015 MN 0.426899 -0.215473 0.042771
 0016 O -0.133652 -0.349149 0.174657
 0017 O -0.011649 -0.079696 -0.154707
 0018 O 0.073132 0.241093 -0.454699
 H019 H 0.462557 -0.095425 0.322359
 H020 H -0.058024 -0.494704 0.321599
 H021 H -0.097654 -0.236972 -0.368173
 H022 H -0.168895 0.091352 0.311394
 B023 B 0.367053 0.211677 -0.356668

Scandium

data_BG_Sc2Mn408_3H20.D1.TZVP2012.121.SPINLOCK500.relax.out

_cell_length_a 5.360131
 _cell_length_b 6.434192
 _cell_length_c 7.249919
 _cell_angle_alpha 63.742434
 _cell_angle_beta 102.985106
 _cell_angle_gamma 83.665250
 _symmetry_space_group_name_H-M 'P 1'
 _symmetry_Int_Tables_number 1

loop_
 _atom_site_label
 _atom_site_type_symbol
 _atom_site_fract_x
 _atom_site_fract_y
 _atom_site_fract_z

MN001 MN -0.120634 0.040274 0.025181
 0002 O 0.265227 0.482574 0.147310

Gallium

```

0003  O   0.357627  0.145461 -0.498083
0004  O   0.467136  0.229818 -0.185880
MN005  MN   0.386788  0.285453  0.030769
0006  O   -0.252503  0.215487  0.192200
SC007  SC  -0.218844  0.046139 -0.484896
0008  O   0.024063  0.360173 -0.115354
H009  H   0.382336  0.173727 -0.368646
H010  H   0.305108  0.308740  0.357401
MN011  MN  -0.101791 -0.453839 -0.000230
0012  O   0.347262 -0.080230  0.271121
0013  O   -0.430052 -0.321693 -0.222681
0014  O   0.037519 -0.259555 -0.467285
MN015  MN   0.370129 -0.186822 -0.056056
0016  O   -0.238652 -0.288879  0.138605
0017  O   -0.015621 -0.069226 -0.184620
0018  O   -0.264434  0.398557 -0.497410
H019  H   -0.119123  0.360306 -0.368532
H020  H   -0.228164 -0.400831  0.292802
H021  H   0.014676 -0.394905 -0.341799
H022  H   0.259264 -0.002682  0.337265
SC023  SC   0.428313 -0.416840 -0.435671

```

Yttrium

data_BG_Y2Mn408_3H2O.D1.121.SPLOCK4.out

```

_cell_length_a          5.223654
_cell_length_b          6.439598
_cell_length_c          7.724351
_cell_angle_alpha        65.342986
_cell_angle_beta         109.763066
_cell_angle_gamma        88.676481
_symmetry_space_group_name_H-M  'P 1'
_symmetry_Int_Tables_number  1

```

```

loop_
_symmetry_equiv_pos_as_xyz
'x, y, z'

```

```

loop_
_atom_site_label
_atom_site_type_symbol
_atom_site_fract_x
_atom_site_fract_y
_atom_site_fract_z
MN001  MN  -0.119676  0.072012  0.006872
0002  O   0.261533 -0.497949  0.168974
0003  O   0.344791  0.125803  0.499331
0004  O   0.445407  0.203253 -0.200771
MN005  MN   0.371759  0.314196  0.015487
0006  O   -0.242448  0.235983  0.170921
Y007  Y   -0.217580  0.039409  0.494118
0008  O   -0.019044  0.415678 -0.140981
H009  H   0.396129  0.117206 -0.284197
H010  H   0.234343  0.181389  0.353187
MN011  MN  -0.123557 -0.430510 -0.005977
0012  O   0.331276 -0.009530  0.190353
0013  O   0.466726 -0.377218 -0.150554
0014  O   0.100754 -0.230107  0.493993
MN015  MN   0.356932 -0.173379 -0.001036
0016  O   -0.205191 -0.285154  0.151926
0017  O   -0.055834 -0.085007 -0.179753
0018  O   -0.204177  0.402898  0.498761
H019  H   -0.097878  0.401339 -0.365967
H020  H   -0.204732 -0.392979  0.291298
H021  H   0.327118 -0.295963 -0.295591
H022  H   0.156643 -0.108114  0.393089
Y023  Y   0.352334  0.497956  0.466655

```

4.5 $M_2^{n+}Mn_4O_8 \cdot 3H_2O$ Parallel Oxidative Pattern**Aluminum**

data_BG_A12Mn408_3H2O.D1.TZVP2012.121.para.relax.out

```

_cell_length_a          5.625758
_cell_length_b          6.258988
_cell_length_c          7.583914
_cell_angle_alpha        58.333106
_cell_angle_beta         111.130387
_cell_angle_gamma        96.381124
_symmetry_space_group_name_H-M  'P 1'
_symmetry_Int_Tables_number  1

```

```

loop_
_symmetry_equiv_pos_as_xyz
'x, y, z'

```

```

loop_
_atom_site_label
_atom_site_type_symbol
_atom_site_fract_x
_atom_site_fract_y
_atom_site_fract_z
MN001  MN  -0.234310  0.067899 -0.049847
0002  O   0.209433  0.458238  0.161783
0003  O   -0.479382  0.142729 -0.476907
0004  O   0.391094  0.146426 -0.095391
MN005  MN   0.304365  0.313963  0.027099
0006  O   -0.304179  0.309988  0.219354
AL007  AL  -0.140033  0.100975 -0.476847
0008  O   -0.164057  0.433927 -0.236363
H009  H   0.451427 -0.001426 -0.378276
H010  H   0.370841  0.283999  0.376921
MN011  MN  -0.202352 -0.435443 -0.056905
0012  O   0.153723  0.005943  0.177396
0013  O   0.395461 -0.334158 -0.164766
0014  O   -0.008630 -0.122835  0.496139
MN015  MN   0.293932 -0.196706  0.046042
0016  O   -0.357437 -0.294808  0.230710
0017  O   -0.055749 -0.089923 -0.167976
0018  O   0.045775  0.361490 -0.472094
H019  H   0.199610  0.282322 -0.324902
H020  H   -0.336704  0.465705  0.221607
H021  H   0.239667 -0.252157 -0.305904
H022  H   0.124367 -0.029412  0.312490
AL023  AL  -0.141230 -0.395528 -0.498730

```

Boron

data_BG_B2Mn408_3H2O.D1.TZVP2012.para.relax.out

```

_cell_length_a          5.130087
_cell_length_b          6.576508
_cell_length_c          8.560683
_cell_angle_alpha        56.437967
_cell_angle_beta         110.775936
_cell_angle_gamma        90.961056
_symmetry_space_group_name_H-M  'P 1'
_symmetry_Int_Tables_number  1

```

```

loop_
_symmetry_equiv_pos_as_xyz
'x, y, z'

```

```

loop_
_atom_site_label
_atom_site_type_symbol

```

_atom_site_fract_x
 _atom_site_fract_y
 _atom_site_fract_z

MN001 MN -0.079040 0.060291 0.015573
 0002 O 0.358807 0.464810 0.171549
 0003 O -0.421996 0.226568 -0.444602
 0004 O 0.484099 0.117101 -0.156628
 MN005 MN 0.392650 0.317605 -0.001908
 0006 O -0.196891 0.197076 0.163899
 B007 B -0.115468 0.073660 -0.369309
 0008 O 0.011674 0.420222 -0.146363
 H009 H 0.344102 -0.239225 -0.312975
 H010 H 0.445992 0.361511 0.327790
 MN011 MN -0.089449 -0.448226 0.008043
 0012 O 0.368801 -0.038719 0.179303
 0013 O 0.460508 -0.344794 -0.166422
 0014 O -0.172389 -0.072933 -0.453939
 MN015 MN 0.419307 -0.207150 0.025701
 0016 O -0.176795 -0.318137 0.177160
 0017 O 0.015881 -0.079787 -0.146348
 0018 O 0.083793 0.235909 -0.460357
 H019 H 0.493077 -0.111587 0.322327
 H020 H -0.094058 -0.472095 0.320891
 H021 H -0.101968 -0.257268 -0.351207
 H022 H -0.155031 0.090592 0.313023
 B023 B 0.380021 0.195787 -0.359453

Lithium

data_BG_Li2Mn408_3H20.121.LiTZVPP.para.1.03.relax.out

_cell_length_a 5.299172
 _cell_length_b 5.734281
 _cell_length_c 7.799298
 _cell_angle_alpha 60.696786
 _cell_angle_beta 100.971870
 _cell_angle_gamma 90.088275
 _symmetry_space_group_name_H-M 'P 1'
 _symmetry_Int_Tables_number 1

loop_
 _symmetry_equiv_pos_as_xyz
 'x, y, z'

loop_
 _atom_site_label
 _atom_site_type_symbol
 _atom_site_fract_x
 _atom_site_fract_y
 _atom_site_fract_z

MN001 MN -0.099143 0.084705 0.012487
 0002 O 0.314675 0.490535 0.158302
 0003 O 0.231032 0.203714 0.496479
 0004 O 0.480016 0.198781 -0.152199
 MN005 MN 0.401357 0.336583 0.009900
 0006 O -0.237958 0.251412 0.143945
 LI007 LI -0.096643 0.058757 0.458487
 0008 O 0.040459 0.420240 -0.123254
 H009 H 0.369768 0.067718 -0.406072
 H010 H 0.289250 0.319574 0.366401
 MN011 MN -0.104265 -0.406933 0.000641
 0012 O 0.321515 -0.019342 0.167215
 0013 O 0.478435 -0.302857 -0.157880
 0014 O 0.148040 -0.269162 -0.498646
 MN015 MN 0.397936 -0.157974 0.003456
 0016 O -0.243359 -0.251156 0.137383
 0017 O 0.038901 -0.067334 -0.129324
 0018 O -0.260242 0.355047 -0.490495
 H019 H -0.385096 0.369135 -0.418967
 H020 H -0.279371 -0.480519 0.376894
 H021 H 0.269124 -0.279057 -0.382207
 H022 H 0.233744 -0.184860 0.385207
 LI023 LI 0.104707 0.340922 -0.348415

Potassium

data_BG_K2Mn408_3H20.121.SPLOCK4.para.relax.out

_cell_length_a 5.356028
 _cell_length_b 5.706639
 _cell_length_c 9.779078
 _cell_angle_alpha 78.441375
 _cell_angle_beta 119.888494
 _cell_angle_gamma 90.640627
 _symmetry_space_group_name_H-M 'P 1'
 _symmetry_Int_Tables_number 1

loop_
 _symmetry_equiv_pos_as_xyz
 'x, y, z'

loop_
 _atom_site_label
 _atom_site_type_symbol
 _atom_site_fract_x
 _atom_site_fract_y
 _atom_site_fract_z

MN001 MN -0.128436 -0.011145 -0.006518
 0002 O 0.343468 0.447637 0.107870
 0003 O 0.477339 0.223838 -0.388259
 0004 O 0.367893 0.035720 -0.148855
 MN005 MN 0.355175 0.241570 -0.021770
 0006 O -0.221342 0.206009 0.093017
 K007 K -0.316624 0.136646 0.379604
 0008 O -0.063103 0.274954 -0.123992
 H009 H 0.398777 0.169652 -0.314702
 H010 H -0.322976 0.253121 -0.307906
 MN011 MN -0.127154 0.487237 -0.006616
 0012 O 0.348587 -0.048892 0.109370
 0013 O 0.361952 -0.462840 -0.147355
 0014 O -0.126989 -0.314061 -0.430209
 MN015 MN 0.354182 -0.257759 -0.017706
 0016 O -0.224600 -0.295925 0.091887
 0017 O -0.060395 -0.225150 -0.117861
 0018 O 0.006089 -0.488874 0.387726
 H019 H 0.189396 0.410916 0.437685
 H020 H -0.081015 -0.413671 0.268187

Sodium

data_BG_Na2Mn408_3H20.121.NaTZVPP.Li.para.02.relax.out

_cell_length_a 5.252349
 _cell_length_b 5.782104
 _cell_length_c 8.111298
 _cell_angle_alpha 58.554531
 _cell_angle_beta 96.995028
 _cell_angle_gamma 89.598294
 _symmetry_space_group_name_H-M 'P 1'
 _symmetry_Int_Tables_number 1

loop_
 _symmetry_equiv_pos_as_xyz
 'x, y, z'

loop_
 _atom_site_label
 _atom_site_type_symbol

_atom_site_fract_x
 _atom_site_fract_y
 _atom_site_fract_z

MN001	MN	-0.124974	0.049931	0.014031	H021	H	0.050786	-0.421941	-0.316187
0002	O	0.234291	0.453533	0.145521	H022	H	0.162799	-0.149166	0.313307
0003	O	0.389825	0.154669	-0.489355	SC023	SC	0.474841	-0.411825	-0.404059
0004	O	-0.474519	0.145411	-0.117739	Yttrium				
MN005	MN	0.382144	0.299210	0.013374	data_BG_Y2Mn408_3H2O.D1.121.SPLOCK4.para.relax.out				
0006	O	-0.216007	0.178459	0.174967	_cell_length_a		5.230074		
NA007	NA	-0.189403	-0.140713	-0.423802	_cell_length_b		6.499303		
0008	O	-0.021300	0.408361	-0.132427	_cell_length_c		7.289624		
H009	H	-0.473592	0.245089	-0.454303	_cell_angle_alpha		67.534268		
H010	H	0.330072	0.279549	0.365846	_cell_angle_beta		103.851021		
MN011	MN	-0.120264	-0.459904	0.021599	_cell_angle_gamma		88.887717		
0012	O	0.225769	-0.045560	0.140670	_symmetry_space_group_name_H-M	'P 1'			
0013	O	-0.461791	-0.360261	-0.114933	_symmetry_Int_Tables_number	1			
0014	O	0.241222	-0.261743	-0.492139	loop_				
MN015	MN	0.378787	-0.199545	0.008623	_symmetry_equiv_pos_as_xyz	'x, y, z'			
0016	O	-0.219701	-0.311230	0.167025	loop_				
0017	O	-0.024894	-0.092107	-0.140481	_atom_site_label				
0018	O	-0.310843	-0.484105	-0.494720	_atom_site_type_symbol				
H019	H	-0.475492	-0.410097	-0.486065	_atom_site_fract_x				
H020	H	-0.286483	-0.400549	0.363556	_atom_site_fract_y				
H021	H	0.309265	-0.132305	-0.456118	_atom_site_fract_z				
H022	H	0.215097	-0.162235	0.360926	MN001	MN	-0.128228	0.094049	-0.001121
NA023	NA	0.105673	0.324071	-0.364718	0002	O	0.270197	-0.439461	0.175936

Scandium

data_BG_Sc2Mn408_3H2O.D1.TZVP2012.121.para.02.relax.out

_cell_length_a		5.546983			0003	O	0.359326	0.125548	0.488755
_cell_length_b		6.370903			0004	O	0.463916	0.118257	-0.169420
_cell_length_c		7.179743			MN005	MN	0.370753	0.331959	0.019818
_cell_angle_alpha		61.910871			0006	O	-0.263381	0.261645	0.165567
_cell_angle_beta		95.538514			Y007	Y	-0.183850	0.058243	0.497751
_cell_angle_gamma		81.737789			0008	O	0.027465	0.401390	-0.144252
_symmetry_space_group_name_H-M		'P 1'			H009	H	0.431687	0.067257	-0.285711
_symmetry_Int_Tables_number		1			H010	H	0.304229	0.093296	0.359063
loop_					MN011	MN	-0.133117	-0.413142	-0.012104
_symmetry_equiv_pos_as_xyz					0012	O	0.288830	0.035137	0.181000
'x, y, z'					0013	O	0.475921	-0.409495	-0.207952
loop_					0014	O	0.068369	-0.223439	0.472935
_atom_site_label					MN015	MN	0.347985	-0.156564	0.017996
_atom_site_type_symbol					0016	O	-0.281650	-0.240235	0.145415
_atom_site_fract_x					0017	O	0.004171	-0.087446	-0.166825
_atom_site_fract_y					0018	O	-0.213026	0.398448	-0.481844
_atom_site_fract_z					H019	H	-0.109709	0.411225	-0.347352
MN001	MN	-0.160363	0.072093	-0.000962	H020	H	-0.237035	-0.347463	0.290908
0002	O	0.224754	-0.498253	0.123889	H021	H	0.319106	-0.296091	-0.292126
0003	O	0.379872	0.180839	0.491789	H022	H	0.132059	-0.125885	0.355473
0004	O	0.476980	0.246734	-0.187054	Y023	Y	0.341611	0.463978	-0.491769
MN005	MN	0.367161	0.210932	0.089824	4.6 $M^{n+}Mn_4O_8 \cdot 3H_2O$ Bulk Water Removal				
0006	O	-0.250960	0.133053	0.223672					
SC007	SC	-0.212347	0.048270	-0.466800					
0008	O	-0.012031	0.341896	-0.102991					
H009	H	0.384956	0.203281	-0.378149					
H010	H	0.300184	0.341118	0.348993					
MN011	MN	-0.098239	-0.422541	-0.019480					
0012	O	0.320660	-0.150507	0.262204					
0013	O	-0.376986	-0.257622	-0.249863					
0014	O	0.101511	-0.269719	-0.409822					
MN015	MN	0.359824	-0.188197	-0.046070					
0016	O	-0.260421	-0.246947	0.114471					
0017	O	-0.009174	-0.028864	-0.180621					
0018	O	-0.236240	0.421483	0.487741					
H019	H	-0.091879	0.383035	-0.403627					
H020	H	-0.240057	-0.365946	0.275410					

Aluminum, Two Waters

data_BG_AlMn408_3H2O.D1.TZVP2012.121.wat1.out

_cell_length_a		5.063664		
_cell_length_b		6.138837		
_cell_length_c		7.138443		
_cell_angle_alpha		64.610925		
_cell_angle_beta		107.063747		
_cell_angle_gamma		88.971646		
_symmetry_space_group_name_H-M		'P 1'		
_symmetry_Int_Tables_number		1		
loop_				
_symmetry_equiv_pos_as_xyz				
'x, y, z'				

loop_					
_atom_site_label					
_atom_site_type_symbol					
_atom_site_fract_x					
_atom_site_fract_y					
_atom_site_fract_z					
MN001 MN -0.197661 0.055602 -0.010558					
0002 O 0.189203 0.441857 0.167170					
0003 O 0.422425 0.166137 -0.150534					
MN004 MN 0.314929 0.279969 0.026070					
0005 O -0.314351 0.173069 0.225386					
AL006 AL -0.102899 0.090555 0.499712					
0007 O -0.079966 0.369786 -0.146523					
MN008 MN -0.183637 -0.450069 -0.010187					
0009 O 0.204515 -0.037372 0.147521					
0010 O 0.414639 -0.406585 -0.132724					
0011 O 0.195059 -0.076403 -0.498268					
MN012 MN 0.315648 -0.206564 -0.004727					
0013 O -0.284498 -0.266900 0.132162					
0014 O -0.071264 -0.097493 -0.218098					
0015 O -0.110762 0.381504 0.498266					
H016 H -0.098389 0.397969 -0.363614					
H017 H -0.178579 -0.457199 0.356584					
H018 H 0.290963 -0.236647 -0.357738					
H019 H 0.216238 -0.077259 0.363282					

Aluminum, One Water

data_BG_AlMn408_3H2O.D1.TZVP2012.121.wat1wat2.out

_cell_length_a	5.089814
_cell_length_b	6.142774
_cell_length_c	7.409986
_cell_angle_alpha	62.812769
_cell_angle_beta	114.465241
_cell_angle_gamma	88.253645
_symmetry_space_group_name_H-M	'P 1'
_symmetry_Int_Tables_number	1

loop_	
_symmetry_equiv_pos_as_xyz	
'x, y, z'	

loop_	
_atom_site_label	
_atom_site_type_symbol	
_atom_site_fract_x	
_atom_site_fract_y	
_atom_site_fract_z	
MN001 MN -0.146578 0.051542 0.003544	
0002 O 0.274711 0.408575 0.187054	
0003 O 0.437859 0.179705 -0.159837	
MN004 MN 0.350164 0.281623 0.014282	
0005 O -0.237080 0.159413 0.242251	
AL006 AL -0.228729 0.144884 0.484237	
0007 O -0.081399 0.381893 -0.148156	
MN008 MN -0.149562 -0.457031 0.000608	
0009 O 0.280980 -0.049944 0.147241	
0010 O 0.420636 -0.388512 -0.142155	
MN011 MN 0.347880 -0.199379 -0.016103	
0012 O -0.210776 -0.275296 0.137026	
0013 O -0.090050 -0.089089 -0.229971	
0014 O -0.163178 0.415980 0.495717	
H015 H -0.146538 0.436045 -0.370365	
H016 H -0.150651 -0.433288 0.360298	

Aluminum, No Waters

data_BG_AlMn408_3H2O.D1.TZVP2012.121.wat1wat2wat3.Gasub.01.out

_cell_length_a	5.183359
_cell_length_b	5.826908
_cell_length_c	6.771608
_cell_angle_alpha	47.838728
_cell_angle_beta	115.282854
_cell_angle_gamma	94.283691
_symmetry_space_group_name_H-M	'P 1'
_symmetry_Int_Tables_number	1

loop_	
_symmetry_equiv_pos_as_xyz	
'x, y, z'	

loop_	
_atom_site_label	
_atom_site_type_symbol	
_atom_site_fract_x	
_atom_site_fract_y	
_atom_site_fract_z	

MN001 MN -0.173198 0.033306 0.009130	
0002 O 0.260573 0.339147 0.263255	
0003 O 0.373262 0.166110 -0.175140	
MN004 MN 0.298613 0.299169 0.013214	
0005 O -0.268696 0.200933 0.187115	
AL006 AL 0.036998 0.172386 0.488554	
0007 O -0.118955 0.453694 -0.229869	
MN008 MN -0.271310 -0.357683 -0.135207	
0009 O 0.264194 -0.120314 0.253333	
0010 O 0.305774 -0.251602 -0.227802	
MN011 MN 0.375477 -0.280822 0.116439	
0012 O -0.184782 -0.395756 0.227029	
0013 O -0.135730 -0.002800 -0.273326	

Beryllium, No Waters

data_BG_BeMn408_3H2O.D1.121.BeTZVPP.wat1wat2wat3.01.out

_cell_length_a	4.971805
_cell_length_b	6.068597
_cell_length_c	6.159036
_cell_angle_alpha	49.087510
_cell_angle_beta	96.933176
_cell_angle_gamma	89.601281
_symmetry_space_group_name_H-M	'P 1'
_symmetry_Int_Tables_number	1

loop_	
_symmetry_equiv_pos_as_xyz	
'x, y, z'	

loop_	
_atom_site_label	
_atom_site_type_symbol	
_atom_site_fract_x	
_atom_site_fract_y	
_atom_site_fract_z	
MN001 MN -0.132417 0.079052 -0.016449	
0002 O 0.194746 0.351750 0.254617	
0003 O -0.490522 0.240187 -0.205179	
MN004 MN 0.362060 0.302850 0.010848	
0005 O -0.260033 0.186481 0.243137	
BE006 BE 0.016437 0.098155 0.460561	
0007 O 0.007209 0.459005 -0.203905	
MN008 MN -0.143516 -0.434389 -0.006703	
0009 O 0.232953 -0.064772 0.200865	
0010 O 0.492752 -0.316434 -0.182902	
MN011 MN 0.381998 -0.206946 0.027757	
0012 O -0.248557 -0.316258 0.193570	
0013 O 0.024569 -0.080803 -0.216231	

Beryllium, One Water

```
data_BG_BeMn408_3H20.D1.121.BeTZVPP.wat2wat3.out
_cell_length_a      5.148550
_cell_length_b      5.869395
_cell_length_c      7.078892
_cell_angle_alpha   60.545867
_cell_angle_beta    106.038576
_cell_angle_gamma   90.944197
_symmetry_space_group_name_H-M   'P 1'
_symmetry_Int_Tables_number     1
```

```
loop_
_symmetry_equiv_pos_as_xyz
'x, y, z'
```

```
loop_
_atom_site_label
_atom_site_type_symbol
_atom_site_fract_x
_atom_site_fract_y
_atom_site_fract_z
MN001 MN -0.095934 0.054669 0.008339
0002 O 0.265936 0.475110 0.149784
0003 O 0.227734 0.179948 -0.482926
0004 O -0.489839 0.157720 -0.137810
MN005 MN 0.388655 0.309051 0.010515
0006 O -0.231799 0.232810 0.191066
BE007 BE -0.029321 0.060467 -0.455107
0008 O 0.001679 0.397018 -0.153162
H009 H 0.352487 0.201678 -0.354631
H010 H 0.258681 0.310623 0.365304
MN011 MN -0.126059 -0.432645 -0.012502
0012 O 0.288984 -0.036313 0.164837
0013 O 0.496320 -0.352687 -0.151487
MN014 MN 0.409579 -0.197977 0.021549
0015 O -0.168754 -0.294194 0.163086
0016 O -0.056082 -0.095234 -0.220502
```

Beryllium, Two Waters

```
data_BG_BeMn408_3H20.D1.121.BeTZVPP.wat3.out
```

```
_cell_length_a      4.986101
_cell_length_b      6.020790
_cell_length_c      7.301666
_cell_angle_alpha   63.294526
_cell_angle_beta    95.261128
_cell_angle_gamma   89.954442
_symmetry_space_group_name_H-M   'P 1'
_symmetry_Int_Tables_number     1
```

```
loop_
_symmetry_equiv_pos_as_xyz
'x, y, z'
```

```
loop_
_atom_site_label
_atom_site_type_symbol
_atom_site_fract_x
_atom_site_fract_y
_atom_site_fract_z
MN001 MN -0.121192 0.081245 -0.012851
0002 O 0.213238 0.458372 0.158415
0003 O 0.238835 0.219090 -0.472966
0004 O -0.469103 0.192316 -0.157003
MN005 MN 0.380867 0.322314 0.002707
0006 O -0.286072 0.263466 0.158917
BE007 BE 0.091770 -0.025677 -0.387058
0008 O 0.024849 0.407380 -0.148295
H009 H 0.370777 0.245268 -0.372305
```

```
H010 H 0.242726 0.330621 0.366334
MN011 MN -0.128484 -0.440582 0.005250
0012 O 0.234442 -0.007384 0.141526
0013 O -0.477930 -0.355254 -0.141827
0014 O 0.051970 -0.186588 0.496949
MN015 MN 0.389632 -0.190093 0.009335
0016 O -0.253107 -0.253475 0.136115
0017 O 0.039444 -0.128453 -0.160976
H018 H 0.041408 -0.365411 -0.408903
H019 H 0.137696 -0.141462 0.364930
```

Boron, Two Waters

```
data_BG_BMn408_3H20.D1.TZVP2012.SPLOCK4.wat1.out
```

```
_cell_length_a      5.114560
_cell_length_b      6.122938
_cell_length_c      7.938243
_cell_angle_alpha   61.271545
_cell_angle_beta    107.375204
_cell_angle_gamma   89.090265
_symmetry_space_group_name_H-M   'P 1'
_symmetry_Int_Tables_number     1
```

```
loop_
_symmetry_equiv_pos_as_xyz
'x, y, z'
```

```
loop_
_atom_site_label
_atom_site_type_symbol
_atom_site_fract_x
_atom_site_fract_y
_atom_site_fract_z
MN001 MN -0.153241 0.048905 0.006298
0002 O 0.251050 0.463846 0.122757
0003 O 0.448985 0.112327 -0.130418
MN004 MN 0.343478 0.283126 -0.003478
0005 O -0.268017 0.193616 0.141543
B006 B -0.092800 0.082003 -0.380772
0007 O -0.036033 0.410889 -0.169074
MN008 MN -0.141030 -0.457975 -0.026097
0009 O 0.237270 -0.017865 0.148137
0010 O 0.448518 -0.381101 -0.173586
0011 O -0.057685 -0.046748 -0.472468
MN012 MN 0.357406 -0.213324 0.010719
0013 O -0.237532 -0.342003 0.144653
0014 O -0.051687 -0.064489 -0.170680
0015 O -0.156270 0.341301 -0.478349
H016 H -0.130728 0.406178 -0.381615
H017 H -0.183776 -0.470540 0.296628
H018 H 0.328865 -0.279579 -0.317379
H019 H -0.128368 0.050988 0.372989
```

Boron, No Waters

```
data_BG_BMn408_3H20.D1.TZVP2012.SPLOCK4.wat1wat2wat3.03.out
```

```
_cell_length_a      5.201320
_cell_length_b      5.916770
_cell_length_c      6.629820
_cell_angle_alpha   47.207819
_cell_angle_beta    107.205597
_cell_angle_gamma   90.418930
_symmetry_space_group_name_H-M   'P 1'
_symmetry_Int_Tables_number     1
```

```
loop_
_symmetry_equiv_pos_as_xyz
'x, y, z'
```

```

loop_
_atom_site_label
_atom_site_type_symbol
_atom_site_fract_x
_atom_site_fract_y
_atom_site_fract_z
MN001 MN -0.140123 -0.003354 0.068013
0002 O 0.208926 0.423552 0.161772
0003 O 0.461530 0.154563 -0.155362
MN004 MN 0.323585 0.291996 -0.005861
0005 O -0.232854 0.128432 0.297691
B006 B -0.169940 0.231788 0.430579
0007 O -0.124198 0.418924 -0.210258
MN008 MN -0.193325 -0.400527 -0.086762
0009 O 0.252235 -0.140911 0.218269
0010 O 0.408583 -0.284156 -0.227119
MN011 MN 0.337782 -0.211347 -0.002192
0012 O -0.249882 -0.429250 0.240833
0013 O -0.051552 0.017820 -0.263349

Boron, One Water

data_BG_BMn408_3H2O.D1.TZVP2012.SPLOCK4.wat1wat3.out

_cell_length_a 5.178435
_cell_length_b 6.072205
_cell_length_c 8.541449
_cell_angle_alpha 64.334940
_cell_angle_beta 111.963405
_cell_angle_gamma 91.538979
_symmetry_space_group_name_H-M 'P 1'
_symmetry_Int_Tables_number 1

loop_
_symmetry_equiv_pos_as_xyz
'x, y, z'

loop_
_atom_site_label
_atom_site_type_symbol
_atom_site_fract_x
_atom_site_fract_y
_atom_site_fract_z
MN001 MN -0.168449 0.057521 -0.001005
0002 O 0.255200 0.483634 0.120244
0003 O 0.422069 0.127854 -0.118115
MN004 MN 0.323170 0.290413 0.006627
0005 O -0.281579 0.217741 0.152344
B006 B -0.063166 -0.032314 -0.356596
0007 O -0.073966 0.378909 -0.130878
MN008 MN -0.151051 -0.456585 -0.004088
0009 O 0.229105 -0.015301 0.133561
0010 O 0.425174 -0.397351 -0.153779
0011 O -0.032122 -0.005572 0.499827
MN012 MN 0.367826 -0.198386 0.020794
0013 O -0.231796 -0.279023 0.109676
0014 O -0.071557 -0.083824 -0.196009
H015 H 0.343935 -0.346273 -0.289176
H016 H -0.165895 0.121178 0.301947

Calcium, Two Waters

data_BG_CaMn408_3H2O.D1.121.wat2.out

_cell_length_a 4.947940
_cell_length_b 6.008190
_cell_length_c 7.634195
_cell_angle_alpha 66.347660
_cell_angle_beta 109.550465
_cell_angle_gamma 90.232683
_symmetry_space_group_name_H-M 'P 1'
_symmetry_Int_Tables_number 1

loop_
_symmetry_equiv_pos_as_xyz
'x, y, z'

loop_
_atom_site_label
_atom_site_type_symbol
_atom_site_fract_x
_atom_site_fract_y
_atom_site_fract_z
MN001 MN -0.131944 0.087857 -0.000915
0002 O 0.258606 0.466519 0.163242
0003 O 0.301586 0.109967 -0.487703
0004 O 0.468673 0.191428 -0.153090
MN005 MN 0.363402 0.336302 -0.001483
0006 O -0.241017 0.270680 0.163250
CA007 CA -0.215337 0.017753 0.496836
0008 O -0.045473 0.419797 -0.147095
H009 H 0.357954 0.167712 -0.376627
H010 H 0.262442 0.260691 0.381227
MN011 MN -0.134704 -0.424613 0.008483
0012 O 0.282969 0.014419 0.143985
0013 O 0.456558 -0.349519 -0.139728
MN014 MN 0.369352 -0.174472 0.005231
0015 O -0.217583 -0.247055 0.150451
0016 O -0.038699 -0.124808 -0.149672
0017 O -0.209961 0.402301 -0.499607
H018 H -0.138093 0.430147 -0.374126
H019 H -0.187912 -0.463601 0.380596

Calcium, One Water

data_BG_CaMn408_3H2O.D1.121.wat1wat2wat3.01.out

_cell_length_a 4.964932
_cell_length_b 6.010349
_cell_length_c 8.733897
_cell_angle_alpha 55.483839
_cell_angle_beta 122.797463
_cell_angle_gamma 93.551203
_symmetry_space_group_name_H-M 'P 1'

```

data_BG_CaMn408_3H20.D1.121.wat2wat3.out

_cell_length_a 4.926011
 _cell_length_b 6.000941
 _cell_length_c 7.436930
 _cell_angle_alpha 65.718841
 _cell_angle_beta 110.903426
 _cell_angle_gamma 90.051271
 _symmetry_space_group_name_H-M 'P 1'
 _symmetry_Int_Tables_number 1

loop_
 _symmetry_equiv_pos_as_xyz
 'x, y, z'

loop_
 _atom_site_label
 _atom_site_type_symbol
 _atom_site_fract_x
 _atom_site_fract_y
 _atom_site_fract_z

MN001	MN	-0.142046	0.101725	-0.010454
0002	O	0.262889	0.471251	0.172306
0003	O	0.335632	0.087794	-0.486130
0004	O	0.451037	0.206659	-0.163162
MN005	MN	0.356979	0.343508	-0.000504
0006	O	-0.238440	0.271905	0.174091
CA007	CA	-0.154959	-0.070340	-0.494703
0008	O	-0.060548	0.436851	-0.156484
H009	H	0.384016	0.144773	-0.372298
H010	H	0.289284	0.244374	0.378108
MN011	MN	-0.137985	-0.418180	0.013570
0012	O	0.281638	0.019584	0.148893
0013	O	0.443474	-0.340754	-0.143117
MN014	MN	0.367695	-0.168592	0.010331
0015	O	-0.215217	-0.235831	0.157090
0016	O	-0.047511	-0.114835	-0.154844

Gallium, No Waters

data_BG_GaMn408_3H20.D1.TZVP2012.121.wat1wat2wat3.out

_cell_length_a 5.247096
 _cell_length_b 5.928687
 _cell_length_c 7.873961
 _cell_angle_alpha 45.125003
 _cell_angle_beta 114.456233
 _cell_angle_gamma 93.670809
 _symmetry_space_group_name_H-M 'P 1'
 _symmetry_Int_Tables_number 1

loop_
 _symmetry_equiv_pos_as_xyz
 'x, y, z'

loop_
 _atom_site_label
 _atom_site_type_symbol
 _atom_site_fract_x
 _atom_site_fract_y
 _atom_site_fract_z

MN001	MN	-0.173398	0.042970	0.018352
0002	O	0.292044	0.345631	0.222820
0003	O	0.395368	0.189364	-0.146308
MN004	MN	0.307018	0.294774	0.017411
0005	O	-0.256316	0.164744	0.203589
GA006	GA	-0.040101	0.120386	0.490030
0007	O	-0.117444	0.474400	-0.198176
MN008	MN	-0.232416	-0.381166	-0.078225
0009	O	0.250467	-0.125421	0.216076

Gallium, Two Waters

data_BG_GaMn408_3H20.D1.TZVP2012.121.wat2.out

_cell_length_a 5.091150
 _cell_length_b 6.141668
 _cell_length_c 7.234827
 _cell_angle_alpha 64.743928
 _cell_angle_beta 106.883211
 _cell_angle_gamma 89.210660
 _symmetry_space_group_name_H-M 'P 1'
 _symmetry_Int_Tables_number 1

loop_
 _symmetry_equiv_pos_as_xyz
 'x, y, z'

loop_
 _atom_site_label
 _atom_site_type_symbol
 _atom_site_fract_x
 _atom_site_fract_y
 _atom_site_fract_z

MN001	MN	-0.145559	0.048791	0.015918
0002	O	0.215408	0.455032	0.154787
0003	O	0.419880	0.145366	-0.480829
0004	O	0.470918	0.167101	-0.143058
MN005	MN	0.342630	0.287335	0.017156
0006	O	-0.282439	0.182417	0.219213
GA007	GA	-0.214201	0.113539	-0.494181
0008	O	-0.048906	0.365900	-0.140452
H009	H	0.417201	0.186375	-0.357551
H010	H	0.303456	0.290409	0.368686
MN011	MN	-0.165433	-0.444117	-0.015177
0012	O	0.244075	-0.034991	0.143011
0013	O	0.442150	-0.399724	-0.138588
MN014	MN	0.344077	-0.197205	-0.017859
0015	O	-0.254585	-0.268135	0.131480
0016	O	-0.039062	-0.106044	-0.210687
0017	O	-0.076493	0.401179	-0.499228
H018	H	-0.070867	0.419753	-0.365066
H019	H	-0.149876	-0.442540	0.355332

Gallium, One Water

data_BG_GaMn408_3H20.D1.TZVP2012.121.wat2wat3.out

_cell_length_a 5.107603
 _cell_length_b 6.083729
 _cell_length_c 7.010553
 _cell_angle_alpha 68.360211
 _cell_angle_beta 109.716801
 _cell_angle_gamma 89.442485
 _symmetry_space_group_name_H-M 'P 1'
 _symmetry_Int_Tables_number 1

loop_
 _symmetry_equiv_pos_as_xyz
 'x, y, z'

loop_
 _atom_site_label
 _atom_site_type_symbol
 _atom_site_fract_x
 _atom_site_fract_y
 _atom_site_fract_z

MN001 MN -0.143065 0.053368 0.018074
 0002 O 0.225430 0.474271 0.155848
 0003 O 0.405314 0.153052 -0.491408
 0004 O 0.460248 0.162413 -0.147007
 MN005 MN 0.328793 0.302861 0.005130
 0006 O -0.273926 0.205349 0.222767
 GA007 GA -0.249741 0.060990 -0.495562
 0008 O -0.063385 0.361428 -0.144488
 H009 H 0.414909 0.183022 -0.347040
 H010 H 0.305253 0.307994 0.360832
 MN011 MN -0.165936 -0.444069 -0.005662
 0012 O 0.256175 -0.015249 0.147815
 0013 O 0.435099 -0.397982 -0.143146
 MN014 MN 0.354034 -0.194483 -0.009840
 0015 O -0.242829 -0.254446 0.139973
 0016 O -0.045718 -0.108698 -0.212165

Potassium, One Water

data_BG_KMn408_3H2O.D1.121.SPLOCK4.wat1wat2.out

_cell_length_a 5.071100
 _cell_length_b 5.696079
 _cell_length_c 7.634285
 _cell_angle_alpha 66.672463
 _cell_angle_beta 102.147255
 _cell_angle_gamma 90.211663
 _symmetry_space_group_name_H-M 'P 1'
 _symmetry_Int_Tables_number 1

loop_
 _symmetry_equiv_pos_as_xyz
 'x, y, z'

loop_
 _atom_site_label
 _atom_site_type_symbol
 _atom_site_fract_x
 _atom_site_fract_y
 _atom_site_fract_z

MN001 MN -0.093417 0.028089 0.003315
 0002 O 0.277806 0.451330 0.139295
 0003 O -0.464617 0.104637 -0.134241
 MN004 MN 0.405134 0.283884 -0.002323
 0005 O -0.221788 0.206471 0.144034
 K006 K -0.436885 0.037443 -0.494992
 0007 O 0.028242 0.356971 -0.139358
 MN008 MN -0.093475 -0.466080 0.003431
 0009 O 0.277552 -0.033234 0.138919
 0010 O -0.464450 -0.396678 -0.133821
 MN011 MN 0.407327 -0.220704 0.007130
 0012 O -0.173086 -0.299351 0.154638
 0013 O -0.011339 -0.137936 -0.149010
 0014 O -0.307333 -0.459407 -0.499984
 H015 H -0.165122 0.478444 -0.379716
 H016 H -0.219336 -0.406252 0.389461

Potassium, Two Waters

data_BG_KMn408_3H2O.D1.121.SPLOCK4.wat1.out

_cell_length_a 4.980844
 _cell_length_b 5.814521
 _cell_length_c 7.770756
 _cell_angle_alpha 66.976792
 _cell_angle_beta 101.810147
 _cell_angle_gamma 88.474047
 _symmetry_space_group_name_H-M 'P 1'
 _symmetry_Int_Tables_number 1

loop_
 _symmetry_equiv_pos_as_xyz
 'x, y, z'

loop_
 _atom_site_label
 _atom_site_type_symbol
 _atom_site_fract_x
 _atom_site_fract_y
 _atom_site_fract_z

MN001 MN -0.098570 0.021582 0.007403
 0002 O 0.244513 0.373466 0.167149
 0003 O -0.438529 0.161736 -0.150311
 MN004 MN 0.399061 0.270583 0.005205
 0005 O -0.241673 0.157383 0.158261
 K006 K -0.342860 0.132966 -0.490285
 0007 O 0.040748 0.380932 -0.140640
 MN008 MN -0.097702 -0.486333 0.013232
 0009 O 0.264094 -0.084817 0.150825
 0010 O -0.458907 -0.373109 -0.134911
 MN011 MN 0.401368 -0.230490 0.009288
 0012 O -0.226739 -0.340073 0.159188
 0013 O 0.028674 -0.125047 -0.139479

Lithium, Two Waters

data_BG_LiMn408_3H2O.D1.121.LiTZVPP.Wat1.out

_cell_length_a 4.985114
 _cell_length_b 5.829611

```

_cell_length_c          7.483441      MN011  MN   0.344810  -0.194900  0.030929
_cell_angle_alpha       66.143424      0012   0   -0.271000  -0.310405  0.205696
_cell_angle_beta        101.688193     0013   0   -0.034721  -0.043812  -0.194082
_cell_angle_gamma       88.709172
_symmetry_space_group_name_H-M   'P 1'
_symmetry_Int_Tables_number      1

Lithium, One Water
data_BG_LiMn408_3H2O.D1.121.LiTZVPP.Wat2Wat3.out

loop_
_symmetry_equiv_pos_as_xyz
'x, y, z'

loop_
_atom_site_label
_atom_site_type_symbol
_atom_site_fract_x
_atom_site_fract_y
_atom_site_fract_z
MN001  MN  -0.149757  0.061824  -0.003140
0002  O   0.214905  0.451468  0.156290
0003  O   0.492651  0.164724  -0.147600
MN004  MN  0.357265  0.303667  0.007751
0005  O   -0.262993  0.227717  0.152290
LI006  LI  -0.114833  0.075313  -0.496511
0007  O   -0.020722  0.381942  -0.138541
MN008  MN  -0.140458  -0.446738  0.006206
0009  O   0.234677  -0.016471  0.140577
0010  O   0.474064  -0.376605  -0.133831
0011  O   0.120537  -0.189829  -0.494629
MN012  MN  0.352799  -0.192476  -0.000148
0013  O   -0.256009  -0.259104  0.140537
0014  O   -0.038050  -0.121166  -0.146077
0015  O   -0.228110  0.387736  -0.499907
HO16   H   -0.137799  0.424006  -0.387721
HO17   H   -0.216115  -0.465001  0.379118
HO18   H   0.271898  -0.271260  -0.375867
HO19   H   0.194175  -0.146349  0.385562

Lithium, No Waters
data_BG_LiMn408_3H2O.D1.121.LiTZVPP.Wat1Wat2Wat3.01.out

loop_
_cell_length_a          4.961301      MN001  MN  -0.130186  0.075969  0.002565
_cell_length_b          5.876166      0002   O   0.238157  0.475431  0.160923
_cell_length_c          6.337289     0003   O   0.273635  0.113331  -0.484380
_cell_angle_alpha        48.460762     0004   O   -0.499263  0.176221  -0.149455
_cell_angle_beta         98.240907     MN005  MN  0.366506  0.323955  0.004620
_cell_angle_gamma        88.767671     0006   O   -0.243995  0.245027  0.161944
loop_
_atom_site_label
_atom_site_type_symbol
_atom_site_fract_x
_atom_site_fract_y
_atom_site_fract_z
MN011  MN  -0.133603  -0.428289  0.008675
0012  O   0.254153  0.006061  0.146815
0013  O   0.483806  -0.359664  -0.133127
MN014  MN  0.371461  -0.179344  0.009924
0015  O   -0.227677  -0.243453  0.155657
0016  O   -0.035350  -0.106552  -0.149447

Magnesium, No Waters
data_BG_MgMn408_3H2O.D1.121.MgTZVPP.01.Wat1Wat2Wat3.out

loop_
_cell_length_a          4.935649      MN001  MN  -0.163355  0.113789  -0.052844
_cell_length_b          6.041566      0002   O   0.205522  0.365556  0.236311
_cell_length_c          6.524992      0003   O   0.463511  0.259474  -0.213167
_cell_angle_alpha        48.805515
_cell_angle_beta         99.983867
_cell_angle_gamma        89.918836
_symmetry_space_group_name_H-M   'P 1'
_symmetry_Int_Tables_number      1

loop_
_atom_site_label
_atom_site_type_symbol
_atom_site_fract_x
_atom_site_fract_y
_atom_site_fract_z
MN001  MN  -0.167093  0.088122  -0.012936
0002  O   0.193359  0.377613  0.231895
0003  O   0.478286  0.259194  -0.214988
MN004  MN  0.339382  0.322008  0.005069
0005  O   -0.281146  0.173565  0.208445
LI006  LI  0.080701  -0.054780  -0.483877
0007  O   -0.031529  0.486345  -0.208091
MN008  MN  -0.159427  -0.430197  0.010089
0009  O   0.210865  -0.059159  0.203721
0010  O   0.458078  -0.289310  -0.184570

```

0005 O -0.276544 0.189938 0.216411
MG006 MG 0.091068 -0.053603 -0.497968
0007 O -0.025402 0.497439 -0.211957
MN008 MN -0.152697 -0.432668 0.010695
0009 O 0.214449 -0.047823 0.192430
0010 O 0.459381 -0.294849 -0.186720
MN011 MN 0.358984 -0.207433 0.039771
0012 O -0.258976 -0.307645 0.190156
0013 O -0.006364 -0.073353 -0.198879

Magnesium, Two Waters

data_BG_MgMn408_3H2O.D1.121.MgTZVPP.Wat1.out

_cell_length_a 4.986334
_cell_length_b 6.062532
_cell_length_c 7.433469
_cell_angle_alpha 61.270884
_cell_angle_beta 102.781954
_cell_angle_gamma 90.712939
_symmetry_space_group_name_H-M 'P 1'
_symmetry_IntTables_number 1

loop_
_symmetry_equiv_pos_as_xyz
'x, y, z'

loop_
_atom_site_label
_atom_site_type_symbol
_atom_site_fract_x
_atom_site_fract_y
_atom_site_fract_z
MN001 MN -0.161973 0.064036 -0.009811
0002 O 0.204686 0.428533 0.171089
0003 O 0.468346 0.184787 -0.150561
MN004 MN 0.346596 0.296175 0.016306
0005 O -0.283807 0.229802 0.183413
MG006 MG -0.097082 0.078220 0.499626
0007 O -0.033476 0.394161 -0.140065
MN008 MN -0.149649 -0.453882 0.005627
0009 O 0.225901 -0.034076 0.140821
0010 O 0.463214 -0.375906 -0.139763
0011 O 0.139379 -0.171603 0.498457
MN012 MN 0.343334 -0.196399 -0.009058
0013 O -0.271186 -0.271907 0.132514
0014 O -0.032332 -0.135774 -0.173034
0015 O -0.155509 0.384406 -0.492046
HO16 H -0.094198 0.424764 -0.377122
HO17 H -0.198947 -0.457322 0.367566
HO18 H 0.284660 -0.273446 -0.368144
HO19 H 0.200353 -0.138935 0.369209

Magnesium, One Water

data_BG_MgMn408_3H2O.D1.121.MgTZVPP.Wat2Wat3.out

_cell_length_a 4.990204
_cell_length_b 6.023620
_cell_length_c 7.481256
_cell_angle_alpha 60.768997
_cell_angle_beta 108.146991
_cell_angle_gamma 90.095680
_symmetry_space_group_name_H-M 'P 1'
_symmetry_IntTables_number 1

loop_
_symmetry_equiv_pos_as_xyz
'x, y, z'

loop_

_atom_site_label
_atom_site_type_symbol
_atom_site_fract_x
_atom_site_fract_y
_atom_site_fract_z
MN001 MN -0.128885 0.076360 -0.005328
0002 O 0.254916 0.450539 0.162043
0003 O 0.287222 0.142709 -0.471340
0004 O 0.476029 0.205685 -0.156115
MN005 MN 0.364675 0.316869 0.005831
0006 O -0.236945 0.232489 0.189127
MG007 MG -0.071977 0.018627 -0.486106
0008 O -0.038297 0.418838 -0.153321
HO09 H 0.359490 0.205618 -0.365930
HO10 H 0.283700 0.280877 0.377196
MN011 MN -0.137927 -0.433655 0.000754
0012 O 0.276702 -0.021333 0.147903
0013 O 0.460703 -0.351174 -0.145771
MN014 MN 0.374950 -0.187734 0.003119
0015 O -0.215977 -0.269578 0.145689
0016 O -0.039525 -0.113103 -0.180452

Sodium, No Waters

data_NaMn408_3H2O.D1.121.W1W2W3.SPLOCK4.out

_cell_length_a 5.061495
_cell_length_b 5.701401
_cell_length_c 6.376581
_cell_angle_alpha 63.500820
_cell_angle_beta 75.056146
_cell_angle_gamma 89.800934
_symmetry_space_group_name_H-M 'P 1'
_symmetry_IntTables_number 1

loop_
_symmetry_equiv_pos_as_xyz
'x, y, z'

loop_
_atom_site_label
_atom_site_type_symbol
_atom_site_fract_x
_atom_site_fract_y
_atom_site_fract_z
MN001 MN -0.122084 0.046520 0.007775
0002 O 0.147358 0.453632 0.182743
0003 O -0.398275 0.131955 -0.159488
MN004 MN 0.375274 0.301819 0.004115
0005 O -0.346488 0.213126 0.182929
NA006 NA -0.157870 0.051083 -0.486671
0007 O 0.104473 0.387561 -0.168560
MN008 MN -0.121865 -0.445910 0.006932
0009 O 0.148383 -0.028288 0.182821
0010 O -0.399389 -0.364496 -0.159177
MN011 MN 0.374067 -0.209545 0.026896
0012 O -0.308235 -0.295037 0.199192
0013 O 0.071328 -0.106396 -0.180448

Sodium, Two Waters

data_NaMn408_3H2O.D1.121.Wat1.SPLOCK4.out

_cell_length_a 5.039140
_cell_length_b 5.698885
_cell_length_c 7.621510
_cell_angle_alpha 66.214739
_cell_angle_beta 101.296326
_cell_angle_gamma 90.015742
_symmetry_space_group_name_H-M 'P 1'
_symmetry_IntTables_number 1

```

loop_
_symmetry_equiv_pos_as_xyz
'x, y, z'

loop_
_atom_site_label
_atom_site_type_symbol
_atom_site_fract_x
_atom_site_fract_y
_atom_site_fract_z
MNO01 MN -0.121647 0.018896 0.005101
0002 O 0.252463 0.444696 0.140957
0003 O -0.488126 0.097228 -0.131702
MNO04 MN 0.381115 0.272327 0.003412
0005 O -0.248897 0.194688 0.149089
NA006 NA -0.293585 0.057791 -0.492627
0007 O 0.006596 0.349036 -0.136022
MNO08 MN -0.116947 -0.476229 0.006800
0009 O 0.248783 -0.046609 0.142125
0010 O -0.486614 -0.409148 -0.133548
0011 O 0.207653 -0.084363 -0.495317
MNO12 MN 0.379700 -0.228025 0.003823
0013 O -0.203302 -0.309258 0.156459
0014 O -0.037371 -0.145576 -0.147474
0015 O -0.320692 0.494069 -0.493507
H016 H -0.179997 0.459748 -0.375916
H017 H -0.238244 -0.425147 0.392398
H018 H 0.297810 -0.240749 -0.386066
H019 H 0.217975 -0.105682 0.385117

Sodium, One Water
data_NaMn408_3H2O.D1.121.Wat2Wat3.SPLOCK4.out

_cell_length_a 4.948427
_cell_length_b 5.809437
_cell_length_c 7.364729
_cell_angle_alpha 69.503932
_cell_angle_beta 108.663971
_cell_angle_gamma 88.838393
_symmetry_space_group_name_H-M 'P 1'
_symmetry_IntTables_number 1

loop_
_symmetry_equiv_pos_as_xyz
'x, y, z'

loop_
_atom_site_label
_atom_site_type_symbol
_atom_site_fract_x
_atom_site_fract_y
_atom_site_fract_z
MNO01 MN -0.128231 0.087813 0.001148
0002 O 0.265089 0.481272 0.167311
0003 O 0.331077 0.068705 -0.489469
0004 O 0.483544 0.181212 -0.152875
MNO05 MN 0.370453 0.335740 0.002672
0006 O -0.222942 0.261508 0.156881
NA007 NA -0.175849 -0.075393 0.493734
0008 O -0.034674 0.407492 -0.144623
H009 H 0.387209 0.125155 -0.373530
H010 H 0.286864 0.220811 0.386906
MNO11 MN -0.124771 -0.420869 0.013933
0012 O 0.280462 0.023564 0.146993
0013 O 0.469779 -0.354725 -0.131690
MNO14 MN 0.376608 -0.169925 0.012045
0015 O -0.206730 -0.224233 0.158731
0016 O -0.042255 -0.108585 -0.140521

Strontium, Two Waters
data_SrMn408_3H2O.D1.121.Zn.wat2.out

_cell_length_a 4.980297
_cell_length_b 5.993698
_cell_length_c 7.761403
_cell_angle_alpha 65.666133
_cell_angle_beta 112.316245
_cell_angle_gamma 90.401143
_symmetry_space_group_name_H-M 'P 1'
_symmetry_IntTables_number 1

loop_
_symmetry_equiv_pos_as_xyz
'x, y, z'

loop_
_atom_site_label
_atom_site_type_symbol
_atom_site_fract_x
_atom_site_fract_y
_atom_site_fract_z
MNO01 MN -0.163571 0.108546 -0.002638
0002 O 0.245881 0.478557 0.156424
0003 O 0.335166 0.099028 -0.493027
0004 O 0.436280 0.211915 -0.162046
MNO05 MN 0.332461 0.354570 -0.008371
0006 O -0.244128 0.267771 0.145736
SR007 SR -0.160834 -0.045603 -0.492265
0008 O -0.071981 0.419364 -0.169535
H009 H 0.383677 0.154389 -0.383368
H010 H 0.291185 0.253627 0.375242
MNO11 MN -0.163137 -0.404442 0.008822
0012 O 0.265386 0.034780 0.150155
0013 O 0.412190 -0.319959 -0.134959

```

MN1014 MN1 0.347499 -0.154082 0.022303	0002 0 0.322015 0.417449 0.193970	
01015 01 -0.235960 -0.193642 0.170203	0003 0 0.395174 0.214760 -0.186742	
0016 0 -0.077773 -0.076522 -0.134201	MN1004 MN1 0.328366 0.345011 -0.027572	
0017 0 -0.178391 0.373702 0.492037	01005 01 -0.205017 0.187602 0.186170	
H018 H -0.125107 0.387364 -0.376660	Y006 Y -0.212554 -0.030444 -0.491046	
H019 H -0.162214 -0.473546 0.385462	0007 0 -0.110295 -0.496414 -0.202102	
Strontium, One Water		
data_SrMn408_3H20.D1.121.Zn.wat2wat3.out		
_cell_length_a 4.940091	MN1008 MN1 -0.133932 -0.440597 0.026824	
_cell_length_b 6.001745	0009 0 0.305938 0.000208 0.165624	
_cell_length_c 7.495073	0010 0 0.385844 -0.320740 -0.169063	
_cell_angle_alpha 67.183599	MN011 MN 0.378239 -0.194077 0.033300	
_cell_angle_beta 111.202686	0012 0 -0.184486 -0.314575 0.197030	
_cell_angle_gamma 87.761514	0013 0 -0.087143 -0.043825 -0.173826	
_symmetry_space_group_name_H-M 'P 1'	Yttrium, Two Waters	
_symmetry_Int_Tables_number 1	data_YMn408_3H20.D1.121.SPLOCK4.wat2.out	
loop_	_cell_length_a 5.005096	
_symmetry_equiv_pos_as_xyz	_cell_length_b 6.092140	
'x, y, z'	_cell_length_c 7.435863	
loop_	_cell_angle_alpha 66.605406	
_atom_site_label	_cell_angle_beta 111.677182	
_atom_site_type_symbol	_cell_angle_gamma 85.681510	
_atom_site_fract_x	_symmetry_space_group_name_H-M 'P 1'	
_atom_site_fract_y	_symmetry_Int_Tables_number 1	
_atom_site_fract_z	loop_	
MN001 MN -0.152611 0.105362 -0.009731	_atom_site_label	
0002 0 0.265338 0.479848 0.167772	_atom_site_type_symbol	
0003 0 0.333934 0.093518 -0.489901	_atom_site_fract_x	
0004 0 0.443558 0.210119 -0.169051	_atom_site_fract_y	
MN005 MN 0.347460 0.343791 -0.001026	_atom_site_fract_z	
0006 0 -0.240303 0.234732 0.163140	MN001 MN -0.154494 0.096024 0.003914	
SR007 SR -0.148758 -0.095155 -0.488891	0002 0 0.251612 0.472637 0.165780	
0008 0 -0.071159 0.427952 -0.156708	0003 0 0.353897 0.091338 -0.486533	
H009 H 0.382349 0.148772 -0.375363	0004 0 0.434066 0.206467 -0.168569	
H010 H 0.288251 0.246568 0.377396	MN005 MN 0.332787 0.353459 -0.012745	
MN011 MN -0.147103 -0.413061 0.012703	0006 0 -0.245405 0.229444 0.173553	
0012 0 0.275323 0.027621 0.150305	Y007 Y -0.128924 -0.024762 -0.475970	
0013 0 0.425132 -0.340333 -0.139338	0008 0 -0.077267 0.492223 -0.195763	
MN1014 MN1 0.356770 -0.154909 0.008679	H009 H 0.393826 0.149478 -0.372229	
01015 01 -0.217595 -0.210805 0.151506	H010 H 0.292368 0.250983 0.372345	
0016 0 -0.057931 -0.051104 -0.161309	MN011 MN -0.162932 -0.406118 -0.000817	
Yttrium, No Waters		
data_YMn408_3H20.D1.121.SPLOCK4.wat1wat2wat3.out		
_cell_length_a 5.041877	0012 0 0.275743 0.036992 0.150442	
_cell_length_b 6.067932	0013 0 0.405219 -0.329717 -0.148365	
_cell_length_c 7.561145	MN1014 MN1 0.357237 -0.167391 0.025631	
_cell_angle_alpha 61.754321	01015 01 -0.225253 -0.264870 0.179527	
_cell_angle_beta 116.905398	0016 0 -0.062110 -0.057625 -0.154281	
_cell_angle_gamma 86.068010	0017 0 -0.170676 0.350168 -0.497434	
_symmetry_space_group_name_H-M 'P 1'	H018 H -0.138347 0.388667 -0.374587	
_symmetry_Int_Tables_number 1	H019 H -0.178894 -0.498627 0.375391	
loop_	Yttrium, One Water	
_symmetry_equiv_pos_as_xyz	data_YMn408_3H20.D1.121.SPLOCK4.wat2wat3.out	
'x, y, z'	_cell_length_a 4.976492	
loop_	_cell_length_b 6.131955	
_atom_site_label	_cell_length_c 7.088481	
_atom_site_type_symbol	_cell_angle_alpha 66.337609	
_atom_site_fract_x	_cell_angle_beta 110.432506	
_atom_site_fract_y	_cell_angle_gamma 85.641317	
_atom_site_fract_z	_symmetry_space_group_name_H-M 'P 1'	
MN001 MN -0.160322 0.087705 -0.007668	_symmetry_Int_Tables_number 1	
loop_		
_symmetry_equiv_pos_as_xyz		
'x, y, z'		

```

loop_
_atom_site_label
_atom_site_type_symbol
_atom_site_fract_x
_atom_site_fract_y
_atom_site_fract_z
MN001 MN -0.156523 0.108221 -0.014557
0002 O 0.263067 0.471282 0.179338
0003 O 0.365629 0.075286 -0.484557
0004 O 0.436534 0.214308 -0.181346
MN005 MN 0.336342 0.352350 -0.012993
0006 O -0.245181 0.220292 0.183724
Y007 Y -0.178803 -0.082802 -0.488815
0008 O -0.072136 0.483970 -0.188587
H009 H 0.395212 0.130090 -0.363854
H010 H 0.299808 0.241864 0.374717
MN011 MN -0.149798 -0.421021 0.024869
0012 O 0.269876 0.034273 0.148435
0013 O 0.423603 -0.341676 -0.145289
MN1014 MN1 0.359726 -0.167848 0.019962
01015 O1 -0.229864 -0.259295 0.187329
0016 O -0.056853 -0.048851 -0.178203

Zinc, One Water
data_BG_ZnMn408_3H2O.D1.121.wat1wat3.out
_cell_length_a 5.133287
_cell_length_b 5.876953
_cell_length_c 7.574872
_cell_angle_alpha 55.907390
_cell_angle_beta 102.833547
_cell_angle_gamma 92.126286
_symmetry_space_group_name_H-M 'P 1'
_symmetry_Int_Tables_number 1

Zinc, Two Waters
data_BG_ZnMn408_3H2O.D1.121.wat1.out
_cell_length_a 4.988872
_cell_length_b 6.045569
_cell_length_c 7.402467
_cell_angle_alpha 61.848253
_cell_angle_beta 103.465884
_cell_angle_gamma 90.584389
_symmetry_space_group_name_H-M 'P 1'
_symmetry_Int_Tables_number 1

loop_
_symmetry_equiv_pos_as_xyz
'x, y, z'

loop_
_atom_site_label
_atom_site_type_symbol
_atom_site_fract_x
_atom_site_fract_y
_atom_site_fract_z
MN001 MN -0.153201 0.053899 -0.006651
0002 O 0.221073 0.446729 0.154891
0003 O 0.468946 0.167755 -0.139972
MN004 MN 0.343886 0.300424 0.011228
0005 O -0.289267 0.203716 0.188837
ZN006 ZN -0.126001 0.031514 0.499951
0007 O -0.029514 0.410332 -0.144697
MN008 MN -0.148240 -0.445340 0.002542
0009 O 0.223881 -0.055363 0.148711
0010 O 0.481326 -0.351738 -0.143284
0011 O 0.176376 -0.150320 0.498488
MN012 MN 0.356403 -0.197258 0.005642
0013 O -0.227129 -0.316069 0.159586
0014 O -0.066358 -0.089684 -0.201353
H015 H 0.328777 -0.237887 -0.368134
H016 H 0.211758 -0.146244 0.372868

```

5 Surface Structures

5.1 $M^{n+}Mn_4O_8 \cdot 3H_2O$ Surfaces

Aluminum

```

data_BG_AlMn408_3H20.001.7_21.optgeom.D1.TZVP2012.121.01.out
loop_
_atom_site_label
_atom_site_type_symbol
_atom_site_fract_x
_atom_site_fract_y
_atom_site_fract_z
_cell_length_a      5.135465      H001  H -0.045749 -0.047147  0.004263
_cell_length_b      6.150245      H002  H 0.141133 -0.444092  0.004939
_cell_length_c      500.000000     H003  H 0.471922  0.274921  0.003812
_cell_angle_alpha   90.000000     0004  O 0.014344 -0.477947  0.003541
_cell_angle_beta    90.000000     0005  O -0.150807  0.064408  0.003466
_cell_angle_gamma   94.954469     0006  O 0.331207  0.182389  0.003012
_symmetry_space_group_name_H-M 'P 1'
_symmetry_Int_Tables_number 1
H007  BE 0.050107  0.285233  0.002199
H008  H -0.253068 -0.012875  0.001999
H009  H 0.048333 -0.334492  0.001290
H010  H 0.420019  0.097303  0.001331
0011  O 0.003199  0.288737 -0.000993
0012  O 0.029240 -0.248183 -0.000580
0013  O -0.463814 -0.000050 -0.000698
0014  O -0.496124 -0.470684 -0.001047
MN015 MN -0.166769 -0.464744 -0.002991
MN016 MN 0.340909  0.291236 -0.003198
MN017 MN -0.156355  0.032926 -0.003038
MN018 MN 0.346963 -0.226652 -0.002783
0019  O -0.329007  0.305182 -0.004884
0020  O 0.186956  0.015642 -0.004529
0021  O 0.151893 -0.434739 -0.004825
0022  O -0.323972 -0.224902 -0.004669

```

Boron

```

data_BG_BMn408_3H20.001.7_22.optgeom.D1.TZVP2012.SPLOCK4.out
loop_
_symmetry_equiv_pos_as_xyz
'x, y, z'

_cell_length_a      5.282011
_cell_length_b      5.920940
_cell_length_c      500.000000
_cell_angle_alpha   90.000000
_cell_angle_beta    90.000000
_cell_angle_gamma   92.186783
_symmetry_space_group_name_H-M 'P 1'
_symmetry_Int_Tables_number 1

```

Beryllium

```

data_BG_BeMn408_3H20.D1.121.001.7_22.optgeom.BeTZVPP.out
loop_
_symmetry_equiv_pos_as_xyz
'x, y, z'

_cell_length_a      5.060533      H001  H -0.380402  0.119016  0.006096
_cell_length_b      6.010191      H002  H 0.202711  0.387734  0.005686
_cell_length_c      500.000000     0003  O 0.027300  0.028025  0.004199
_cell_angle_alpha   90.000000     0004  O -0.434735  0.227426  0.004798
_cell_angle_beta    90.000000     0005  O 0.100007  0.425934  0.004160
_cell_angle_gamma   93.474020     B006  B -0.001432  0.231882  0.002986
_symmetry_space_group_name_H-M 'P 1'
_symmetry_Int_Tables_number 1
H007  H -0.000789 -0.102652  0.003008
H008  H 0.496015  0.136220  0.003317
H009  H 0.379335 -0.481685  0.001855
H010  O -0.079653  0.252948  0.000329
H011  O -0.028544 -0.241888 -0.000019
H012  O 0.434382  0.038134 -0.000225
H013  O 0.436331 -0.468485 -0.000013
MN014 MN -0.199018 -0.458598 -0.002001
MN015 MN 0.274664 -0.215144 -0.002081

```

MN016 MN -0.232383 0.016459 -0.001924
 MN017 MN 0.279232 0.273769 -0.002239
 0018 O 0.108662 0.016175 -0.003859
 0019 O -0.404898 -0.211320 -0.003801
 0020 O 0.124804 -0.474471 -0.003877
 0021 O -0.358902 0.307904 -0.004171
 H022 H -0.337798 0.322311 -0.006083

Calcium

data_BG_CaMn408_3H20.D1.121.001.7_20.optgeom.511d21G.FMIX90
 _cell_length_a 4.973278
 _cell_length_b 6.044058
 _cell_length_c 500.000000
 _cell_angle_alpha 90.000000
 _cell_angle_beta 90.000000
 _cell_angle_gamma 90.450419
 _symmetry_space_group_name_H-M 'P 1'
 _symmetry_Int_Tables_number 1

loop_
 _atom_site_label
 _atom_site_type_symbol
 _atom_site_fract_x
 _atom_site_fract_y
 _atom_site_fract_z

H001 H 0.120519 -0.129120 0.004079
 H002 H -0.481143 0.086104 0.004880
 H003 H 0.389461 -0.496387 0.004448
 H004 O -0.027991 -0.049550 0.003472
 H005 O 0.339559 -0.357625 0.003670

GA006 GA -0.102393 0.274380 0.003186
 GA007 O -0.462528 0.198661 0.003510
 H008 H -0.088908 -0.123219 0.001719
 H009 H 0.361243 -0.379857 0.001716
 H010 H 0.434525 0.076765 0.000892
 H011 O -0.077403 0.324384 -0.000470
 H012 O 0.403800 0.041186 -0.001071
 H013 O -0.153845 -0.174621 -0.001105
 H014 O 0.384654 -0.411189 -0.001511

MN015 MN -0.277158 -0.440075 -0.002814
 MN016 MN 0.225572 0.333478 -0.003165
 MN017 MN -0.266434 0.081530 -0.002880
 MN018 MN 0.183251 -0.178570 -0.002895
 MN019 O -0.422761 0.312018 -0.004658
 MN020 O 0.052923 0.081996 -0.004670
 MN021 O 0.024373 -0.406000 -0.004819

KMn₄O₈·3H₂O

data_BG_KMn408_3H20.D1.121.001.8_22.opt.SPLOCK4.SHINK881.out

_cell_length_a 5.001752
 _cell_length_b 5.845886
 _cell_length_c 500.000000
 _cell_angle_alpha 90.000000
 _cell_angle_beta 90.000000
 _cell_angle_gamma 91.768021
 _symmetry_space_group_name_H-M 'P 1'
 _symmetry_Int_Tables_number 1

loop_
 _atom_site_label
 _atom_site_type_symbol
 _atom_site_fract_x
 _atom_site_fract_y
 _atom_site_fract_z

'x, y, z'

loop_
 _atom_site_label
 _atom_site_type_symbol
 _atom_site_fract_x
 _atom_site_fract_y
 _atom_site_fract_z

H001 H 0.118270 -0.315342 0.004129
 H002 H 0.471426 -0.110399 0.004321
 H003 H -0.385383 -0.411068 0.004113
 H004 O -0.068398 -0.273148 0.003866

Gallium

data_BG_GaMn408_3H20.D1.TZVP2012.121.001.7_21.optgeom.out

_cell_length_a 5.254631
 _cell_length_b 6.049414
 _cell_length_c 500.000000
 _cell_angle_alpha 90.000000
 _cell_angle_beta 90.000000
 _cell_angle_gamma 92.279361
 _symmetry_space_group_name_H-M 'P 1'
 _symmetry_Int_Tables_number 1

K007 K -0.019547 0.227072 0.003513
 H008 H 0.452671 0.070282 0.002063
 H009 H -0.084476 -0.228148 0.001970
 H010 H 0.413710 -0.412561 0.001689
 H011 O 0.378115 0.123758 -0.001091
 H012 O -0.139215 -0.104275 -0.001183
 H013 O 0.355283 -0.353519 -0.001362
 H014 O -0.147785 0.404239 -0.001321
 MN015 MN 0.191431 0.398666 -0.003356
 MN016 MN -0.307903 0.146647 -0.003160
 MN017 MN 0.191777 -0.101746 -0.003195
 MN018 MN -0.306079 -0.351124 -0.003293
 MN019 O 0.026974 0.140737 -0.004990

0020 0 -0.460733 0.389329 -0.005068
 0021 0 -0.475742 -0.101374 -0.005044
 0022 0 0.005233 -0.322487 -0.005195

Lithium

data_BG_LiMn408_3H2O.D1.121.001.8_22.optgeom.LiTZVPP.01.out

_cell_length_a 4.977513
 _cell_length_b 5.786088
 _cell_length_c 500.000000
 _cell_angle_alpha 90.000000
 _cell_angle_beta 90.000000
 _cell_angle_gamma 91.375220
 _symmetry_space_group_name_H-M 'P 1'
 _symmetry_Int_Tables_number 1

loop_
 _symmetry_equiv_pos_as_xyz
 'x, y, z'

_atom_site_label
 _atom_site_type_symbol
 _atom_site_fract_x
 _atom_site_fract_y
 _atom_site_fract_z

H001 H 0.227976 -0.009481 0.005233
 H002 H -0.291815 0.012312 0.004306
 H003 H 0.362631 0.404927 0.004060
 0004 O 0.059102 -0.077282 0.004611
 0005 O 0.206297 0.478592 0.003298
 LI006 LI -0.022930 0.197854 0.001828
 0007 O -0.418054 0.127932 0.003701
 H008 H 0.097851 -0.239178 0.004177
 H009 H -0.493598 0.082874 0.001926
 H010 H 0.268417 -0.462844 0.001501
 0011 O 0.360317 0.097299 -0.001135
 0012 O -0.159419 0.370842 -0.001371
 0013 O -0.155613 -0.125099 -0.001253
 0014 O 0.337327 -0.382300 -0.001419
 MN015 MN 0.176528 0.372103 -0.003515

MN016 MN -0.323425 0.118267 -0.003272
 MN017 MN 0.173576 -0.128955 -0.003241
 MN018 MN -0.322552 -0.377172 -0.003294
 0019 O -0.474215 0.365282 -0.005165
 0020 O 0.010931 0.112774 -0.005130
 0021 O -0.492793 -0.131207 -0.005114
 0022 O -0.013444 -0.349354 -0.005254

MgMn₄O₈·3H₂O

data_BG_MgMn408_3H2O.D1.121.001.7_21.optgeom.MgTZVPP.out

_cell_length_a 4.966687
 _cell_length_b 6.057496
 _cell_length_c 500.000000
 _cell_angle_alpha 90.000000
 _cell_angle_beta 90.000000
 _cell_angle_gamma 89.790627
 _symmetry_space_group_name_H-M 'P 1'
 _symmetry_Int_Tables_number 1

loop_
 _symmetry_equiv_pos_as_xyz
 'x, y, z'

_atom_site_label
 _atom_site_type_symbol
 _atom_site_fract_x

H001 H 0.033223 -0.211597 0.004674
 H002 H -0.471122 0.022679 0.004668
 H003 H 0.409298 0.476838 0.004457
 0004 O -0.119851 -0.127123 0.004071
 0005 O 0.297147 -0.404918 0.003752
 H001 H 0.033223 -0.211597 0.004674
 H002 H -0.471122 0.022679 0.004668
 H003 H 0.409298 0.476838 0.004457
 0004 O -0.119851 -0.127123 0.004071
 0005 O 0.297147 -0.404918 0.003752
 NA006 NA -0.028074 0.269854 0.003100
 0007 O 0.467685 0.162079 0.003839
 H008 H -0.124348 -0.154106 0.002118
 H009 H 0.453355 0.122801 0.001878
 H010 H 0.347180 -0.391788 0.001831
 0011 O 0.424282 0.076520 -0.001168
 0012 O -0.102276 0.353999 -0.001339
 0013 O -0.096131 -0.150264 -0.001271
 0014 O 0.399118 -0.400001 -0.001397
 MN015 MN 0.237111 0.350586 -0.003393
 MN016 MN -0.261915 0.098343 -0.003238
 MN017 MN 0.235935 -0.150381 -0.003256
 MN018 MN -0.262355 -0.398812 -0.003315
 0019 O -0.415343 0.342661 -0.005119
 0020 O 0.072440 0.093626 -0.005065
 0021 O -0.431245 -0.150996 -0.005110
 0022 O 0.048980 -0.371813 -0.005239

Scandium

data_BG_ScMn408_3H20.D1.TZVP2012.121.001.7_21.optgeom.out

_cell_length_a 5.144232
 _cell_length_b 6.138463
 _cell_length_c 500.000000
 _cell_angle_alpha 90.000000
 _cell_angle_beta 90.000000
 _cell_angle_gamma 94.937327
 _symmetry_space_group_name_H-M 'P 1'
 _symmetry_Int_Tables_number 1

loop_
 _symmetry_equiv_pos_as_xyz
 'x, y, z'

loop_
 _atom_site_label
 _atom_site_type_symbol
 _atom_site_fract_x
 _atom_site_fract_y
 _atom_site_fract_z

H001 H 0.120104 -0.395497 0.004635
 H002 H -0.495382 -0.085854 0.005456
 H003 H 0.366300 0.255811 0.004690
 0004 O 0.082085 -0.256065 0.003881
 0005 O 0.207059 0.296750 0.003825
 SC006 SC -0.039797 0.028501 0.003075
 0007 O -0.387047 0.028700 0.004588
 H008 H -0.051976 -0.387312 0.001200
 H009 H 0.393970 -0.190972 0.001250
 H010 H 0.324792 0.345057 0.001063
 0011 O -0.087662 0.071206 -0.000869
 0012 O -0.095413 -0.416412 -0.000715
 0013 O 0.398860 -0.168625 -0.000676
 0014 O 0.378106 0.361847 -0.000924
 MN015 MN -0.281535 0.355818 -0.002906
 MN016 MN -0.277272 -0.144018 -0.003102
 MN017 MN 0.218371 0.103917 -0.003182
 MN018 MN 0.220456 -0.395706 -0.002999
 0019 O 0.071933 -0.168173 -0.004678
 0020 O -0.451435 0.116868 -0.004675
 0021 O 0.041795 0.376801 -0.004749
 0022 O -0.467386 -0.375251 -0.004760

Strontium

data_BG_SrMn408_3H20.D1.121.001.8_22.optgeom.out

_cell_length_a 4.971114
 _cell_length_b 6.045490
 _cell_length_c 500.000000
 _cell_angle_alpha 90.000000
 _cell_angle_beta 90.000000
 _cell_angle_gamma 93.461490
 _symmetry_space_group_name_H-M 'P 1'
 _symmetry_Int_Tables_number 1

loop_
 _symmetry_equiv_pos_as_xyz
 'x, y, z'

loop_
 _atom_site_label
 _atom_site_type_symbol
 _atom_site_fract_x
 _atom_site_fract_y
 _atom_site_fract_z

H001 H -0.279156 -0.003657 0.004942

H002 H -0.260825 -0.367624 0.004423
 H003 H 0.300054 -0.244682 0.004186
 0004 O 0.117911 -0.188002 0.003987
 0005 O -0.438970 -0.394360 0.003662

SR006 SR 0.219016 0.254346 0.003555
 0007 O -0.295377 0.144275 0.004255
 H008 H -0.324864 0.087945 0.001306
 H009 H 0.100310 -0.182886 0.001938
 H010 H -0.408348 -0.388544 0.001548
 0011 O -0.356309 0.074534 -0.000731
 0012 O 0.146931 0.321872 -0.000928
 0013 O 0.118718 -0.150341 -0.001046
 0014 O -0.385089 -0.395452 -0.001220

MN015 MN -0.037350 0.094979 -0.002991
 MN016 MN 0.451624 -0.152444 -0.003089
 MN017 MN 0.457634 0.347397 -0.003212
 MN018 MN -0.046211 -0.396581 -0.003197
 0019 O -0.194671 0.331636 -0.004751
 0020 O 0.291209 0.088608 -0.004816
 0021 O 0.280475 -0.372791 -0.005015
 0022 O -0.231377 -0.118991 -0.004949

Yttrium

data_BG_YMn408_3H20.D1.121.001.7_21.optgeom.SPLOCK4.out

_cell_length_a 5.087514
 _cell_length_b 6.199215
 _cell_length_c 500.000000
 _cell_angle_alpha 90.000000
 _cell_angle_beta 90.000000
 _cell_angle_gamma 95.180388
 _symmetry_space_group_name_H-M 'P 1'
 _symmetry_Int_Tables_number 1

loop_
 _symmetry_equiv_pos_as_xyz
 'x, y, z'

loop_
 _atom_site_label
 _atom_site_type_symbol
 _atom_site_fract_x
 _atom_site_fract_y
 _atom_site_fract_z

H001 H 0.099572 -0.445687 0.004580
 H002 H -0.459366 -0.170686 0.005191
 H003 H 0.399448 0.271820 0.004873
 0004 O 0.239333 0.304305 0.003973
 0005 O -0.003495 -0.326142 0.004091
 Y006 Y -0.005129 0.003777 0.003016
 0007 O -0.435915 -0.042462 0.004081
 H008 H -0.075626 -0.401169 0.001330
 H009 H 0.339662 0.362001 0.001060
 H010 H 0.460196 -0.142512 0.001190
 0011 O -0.095848 0.086060 -0.001052
 0012 O -0.103922 -0.407182 -0.000726
 0013 O 0.392695 -0.148471 -0.000699
 0014 O 0.374533 0.376257 -0.000947
 MN015 MN -0.286806 -0.127987 -0.003268
 MN016 MN 0.214635 -0.381750 -0.002956
 MN017 MN -0.287304 0.372127 -0.002987
 MN018 MN 0.209196 0.120599 -0.003374
 0019 O 0.065371 -0.158573 -0.004715
 0020 O -0.458363 0.136160 -0.004829
 0021 O 0.041918 0.393322 -0.004794
 0022 O -0.475466 -0.362373 -0.004815

Zinc

data_BG_ZnMn408_3H20.D1.121.001.6_22.optgeom.511d21G.FMIX90.out

```

H001 H -0.054365 -0.100977 0.003824
H002 H 0.007163 -0.473480 0.005385
H003 H 0.467428 0.356753 0.003294
H004 O -0.040868 -0.494704 0.003538
H005 O -0.141011 0.037184 0.003460
H006 O 0.347420 0.220113 0.003340
BE007 BE 0.047139 0.273570 0.002335
H008 H -0.267944 -0.005011 0.002015
H009 H 0.038617 -0.329490 0.001041
H010 H 0.414480 0.124705 0.001810
H011 O 0.040584 0.262753 -0.000849
H012 O 0.043554 -0.249323 -0.000738
H013 O -0.474396 0.032638 -0.000803
H014 O -0.479277 -0.467660 -0.000965
MN015 MN -0.145951 -0.468316 -0.003118
MN016 MN 0.363531 0.283232 -0.002966
MN017 MN -0.141104 0.037862 -0.003072
MN018 MN 0.369971 -0.224039 -0.002870
H019 O -0.329283 0.297480 -0.004869
H020 O 0.203187 0.015126 -0.004625
H021 O 0.208106 -0.478707 -0.004741
H022 O -0.326421 -0.198238 -0.004806

Calcium
data_BG_CaMn408_3H2O.D1.121.SLAB.511d21G.para.SPIN2.relax.out

H001 H 0.028345 -0.146179 0.004488
H002 H 0.355526 -0.487938 0.004755
H003 H 0.459247 0.070913 0.005095
H004 O 0.211054 -0.412174 0.003816
H005 O -0.106283 -0.045608 0.003745
ZN006 ZN 0.045037 0.256969 0.002807
H007 O 0.414316 0.190018 0.003885
H008 H -0.121166 -0.114039 0.001834
H009 H 0.291152 -0.396778 0.001939
H010 H 0.457636 0.080235 0.001197
H011 O -0.052428 0.343132 -0.000734
H012 O 0.450127 0.041534 -0.000802
H013 O 0.417765 -0.426981 -0.000899
H014 O -0.077218 -0.179006 -0.000936
MN015 MN 0.266667 0.327203 -0.003027
MN016 MN -0.228583 0.066322 -0.003054
MN017 MN -0.243657 -0.425096 -0.002835
MN018 MN 0.256903 -0.187687 -0.002929
H019 O -0.388096 0.324946 -0.004618
H020 O 0.113644 0.067873 -0.004661
H021 O 0.068347 -0.399340 -0.004803
H022 O -0.428708 -0.212768 -0.004795

5.2 Mnn+Mn4O8·3H2O Parallel Oxidative Pattern

Beryllium
data_BG_BeMn408_3H2O.D1.121.SLAB.BeTZVPP.para.relax.out

H001 H 0.050010 -0.323433 0.004763
H002 H 0.400551 0.386320 0.004185
H003 H -0.434840 0.044587 0.004942
H004 O 0.252629 0.489091 0.003791
H005 O -0.089194 -0.209729 0.004644
CA006 CA -0.003996 0.157869 0.002392
H007 O -0.417684 0.173191 0.003700
H008 H -0.191744 -0.269950 0.003194
H009 H 0.462420 0.141299 0.001041
H010 H 0.294283 -0.437717 0.001953
H011 O -0.088792 0.389646 -0.001309
H012 O 0.346088 0.142281 -0.000615
H013 O -0.089825 -0.101487 -0.001273
H014 O 0.362110 -0.357576 -0.000810
MN015 MN 0.239073 0.398888 -0.003084
MN016 MN -0.247741 0.143514 -0.003512
MN017 MN 0.237919 -0.113001 -0.003032
MN018 MN -0.267483 -0.356158 -0.003028
H019 O -0.444668 0.394711 -0.004713
H020 O 0.120058 0.141021 -0.005009
H021 O 0.116414 -0.357367 -0.005030
H022 O -0.445628 -0.108831 -0.004698

Magnesium

```

data_BG_MgMn408_3H20.D1.121.SLAB.MgTZVPP.para.relax.out

_cell_length_a	5.285815	H002	H	-0.279918	-0.493929	0.004630
_cell_length_b	5.725518	H003	H	0.321580	-0.332970	0.004386
_cell_length_c	500.000000	0004	O	0.140936	-0.277903	0.004379
_cell_angle_alpha	90.000000	0005	O	-0.431364	-0.453869	0.003672
_cell_angle_beta	90.000000	SR006	SR	0.245038	0.190532	0.002913
_cell_angle_gamma	89.881711	0007	O	-0.273791	0.052198	0.003744
_symmetry_space_group_name_H-M	'P 1'	H008	H	-0.286652	0.077981	0.001757
_symmetry_Int_Tables_number	1	H009	H	0.094187	-0.274554	0.002478
loop_		H010	H	-0.386981	-0.396254	0.001056
_symmetry_equiv_pos_as_xyz		H011	O	-0.389569	0.157051	-0.001129
'x, y, z'		H012	O	0.083088	0.409306	-0.000704
loop_		H013	O	0.088774	-0.082848	-0.000703
_atom_site_label		H014	O	-0.377058	-0.348742	-0.001033
_atom_site_type_symbol		MN015	MN	-0.052271	0.160450	-0.002982
_atom_site_fract_x		MN016	MN	0.447533	-0.085639	-0.003162
_atom_site_fract_y		MN017	MN	0.449807	0.410828	-0.003278
_atom_site_fract_z		MN018	MN	-0.044056	-0.341210	-0.002888
H001 H 0.271813 -0.315408 0.005333		0019	O	-0.179527	0.409385	-0.004890
H002 H 0.163195 0.213598 0.004878		0020	O	0.258892	0.164491	-0.004800
H003 H -0.148699 -0.116136 0.004254		0021	O	0.266863	-0.336626	-0.004734
0004 O 0.222278 -0.446178 0.004252		0022	O	-0.187426	-0.099731	-0.004825
MG005 MG -0.106528 0.470541 0.002665						
0006 O -0.276550 -0.227793 0.003624						
0007 O 0.040777 0.141885 0.003666						
H008 H 0.291695 -0.370969 0.001553						
H009 H 0.151202 0.124116 0.001881						
H010 H -0.305233 -0.162263 0.001739						
0011 O -0.254604 0.408644 -0.000903						
0012 O 0.273410 -0.346843 -0.000516						
0013 O 0.276765 0.151395 -0.000575						
0014 O -0.266611 -0.096074 -0.001137						
MN015 MN 0.405465 0.401403 -0.002751						
MN016 MN -0.101898 -0.342529 -0.003197						
MN017 MN -0.091704 0.155103 -0.002972						
MN018 MN 0.406024 -0.091430 -0.002813						
0019 O 0.092358 0.404795 -0.004530						
0020 O -0.471649 -0.349711 -0.004737						
0021 O -0.468212 0.157154 -0.004744						
0022 O 0.090592 -0.093798 -0.004580						
Zinc						
data_BG_ZnMn408_3H20.D1.121.511d21G.para.relax.1.out						
_cell_length_a						5.319398
_cell_length_b						5.713121
_cell_length_c						500.000000
_cell_angle_alpha						90.000000
_cell_angle_beta						90.000000
_cell_angle_gamma						90.277227
_symmetry_space_group_name_H-M						'P 1'
_symmetry_Int_Tables_number						1
loop_						
_atom_site_label						
_atom_site_type_symbol						
_atom_site_fract_x						
_atom_site_fract_y						
_atom_site_fract_z						
H001 H -0.010776 -0.185056 0.004273						
H002 H 0.248528 -0.453902 0.005540						
H003 H 0.465568 0.043178 0.004984						
0004 O 0.115408 -0.429722 0.004260						
0005 O -0.115081 -0.049141 0.003545						
ZN006 ZN 0.031805 0.263983 0.002869						
0007 O 0.407381 0.171994 0.003906						
H008 H -0.117036 -0.107968 0.001622						
H009 H 0.325484 -0.410545 0.001234						
H010 H 0.438785 0.118288 0.001935						
0011 O -0.038325 0.315318 -0.001013						
0012 O 0.416700 0.073012 -0.000823						
0013 O 0.406700 -0.423022 -0.000540						
0014 O -0.045694 -0.174014 -0.001225						
MN015 MN 0.285624 0.318986 -0.002968						
MN016 MN -0.218058 0.071877 -0.003117						
MN017 MN -0.208571 -0.426072 -0.003048						
MN018 MN 0.281949 -0.172798 -0.002964						
0019 O -0.395757 0.328365 -0.004590						
0020 O 0.161216 0.075266 -0.004950						
0021 O 0.155498 -0.429593 -0.004845						
0022 O -0.401720 -0.182885 -0.004618						
Sr						
Strontium						
data_BG_SrMn408_3H20.D1.121.SLAB.para.relax.out						
_cell_length_a	5.253048	H001	H	-0.010776	-0.185056	0.004273
_cell_length_b	5.692729	H002	H	0.248528	-0.453902	0.005540
_cell_length_c	500.000000	H003	H	0.465568	0.043178	0.004984
_cell_angle_alpha	90.000000	0004	O	0.115408	-0.429722	0.004260
_cell_angle_beta	90.000000	0005	O	-0.115081	-0.049141	0.003545
_cell_angle_gamma	92.188637	ZN006	ZN	0.031805	0.263983	0.002869
_symmetry_space_group_name_H-M	'P 1'	0007	O	0.407381	0.171994	0.003906
_symmetry_Int_Tables_number	1	H008	H	-0.117036	-0.107968	0.001622
loop_		H009	H	0.325484	-0.410545	0.001234
_atom_site_label		H010	H	0.438785	0.118288	0.001935
_atom_site_type_symbol		0011	O	-0.038325	0.315318	-0.001013
_atom_site_fract_x		0012	O	0.416700	0.073012	-0.000823
_atom_site_fract_y		0013	O	0.406700	-0.423022	-0.000540
_atom_site_fract_z		0014	O	-0.045694	-0.174014	-0.001225
H001 H -0.282752 -0.118711 0.003968		MN015	MN	0.285624	0.318986	-0.002968
loop_		MN016	MN	-0.218058	0.071877	-0.003117
_atom_site_label		MN017	MN	-0.208571	-0.426072	-0.003048
_atom_site_type_symbol		MN018	MN	0.281949	-0.172798	-0.002964
_atom_site_fract_x		0019	O	-0.395757	0.328365	-0.004590
_atom_site_fract_y		0020	O	0.161216	0.075266	-0.004950
_atom_site_fract_z		0021	O	0.155498	-0.429593	-0.004845
H001 H -0.282752 -0.118711 0.003968		0022	O	-0.401720	-0.182885	-0.004618

6 Two Cation Surface Structures

6.1 $M_2^{n+}Mn_4O_8 \cdot 6H_2O$ Parallel Pattern, Manganese Hollow Sites

Potassium

data_BG_KMn204_3_H2O.SLAB.001.3_16.optgeom.MnECP.out

```
_cell_length_a          3.013323
_cell_length_b          5.186884
_cell_length_c          500.000000
_cell_angle_alpha       90.000000
_cell_angle_beta        90.000000
_cell_angle_gamma       93.913540
_symmetry_space_group_name_H-M   'P 1'
_symmetry_Int_Tables_number      1
```

```
loop_
_symmetry_equiv_pos_as_xyz
'x, y, z'
```

```
loop_
_atom_site_label
_atom_site_type_symbol
_atom_site_fract_x
_atom_site_fract_y
_atom_site_fract_z
```

```
H001 H -0.241333 0.370319 0.007637
K002 K 0.456112 -0.135596 0.005226
0003 O 0.066041 0.374619 0.007055
H004 H 0.073762 0.328242 0.004910
0005 O -0.111749 -0.282500 0.001351
H006 H -0.025282 -0.461974 0.001553
H007 H 0.048981 -0.218985 -0.000255
H008 H 0.408680 0.259471 0.001749
0009 O 0.100409 0.254583 0.002311
H010 H -0.080506 0.254591 -0.001133
0011 O 0.264211 -0.190772 -0.003365
0012 O -0.172663 0.280314 -0.003004
MN013 MN 0.271258 0.475392 -0.005308
MN014 MN -0.221267 -0.037321 -0.005283
0015 O -0.265393 -0.346590 -0.007131
0016 O 0.299292 0.133634 -0.006976
```

Lithium

data_BG_LiMn204_3_H2O.SLAB.001.3_16.optgeom.MnECP.Na.out

```
_cell_length_a          3.016273
_cell_length_b          5.036807
_cell_length_c          500.000000
_cell_angle_alpha       90.000000
_cell_angle_beta        90.000000
_cell_angle_gamma       92.758189
_symmetry_space_group_name_H-M   'P 1'
_symmetry_Int_Tables_number      1
```

```
loop_
_symmetry_equiv_pos_as_xyz
'x, y, z'
```

```
loop_
_atom_site_label
_atom_site_type_symbol
_atom_site_fract_x
_atom_site_fract_y
_atom_site_fract_z
H001 H -0.120478 0.203909 0.007432
LI002 LI 0.327196 -0.293566 0.005384
```

0003	O	0.179353	0.204794	0.006747
H004	H	0.149873	0.227470	0.004590
0005	O	-0.178442	-0.226676	0.002334
H006	H	-0.068543	-0.373082	0.001280
H007	H	-0.059014	-0.054233	0.001609
H008	H	0.428629	0.267496	0.001196
0009	O	0.125817	0.271084	0.001824
H010	H	-0.061712	0.293002	-0.001309
0011	O	0.264191	-0.155718	-0.003399
0012	O	-0.180649	0.324248	-0.003123
MN013	MN	0.266435	-0.485969	-0.005468
MN014	MN	-0.226153	-0.001714	-0.005364
0015	O	-0.266894	-0.310304	-0.007290
0016	O	0.290944	0.166685	-0.007106

Sodium

data_BG_NaMn204_3_H2O.SLAB.001.3_16.optgeom.MnECP.out

_cell_length_a		3.016273
_cell_length_b		5.036807
_cell_length_c		500.000000
_cell_angle_alpha		90.000000
_cell_angle_beta		90.000000
_cell_angle_gamma		92.758189
_symmetry_space_group_name_H-M		'P 1'
_symmetry_Int_Tables_number		1

```
loop_
_symmetry_equiv_pos_as_xyz
'x, y, z'
```

```
loop_
_atom_site_label
_atom_site_type_symbol
_atom_site_fract_x
_atom_site_fract_y
_atom_site_fract_z
```

H001	H	-0.120478	0.203909	0.007432
NA002	NA	0.327196	-0.293566	0.005384
0003	O	0.179353	0.204794	0.006747
H004	H	0.149873	0.227470	0.004590
0005	O	-0.178442	-0.226676	0.002334
H006	H	-0.068543	-0.373082	0.001280
H007	H	-0.059014	-0.054233	0.001609
H008	H	0.428629	0.267496	0.001196
0009	O	0.125817	0.271084	0.001824
H010	H	-0.061712	0.293002	-0.001309
0011	O	0.264191	-0.155718	-0.003399
0012	O	-0.180649	0.324248	-0.003123
MN013	MN	0.266435	-0.485969	-0.005468
MN014	MN	-0.226153	-0.001714	-0.005364
0015	O	-0.266894	-0.310304	-0.007290
0016	O	0.290944	0.166685	-0.007106

6.2 $M_2^{n+}Mn_4O_8 \cdot 6H_2O$ Parallel Pattern, Oxygen Hollow Sites

Potassium

data_BG_K2Mn408_6_H2O.SLAB.MnECP.para.1.relax.out

_cell_length_a		6.010614
_cell_length_b		5.142610
_cell_length_c		500.000000
_cell_angle_alpha		90.000000
_cell_angle_beta		90.000000

_cell_angle_gamma 92.736003
 _symmetry_space_group_name_H-M 'P 1'
 _symmetry_Int_Tables_number 1
 loop_
 _symmetry_equiv_pos_as_xyz
 'x, y, z'
 loop_
 _atom_site_label
 _atom_site_type_symbol
 _atom_site_fract_x
 _atom_site_fract_y
 _atom_site_fract_z
 H001 H 0.009858 0.389474 0.008239
 H002 H 0.375262 0.360646 0.007306
 K003 K 0.228864 -0.059362 0.004540
 K004 K -0.280829 -0.222237 0.006106
 O005 O 0.106233 0.464897 0.006882
 O006 O -0.470476 0.294775 0.007249
 H007 H 0.060898 0.395970 0.003900
 H008 H -0.438619 0.265270 0.005278
 O009 O -0.088855 -0.167971 0.001221
 O010 O 0.462860 -0.365217 0.001623
 H011 H -0.101151 -0.358100 0.001266
 H012 H -0.465503 0.456817 0.001735
 H013 H 0.010005 -0.143050 -0.000354
 H014 H -0.478426 -0.278799 0.000002
 H015 H 0.208246 0.462931 0.001363
 H016 H -0.298151 0.091037 0.001596
 O017 O 0.068547 0.366147 0.001880
 O018 O -0.423549 0.187447 0.002191
 H019 H -0.061132 0.279278 -0.001053
 H020 H 0.455154 0.225993 -0.001062
 O021 O 0.120036 -0.204790 -0.003258
 O022 O -0.383791 -0.207690 -0.003276
 O023 O -0.103631 0.275486 -0.002963
 O024 O 0.400782 0.264241 -0.002901
 MN025 MN 0.121149 0.461985 -0.005246
 MN026 MN -0.378874 0.460635 -0.005227
 MN027 MN -0.127513 -0.050310 -0.005202
 MN028 MN 0.373818 -0.051500 -0.005202
 O029 O -0.147591 -0.357185 -0.007069
 O030 O 0.351846 -0.360646 -0.007073
 O031 O 0.132150 0.119773 -0.006899
 O032 O -0.367063 0.118903 -0.006916

Sodium

data_BG_Na2Mn408_6_H2O.SLAB.para.1.relax.out

_cell_length_a 5.927843
 _cell_length_b 5.172349
 _cell_length_c 500.000000
 _cell_angle_alpha 90.000000
 _cell_angle_beta 90.000000
 _cell_angle_gamma 93.615025
 _symmetry_space_group_name_H-M 'P 1'
 _symmetry_Int_Tables_number 1

loop_
 _symmetry_equiv_pos_as_xyz
 'x, y, z'

loop_
 _atom_site_label
 _atom_site_type_symbol
 _atom_site_fract_x
 _atom_site_fract_y
 _atom_site_fract_z
 H001 H 0.070746 0.082669 0.008701
 H002 H 0.408627 0.201867 0.007197
 NA003 NA 0.292652 -0.321816 0.005528
 NA004 NA -0.199110 0.020596 0.004041
 O005 O 0.139801 0.031167 0.007064
 O006 O -0.452767 0.313387 0.006815
 H007 H 0.141513 0.207231 0.004830
 H008 H -0.451225 0.332820 0.004819
 O009 O -0.077952 -0.291538 0.001399
 O010 O 0.445768 -0.146140 0.001796
 H011 H 0.007366 -0.434333 0.002116
 H012 H 0.496576 -0.210332 0.000070
 H013 H -0.002494 -0.237697 -0.000300
 H014 H 0.477382 0.041861 0.001597

H015	H	0.284290	0.335646	0.002270	MN025	MN	0.134084	0.462979	-0.005323
H016	H	-0.331331	0.486207	0.001323	MN026	MN	-0.373551	0.461453	-0.005064
0017	O	0.132320	0.321122	0.003105	MN027	MN	-0.117297	-0.047662	-0.005407
0018	O	-0.438750	0.337391	0.001583	MN028	MN	0.385831	-0.049348	-0.005146
H019	H	-0.106769	0.291418	-0.001184	0029	O	-0.155560	-0.390723	-0.007005
H020	H	0.451127	0.304197	-0.001254	0030	O	0.394318	-0.380139	-0.006954
0021	O	0.100970	-0.185657	-0.003335	0031	O	0.159994	0.140222	-0.006980
0022	O	-0.398325	-0.188171	-0.003353	0032	O	-0.372558	0.121272	-0.006853
0023	O	-0.121894	0.295691	-0.003105	Lithium				
0024	O	0.383931	0.297737	-0.003128	data_BG_LiMn204_3_H2O.SLAB.Na.alt.1.01.relax.out				
MN025	MN	0.107504	0.484593	-0.005342	_cell_length_a		5.874745		
MN026	MN	-0.396166	0.483797	-0.005482	_cell_length_b		5.204174		
MN027	MN	-0.141927	-0.031561	-0.005307	_cell_length_c		500.000000		
MN028	MN	0.359845	-0.027540	-0.005273	_cell_angle_alpha		90.000000		
0029	O	-0.160832	-0.333457	-0.007244	_cell_angle_beta		90.000000		
0030	O	0.336197	-0.332204	-0.007216	_cell_angle_gamma		90.595122		
0031	O	0.118247	0.141167	-0.007000	_symmetry_space_group_name_H-M		'P 1'		
0032	O	-0.381441	0.136584	-0.007054	_symmetry_Int_Tables_number		1		

6.3 $M_2^{n+}Mn_4O_8 \cdot 6H_2O$ Alternating Pattern, Oxygen Hollow Sites

Potassium

data_BG_K2Mn408_6_H2O.SLAB.MnECP.alt.relax.out

_cell_length_a		6.054967
_cell_length_b		5.145689
_cell_length_c		500.000000
_cell_angle_alpha		90.000000
_cell_angle_beta		90.000000
_cell_angle_gamma		88.945835
_symmetry_space_group_name_H-M		'P 1'
_symmetry_Int_Tables_number		1

loop_
_symmetry_equiv_pos_as_xyz
'x, y, z'

loop_				
_atom_site_label				
_atom_site_type_symbol				
_atom_site_fract_x				
_atom_site_fract_y				
_atom_site_fract_z				
H001	H	0.042524	0.404803	0.008507
H002	H	0.388266	0.354960	0.007266
K003	K	0.218004	-0.052049	0.004635
K004	K	-0.283169	-0.248643	0.005958
0005	O	0.123812	0.481189	0.007065
0006	O	-0.460227	0.274443	0.007086
H007	H	0.062798	0.417790	0.004128
H008	H	-0.442337	0.244827	0.005089
0009	O	-0.082344	-0.139608	0.001049
0010	O	0.456146	-0.369009	0.001726
H011	H	-0.091753	-0.329100	0.001159
H012	H	-0.479742	0.445568	0.001751
H013	H	0.015050	-0.124275	-0.000525
H014	H	-0.496186	-0.292729	0.000009
H015	H	0.191694	0.463828	0.001473
H016	H	-0.312058	0.069865	0.001450
0017	O	0.052101	0.389428	0.002106
0018	O	-0.444280	0.167665	0.001977
H019	H	-0.104132	0.300352	-0.001101
H020	H	0.450210	0.216494	-0.000959
0021	O	0.128368	-0.205603	-0.003476
0022	O	-0.397510	-0.231790	-0.003066
0023	O	-0.119888	0.297036	-0.003045
0024	O	0.399944	0.261355	-0.002857

MN025	MN	0.134084	0.462979	-0.005323
MN026	MN	-0.373551	0.461453	-0.005064
MN027	MN	-0.117297	-0.047662	-0.005407
MN028	MN	0.385831	-0.049348	-0.005146
0029	O	-0.155560	-0.390723	-0.007005
0030	O	0.394318	-0.380139	-0.006954
0031	O	0.159994	0.140222	-0.006980
0032	O	-0.372558	0.121272	-0.006853
Lithium				
data_BG_LiMn204_3_H2O.SLAB.Na.alt.1.01.relax.out				
_cell_length_a		5.874745		
_cell_length_b		5.204174		
_cell_length_c		500.000000		
_cell_angle_alpha		90.000000		
_cell_angle_beta		90.000000		
_cell_angle_gamma		90.595122		
_symmetry_space_group_name_H-M		'P 1'		
_symmetry_Int_Tables_number		1		
loop_				
_symmetry_equiv_pos_as_xyz				
'x, y, z'				

loop_				
_atom_site_label				
_atom_site_type_symbol				
_atom_site_fract_x				
_atom_site_fract_y				
_atom_site_fract_z				
H001	H	0.057725	0.400696	0.007616
H002	H	-0.444300	0.204321	0.007577
LI003	LI	0.308750	-0.355938	0.003487
LI004	LI	-0.194584	-0.050088	0.003523
0005	O	0.193694	0.379234	0.006556
0006	O	-0.309750	0.221808	0.006479
H007	H	0.134108	0.282805	0.004979
H008	H	-0.369971	0.314027	0.004881
0009	O	-0.009465	-0.335972	0.001974
0010	O	0.493959	-0.072204	0.001835
H011	H	0.000657	0.468867	0.001960
H012	H	-0.473741	-0.134865	0.000003
H013	H	0.021610	-0.278775	0.000104
H014	H	-0.497162	0.125589	0.001783
H015	H	0.153686	0.097931	0.001408
H016	H	-0.357105	0.487462	0.001189
0017	O	0.018400	0.184592	0.002007
0018	O	-0.489948	0.404291	0.001944
H019	H	-0.089727	0.226586	-0.000798
H020	H	0.370946	0.366806	-0.000866
0021	O	0.085144	-0.216599	-0.003003
0022	O	-0.412112	-0.213324	-0.003158
0023	O	-0.143722	0.263040	-0.002699
0024	O	0.335869	0.322335	-0.002781
MN025	MN	0.090402	0.463790	-0.004974
MN026	MN	-0.411565	0.462990	-0.005109
MN027	MN	-0.155605	-0.047595	-0.004943
MN028	MN	0.341705	-0.047530	-0.005111
0029	O	-0.151419	-0.375272	-0.006775
0030	O	0.305601	-0.401218	-0.007037
0031	O	0.087397	0.130037	-0.006681
0032	O	-0.395600	0.128877	-0.006696

Sodium

data_BG_Na2Mn408_6_H2O.SLAB.alt.1.01.relax.out

_cell_length_a		6.045242
_cell_length_b		5.134088

```

_cell_length_c          500.000000      _atom_site_type_symbol
_cell_angle_alpha       90.000000      _atom_site_fract_x
_cell_angle_beta        90.000000      _atom_site_fract_y
_cell_angle_gamma       89.576117      _atom_site_fract_z
_symmetry_space_group_name_H-M   'P 1'
_symmetry_Int_Tables_number      1
loop_
_symmetry_equiv_pos_as_xyz
'x, y, z'

loop_
_atom_site_label
_atom_site_type_symbol
_atom_site_fract_x
_atom_site_fract_y
_atom_site_fract_z
H001 H 0.085916 0.077295 0.008541
H002 H 0.423646 0.195382 0.006932
NA003 NA 0.277744 -0.344084 0.004067
NA004 NA -0.223844 -0.025033 0.004243
O005 O 0.157899 0.007527 0.006980
O006 O -0.447015 0.303955 0.006583
H007 H 0.117289 0.122663 0.005219
H008 H -0.454549 0.347883 0.004623
O009 O -0.066997 -0.325605 0.001707
O010 O 0.465628 -0.053978 0.001546
H011 H -0.015004 0.488787 0.002027
H012 H -0.481951 -0.132629 -0.000132
H013 H -0.008953 -0.268972 -0.000076
H014 H -0.496364 0.138160 0.001396
H015 H 0.176885 0.134351 0.001684
H016 H -0.337116 -0.484607 0.001181
O017 O 0.067795 0.225524 0.002765
O018 O -0.472977 0.419597 0.001504
H019 H -0.074140 0.266868 -0.000897
H020 H 0.421516 0.382865 -0.001084
O021 O 0.095467 -0.193109 -0.002899
O022 O -0.380357 -0.171477 -0.003358
O023 O -0.108005 0.301860 -0.002768
O024 O 0.374999 0.343364 -0.003069
MN025 MN 0.122566 -0.496771 -0.004987
MN026 MN -0.374876 -0.496936 -0.005339
MN027 MN -0.122967 -0.012131 -0.005038
MN028 MN 0.373850 -0.004188 -0.005204
O029 O -0.113578 -0.339453 -0.006863
O030 O 0.332934 -0.338012 -0.006966
O031 O 0.119898 0.162393 -0.006726
O032 O -0.341459 0.175212 -0.006917

subsectionM2n+Mn4O8·6H2O Surfaces Water Removal
Potassium, No Waters
data_BG_K2Mn408_3H2O.SLAB.211.MnECP.wat1wat2wat3wat4wat5wat6.out

_cell_length_a          6.072054
_cell_length_b          5.092823
_cell_length_c          500.000000
_cell_angle_alpha        90.000000
_cell_angle_beta         90.000000
_cell_angle_gamma        89.877484
_symmetry_space_group_name_H-M   'P 1'
_symmetry_Int_Tables_number      1
loop_
_symmetry_equiv_pos_as_xyz
'x, y, z'

loop_
_atom_site_label
_atom_site_type_symbol
_atom_site_fract_x
_atom_site_fract_y
_atom_site_fract_z
K001 K 0.263864 0.062462 0.000948
K002 K -0.223597 -0.358847 0.001095
O003 O 0.096927 -0.234243 -0.002099
O004 O -0.382930 -0.180917 -0.002774
O005 O -0.077697 0.262538 -0.002019
O006 O 0.394981 0.318856 -0.002789
MN007 MN 0.128793 0.471747 -0.004362
MN008 MN -0.371598 0.482306 -0.004910
MN009 MN -0.112659 -0.026755 -0.004370
MN010 MN 0.387740 -0.017206 -0.005041
O011 O -0.108895 -0.362171 -0.006200
O012 O 0.334930 -0.349823 -0.006481
O013 O 0.121632 0.138516 -0.006233
O014 O -0.319943 0.151656 -0.006448

Potassium, One Water
data_BG_K2Mn408_3H2O.SLAB.211.MnECP.wat1wat2wat3wat4wat6.02.out

_cell_length_a          6.050259
_cell_length_b          5.027739
_cell_length_c          500.000000
_cell_angle_alpha        90.000000
_cell_angle_beta         90.000000
_cell_angle_gamma        93.217845
_symmetry_space_group_name_H-M   'P 1'
_symmetry_Int_Tables_number      1

loop_
_symmetry_equiv_pos_as_xyz
'x, y, z'

loop_
_atom_site_label
_atom_site_type_symbol
_atom_site_fract_x
_atom_site_fract_y
_atom_site_fract_z
K001 K 0.344580 -0.281866 0.001406
K002 K -0.144087 -0.255852 0.001527
H003 H 0.207658 0.222349 0.000863
O004 O 0.101556 0.230714 0.002327
H005 H -0.040762 0.269013 -0.000522
O006 O 0.109757 -0.166779 -0.002648
O007 O -0.388067 -0.164291 -0.002572
O008 O -0.107931 0.311612 -0.002301
O009 O 0.386130 0.312232 -0.002414
MN010 MN 0.115095 -0.499987 -0.004741
MN011 MN -0.396426 0.497148 -0.004641
MN012 MN -0.136782 -0.012297 -0.004671
MN013 MN 0.364017 -0.000687 -0.004602
O014 O -0.159232 -0.324241 -0.006482
O015 O 0.345456 -0.317267 -0.006521
O016 O 0.120374 0.152600 -0.006415
O017 O -0.375494 0.154365 -0.006350

Potassium, Three Waters
data_BG_K2Mn408_3H2O.SLAB.211.MnECP.wat1wat3wat4.01.out

_cell_length_a          6.035642
_cell_length_b          5.067420
_cell_length_c          500.000000
_cell_angle_alpha        90.000000
_cell_angle_beta         90.000000
_cell_angle_gamma        93.110231
_symmetry_space_group_name_H-M   'P 1'

```

```

_symmetry_Int_Tables_number      1
loop_
_symmetry_equiv_pos_as_xyz
'x, y, z'

loop_
_atom_site_label
_atom_site_type_symbol
_atom_site_fract_x
_atom_site_fract_y
_atom_site_fract_z
H001  H  -0.488051   0.448993  0.007703
K002  K   0.329739  -0.277286  0.001598
K003  K  -0.171408  -0.264995  0.001910
0004  O  -0.430644  -0.482909  0.006039
H005  H  -0.436023   0.368247  0.004644
H006  H   0.231091   0.217763  0.002033
H007  H  -0.324182   0.217395  0.000964
0008  O   0.071238   0.230019  0.002136
0009  O  -0.454324   0.208696  0.002108
H010  H   0.011922   0.246119  0.000188
H011  H   0.437513   0.259719  -0.000682
0012  O   0.098828  -0.177722  -0.002642
0013  O  -0.404142  -0.180091  -0.002678
0014  O  -0.119345   0.296961  -0.002338
0015  O   0.376345   0.302211  -0.002490
MN016 MN   0.092755   0.485419  -0.004696
MN017 MN  -0.398318   0.489829  -0.004797
MN018 MN  -0.147384  -0.016028  -0.004599
MN019 MN   0.350561  -0.025051  -0.004726
0020  O  -0.166399  -0.328568  -0.006540
0021  O   0.327992  -0.334696  -0.006553
0022  O   0.109839   0.142352  -0.006395
0023  O  -0.388236   0.142215  -0.006414

Potassium, Four Waters
data_BG_K2Mn408_3H2O.SLAB.211.MnECP.wat3wat4.01.out

_cell_length_a                  6.005681
_cell_length_b                  5.083870
_cell_length_c                  500.000000
_cell_angle_alpha                90.000000
_cell_angle_beta                 90.000000
_cell_angle_gamma                93.369483
_symmetry_space_group_name_H-M   'P 1'
_symmetry_Int_Tables_number       1

loop_
_symmetry_equiv_pos_as_xyz
'x, y, z'

loop_
_atom_site_label
_atom_site_type_symbol
_atom_site_fract_x
_atom_site_fract_y
_atom_site_fract_z
H001  H  -0.082069   -0.471089  0.007326
H002  H   0.420690  -0.471183  0.007358
K003  K   0.324136  -0.277865  0.001978
K004  K  -0.175720  -0.280562  0.001942
0005  O   0.058861  -0.475747  0.006390
0006  O  -0.439526  -0.474833  0.006398
H007  H   0.040127   0.376865  0.005064
H008  H  -0.459101   0.378416  0.005066
H009  H   0.195589   0.204601  0.001957
H010  H  -0.304058   0.203013  0.001983
0011  O   0.036941   0.213803  0.002200
0012  O  -0.462721   0.215568  0.002201
H013  H  -0.041740   0.240974  -0.000533
H014  H   0.459091   0.241675  -0.000534
0015  O   0.108008  -0.212086  -0.002717
0016  O  -0.392003  -0.212058  -0.002718
0017  O  -0.108459   0.268091  -0.002457
0018  O   0.391745   0.268156  -0.002456
MN019 MN   0.110894   0.456811  -0.004793
MN020 MN  -0.389179   0.456845  -0.004797
MN021 MN  -0.135019  -0.053879  -0.004698
MN022 MN   0.365025  -0.053863  -0.004696
0023  O  -0.156072  -0.361922  -0.006608
0024  O   0.343879  -0.361874  -0.006607
0025  O   0.124659   0.112009  -0.006436
0026  O  -0.375374   0.111903  -0.006437

Potassium, Two Waters
data_BG_K2Mn408_3H2O.SLAB.211.MnECP.wat2wat3wat4wat6.03.out

_cell_length_a                  6.125609
_cell_length_b                  5.013676
_cell_length_c                  500.000000
_cell_angle_alpha                90.000000
_cell_angle_beta                 90.000000
_cell_angle_gamma                93.455875
_symmetry_space_group_name_H-M   'P 1'
_symmetry_Int_Tables_number       1

loop_
_symmetry_equiv_pos_as_xyz
'x, y, z'

loop_
_atom_site_label
_atom_site_type_symbol
_atom_site_fract_x
_atom_site_fract_y
_atom_site_fract_z
H001  H   0.446566   0.409481  0.006711
K002  K   0.316661  -0.112980  0.001874
K003  K  -0.207732  -0.332884  0.002058
0004  O   0.453899   0.424537  0.004799
H005  H   0.265189   0.378311  0.003725
H006  H   0.175538   0.349463  0.000601
0007  O   0.111784   0.343871  0.002433
H008  H  -0.102586   0.225826  -0.000272
0009  O   0.027219  -0.202693  -0.002359
0010  O  -0.444490  -0.227463  -0.002153
0011  O  -0.189103   0.266035  -0.001836

Potassium, Five Waters
data_BG_K2Mn408_3H2O.SLAB.211.MnECP.wat4.01.out

_cell_length_a                  5.925605
_cell_length_b                  5.131714
_cell_length_c                  500.000000
_cell_angle_alpha                90.000000
_cell_angle_beta                 90.000000
_cell_angle_gamma                92.820127
_symmetry_space_group_name_H-M   'P 1'

```

```

_symmetry_Int_Tables_number      1
loop_
_symmetry_equiv_pos_as_xyz
'x, y, z'

loop_
_atom_site_label
_atom_site_type_symbol
_atom_site_fract_x
_atom_site_fract_y
_atom_site_fract_z
H001 H -0.107597 0.477940 0.007658
H002 H 0.363858 0.477380 0.007421
K003 K 0.299795 -0.032799 0.005670
K004 K -0.155780 -0.236433 0.001685
0005 O 0.036689 0.490787 0.006748
0006 O -0.473598 0.477823 0.007128
H007 H 0.017997 0.386683 0.004972
H008 H -0.452951 0.400604 0.005293
0009 O 0.353256 -0.340897 0.001667
H010 H 0.452285 -0.498884 0.001766
H011 H 0.340441 -0.289034 -0.000186
H012 H 0.153821 0.367454 0.001769
H013 H -0.264050 0.265258 0.002179
0014 O 0.025936 0.252740 0.002292
0015 O -0.428635 0.258789 0.002335
H016 H -0.039203 0.236305 -0.000930
H017 H 0.478443 0.225814 -0.000930
0018 O 0.143772 -0.233116 -0.003166
0019 O -0.354708 -0.234100 -0.003195
0020 O -0.077904 0.246389 -0.002881
0021 O 0.426758 0.243209 -0.002832
MN022 MN 0.148219 0.435670 -0.005168
MN023 MN -0.351663 0.434821 -0.005190
MN024 MN -0.100006 -0.077000 -0.005150
MN025 MN 0.400687 -0.076300 -0.005133
0026 O -0.120006 -0.383452 -0.007048
0027 O 0.379119 -0.383611 -0.007025
0028 O 0.160376 0.093915 -0.006849
0029 O -0.340772 0.092354 -0.006874

```

Lithium, Five Waters

data_BG_Li2Mn408_6H2O.SLAB.MnCEP.Na.wat1.out

```

_cell_length_a 5.924555
_cell_length_b 5.070790
_cell_length_c 500.000000
_cell_angle_alpha 90.000000
_cell_angle_beta 90.000000
_cell_angle_gamma 92.579357
_symmetry_space_group_name_H-M 'P 1'
_symmetry_Int_Tables_number 1

```

```

loop_
_symmetry_equiv_pos_as_xyz
'x, y, z'

```

```

loop_
_atom_site_label
_atom_site_type_symbol
_atom_site_fract_x
_atom_site_fract_y
_atom_site_fract_z

```

```

H001 H 0.339990 0.224957 0.007290
LI002 LI 0.166089 -0.421800 0.003622
LI003 LI -0.359560 -0.386483 0.003878
0004 O 0.483000 0.303450 0.006741
H005 H -0.485188 0.246127 0.004805

```

```

0006 O -0.089691 -0.233020 0.002398
0007 O 0.411766 -0.224689 0.001978
H008 H -0.092077 -0.289469 0.000542
H009 H 0.427566 -0.292525 0.000177
H010 H -0.026567 -0.033468 0.002249
H011 H 0.480049 -0.034038 0.001898
H012 H 0.192210 0.173836 0.000764
H013 H -0.253757 0.212272 0.001740
0014 O 0.061392 0.226217 0.001751
0015 O -0.413818 0.238730 0.001986
H016 H -0.040621 0.317876 -0.001081
H017 H 0.498156 0.294396 -0.000905
0018 O 0.156656 -0.155777 -0.003153
0019 O -0.338817 -0.146265 -0.003037
0020 O -0.080961 0.346504 -0.003011
0021 O 0.435297 0.328429 -0.002746
MN022 MN 0.161922 -0.480642 -0.005243
MN023 MN -0.337107 -0.480051 -0.005029
MN024 MN -0.089980 0.004540 -0.005122
MN025 MN 0.417957 0.005335 -0.005043
0026 O -0.112257 -0.299481 -0.007036
0027 O 0.415249 -0.314669 -0.006884
0028 O 0.173208 0.173781 -0.006812
0029 O -0.333928 0.174602 -0.006812

```

Lithium, No Waters

data_BG_Li2Mn408_6H2O.SLAB.MnCEP.Na.wat1wat2wat3wat4wat5wat6.out

```

_cell_length_a 5.731962
_cell_length_b 4.956751
_cell_length_c 500.000000
_cell_angle_alpha 90.000000
_cell_angle_beta 90.000000
_cell_angle_gamma 90.189474
_symmetry_space_group_name_H-M 'P 1'
_symmetry_Int_Tables_number 1

```

```

loop_
_symmetry_equiv_pos_as_xyz
'x, y, z'

```

```

loop_
_atom_site_label
_atom_site_type_symbol
_atom_site_fract_x
_atom_site_fract_y
_atom_site_fract_z
LI001 LI 0.170520 -0.320131 0.002743
LI002 LI -0.330505 -0.353599 0.002759
0003 O 0.138276 -0.155695 -0.002931
0004 O -0.366934 -0.156422 -0.002922
0005 O -0.112070 0.349396 -0.002888
0006 O 0.387700 0.346678 -0.002884
MN007 MN 0.135211 -0.487366 -0.004898
MN008 MN -0.363319 -0.486775 -0.004897
MN009 MN -0.113880 0.013410 -0.004873
MN010 MN 0.386347 0.014068 -0.004875
0011 O -0.114938 -0.322827 -0.006781
0012 O 0.385241 -0.319185 -0.006778
0013 O 0.140003 0.183006 -0.006754
0014 O -0.366582 0.182765 -0.006754

```

Lithium, One Water

data_BG_Li2Mn408_6H2O.SLAB.MnCEP.Na.wat1wat2wat3wat5wat6.out

```

_cell_length_a 5.878840
_cell_length_b 4.993581
_cell_length_c 500.000000
_cell_angle_alpha 90.000000

```

```

_cell_angle_beta          90.000000      MN015  MN -0.157859  0.038922 -0.004416
_cell_angle_gamma         91.419802      MN016  MN  0.348826  0.024921 -0.004219
_symmetry_space_group_name_H-M   'P 1'      0017   0 -0.175980 -0.289718 -0.006280
_symmetry_Int_Tables_number    1           0018   0  0.351018 -0.299814 -0.006073
                                         0019   0  0.111893  0.191392 -0.005912
                                         0020   0 -0.435611  0.220685 -0.006228

loop_
_symmetry_equiv_pos_as_xyz
'x, y, z'

loop_
_atom_site_label
_atom_site_type_symbol
_atom_site_fract_x
_atom_site_fract_y
_atom_site_fract_z
LI001  LI  0.209196 -0.405538  0.003116
LI002  LI -0.370525 -0.265048  0.003036
0003   O -0.072052 -0.307009  0.001696
H004   H -0.090037 -0.446118  0.000240
H005   H -0.020431 -0.152729  0.000597
0006   O  0.138698 -0.133553 -0.002721
0007   O -0.365335 -0.124928 -0.002781
0008   O -0.086844  0.350698 -0.002536
0009   O  0.389744  0.370144 -0.002836
MN010  MN  0.139565 -0.465821 -0.004723
MN011  MN -0.363331 -0.465515 -0.004817
MN012  MN -0.110736  0.033076 -0.004672
MN013  MN  0.388025  0.034702 -0.004757
0014   O -0.107445 -0.298666 -0.006519
0015   O  0.360414 -0.279329 -0.006701
0016   O  0.137413  0.201810 -0.006564
0017   O -0.354247  0.187157 -0.006569

Lithium, Three Waters

data_BG_Li2Mn408_6H2O.SLAB.MnCEP.Na.wat1wat4wat5.03.out

_cell_length_a            5.844049
_cell_length_b            5.139720
_cell_length_c            500.000000
_cell_angle_alpha          90.000000
_cell_angle_beta           90.000000
_cell_angle_gamma          91.173838
_symmetry_space_group_name_H-M   'P 1'
_symmetry_Int_Tables_number    1

loop_
_symmetry_equiv_pos_as_xyz
'x, y, z'

loop_
_atom_site_label
_atom_site_type_symbol
_atom_site_fract_x
_atom_site_fract_y
_atom_site_fract_z
H001   H -0.229642 -0.389302  0.005267
LI002  LI  0.056555 -0.183357  0.001814
LI003  LI -0.406252 -0.446086  0.000851
0004   O -0.158051 -0.457953  0.003695
H005   H -0.169070  0.345559  0.003671
0006   O  0.383443 -0.122583  0.002332
H007   H  0.389396 -0.161757  0.000435
H008   H -0.382095 -0.009659  0.002571
H009   H -0.202927  0.139694  0.000587
0010   O -0.215055  0.069707  0.002449
H011   H  0.370040  0.184745 -0.000116
0012   O  0.054490 -0.216834 -0.002391
0013   O -0.435632 -0.225999 -0.002422
0014   O -0.193060  0.281590 -0.002256
0015   O  0.347310  0.314835 -0.001516
MN016  MN  0.060779  0.438677 -0.004200
MN017  MN -0.434696  0.444466 -0.004324
MN018  MN -0.192407 -0.056516 -0.004357
MN019  MN  0.307080 -0.068405 -0.004556
0020   O -0.214865 -0.370468 -0.006259
0021   O  0.315847 -0.439124 -0.006132
0022   O  0.058520  0.111371 -0.006071
0023   O -0.436895  0.118487 -0.006099

Lithium, Two Waters

data_BG_Li2Mn408_6H2O.SLAB.MnCEP.Na.wat1wat3wat4wat5.02.out

_cell_length_a            6.046226
_cell_length_b            5.022475
_cell_length_c            500.000000
_cell_angle_alpha          90.000000
_cell_angle_beta           90.000000
_cell_angle_gamma          92.530857
_symmetry_space_group_name_H-M   'P 1'
_symmetry_Int_Tables_number    1

loop_
_symmetry_equiv_pos_as_xyz
'x, y, z'

loop_
_atom_site_label
_atom_site_type_symbol
_atom_site_fract_x
_atom_site_fract_y
_atom_site_fract_z
H001   H -0.477446 -0.082613  0.005780
LI002  LI  0.364217 -0.316718  0.001529
LI003  LI -0.240846 -0.254159  0.002220
0004   O -0.458678 -0.069433  0.003883
H005   H -0.382829  0.208153  0.002946
H006   H -0.254472  0.360975  0.000254
0007   O -0.342912  0.387414  0.002055
H008   H  0.450596  0.311926 -0.000288
0009   O  0.127805 -0.153685 -0.002065
0010   O -0.402302 -0.129679 -0.002360
0011   O -0.165834  0.377542 -0.002389
0012   O  0.371801  0.349936 -0.001937
MN013  MN  0.095653 -0.462260 -0.004293
MN014  MN -0.401229 -0.458707 -0.004460

Lithium, Four Waters

data_BG_Li2Mn408_6H2O.SLAB.MnCEP.Na.wat2wat4.01.out

_cell_length_a            5.944390
_cell_length_b            5.119654
_cell_length_c            500.000000
_cell_angle_alpha          90.000000
_cell_angle_beta           90.000000
_cell_angle_gamma          93.832363
_symmetry_space_group_name_H-M   'P 1'
_symmetry_Int_Tables_number    1

loop_
_symmetry_equiv_pos_as_xyz
'x, y, z'

```

```

loop_
_atom_site_label
_atom_site_type_symbol
_atom_site_fract_x
_atom_site_fract_y
_atom_site_fract_z
H001 H -0.190718 -0.081339 0.005784
LI002 LI 0.108867 -0.323762 0.003627
LI003 LI -0.339045 -0.331771 0.002011
0004 O -0.119798 -0.107682 0.004092
H005 H 0.020044 0.145484 0.003318
0006 O 0.373361 -0.172490 0.002007
H007 H 0.317150 -0.183052 0.000151
H008 H 0.436014 0.014023 0.002179
H009 H 0.264608 0.300634 0.002626
H010 H -0.308074 0.211328 0.002359
0011 O 0.100841 0.318232 0.002697
0012 O -0.444091 0.302928 0.002195
H013 H 0.010322 0.328586 -0.000691
H014 H -0.497180 0.325852 -0.000675
0015 O 0.177381 -0.132423 -0.002857
0016 O -0.326382 -0.132243 -0.002852
0017 O -0.043863 0.348980 -0.002537
0018 O 0.453587 0.349309 -0.002646
MN019 MN 0.179016 -0.462957 -0.004929
MN020 MN -0.323224 -0.461737 -0.004928
MN021 MN -0.069047 0.024405 -0.004788
MN022 MN 0.432295 0.026187 -0.004844
0023 O -0.088750 -0.279777 -0.006729
0024 O 0.410675 -0.280598 -0.006775
0025 O 0.190327 0.192763 -0.006563
0026 O -0.305139 0.193790 -0.006550

```

Sodium, No Waters

data_BG_Na2Mn408_6_H2O.SLAB.MnECP.wat1wat2wat3wat4wat5wat6.02.out

```

_cell_length_a 5.877845
_cell_length_b 4.989578
_cell_length_c 500.000000
_cell_angle_alpha 90.000000
_cell_angle_beta 90.000000
_cell_angle_gamma 91.605562
_symmetry_space_group_name_H-M 'P 1'
_symmetry_Int_Tables_number 1

loop_
_symmetry_equiv_pos_as_xyz
'x, y, z'

loop_
_atom_site_label
_atom_site_type_symbol
_atom_site_fract_x
_atom_site_fract_y
_atom_site_fract_z
NA001 NA 0.177373 -0.423600 0.001080
NA002 NA -0.328720 -0.407067 0.001211
0003 O 0.132968 -0.141198 -0.002643
0004 O -0.366691 -0.145452 -0.002665
0005 O -0.113618 0.367727 -0.002684
0006 O 0.411092 0.345286 -0.002444
MN007 MN 0.132451 -0.472299 -0.004865
MN008 MN -0.366919 -0.472169 -0.004680
MN009 MN -0.117054 0.026311 -0.004625
MN010 MN 0.387576 0.026767 -0.004515
0011 O -0.143183 -0.285412 -0.006617
0012 O 0.392349 -0.306379 -0.006465
0013 O 0.147092 0.179354 -0.006451
0014 O -0.369646 0.195455 -0.006467

```

Sodium, One Water

data_BG_Na2Mn408_6_H2O.SLAB.MnECP.wat1wat2wat3wat5wat6.02.out

```

_cell_length_a 6.008215
_cell_length_b 5.041194
_cell_length_c 500.000000
_cell_angle_alpha 90.000000
_cell_angle_beta 90.000000
_cell_angle_gamma 92.873648
_symmetry_space_group_name_H-M 'P 1'
_symmetry_Int_Tables_number 1

loop_
_symmetry_equiv_pos_as_xyz
'x, y, z'

loop_
_atom_site_label
_atom_site_type_symbol

```

```

_atom_site_fract_x
_atom_site_fract_y
_atom_site_fract_z
NA001 NA 0.138234 0.260926 0.000622
NA002 NA -0.494502 -0.265123 0.000838
0003 O -0.067545 -0.335733 0.001800
H004 H -0.126804 -0.447959 0.000246
H005 H 0.031652 -0.222338 0.000551
0006 O 0.184433 -0.120135 -0.001911
0007 O -0.341506 -0.091071 -0.002484
0008 O -0.106077 0.409664 -0.002555
0009 O 0.432551 0.384365 -0.001991
MN010 MN 0.151708 -0.426178 -0.004455
MN011 MN -0.352221 -0.425589 -0.004496
MN012 MN -0.105479 0.073856 -0.004649
MN013 MN 0.407869 0.072962 -0.004195
0014 O -0.120372 -0.255630 -0.006382
0015 O 0.404995 -0.259105 -0.006106
0016 O 0.169332 0.223111 -0.006008
0017 O -0.384195 0.257311 -0.006333

```

Sodium, Two Waters

data_BG_Na2Mn408_6_H2O.SLAB.MnECP.wat1wat2wat4wat5.01.out

```

_cell_length_a 5.802513
_cell_length_b 5.189034
_cell_length_c 500.000000
_cell_angle_alpha 90.000000
_cell_angle_beta 90.000000
_cell_angle_gamma 92.499948
_symmetry_space_group_name_H-M 'P 1'
_symmetry_Int_Tables_number 1

```

```

loop_
_symmetry_equiv_pos_as_xyz
'x, y, z'

```

```

loop_
_atom_site_label
_atom_site_type_symbol
_atom_site_fract_x
_atom_site_fract_y
_atom_site_fract_z
NA001 NA 0.240607 0.479150 0.001715
NA002 NA -0.234475 -0.264267 0.002510
0003 O 0.411187 -0.091128 0.002266
H004 H 0.442574 -0.123867 0.000318
H005 H -0.482776 0.078748 0.002446
H006 H -0.245297 0.296479 0.000386
0007 O -0.325780 0.305846 0.002135
H008 H 0.481550 0.261839 -0.001045
0009 O 0.104541 -0.190436 -0.002720
0010 O -0.402413 -0.161679 -0.002548
0011 O -0.141198 0.315187 -0.002835
0012 O 0.382687 0.287950 -0.002585
MN013 MN 0.098239 0.480692 -0.004909
MN014 MN -0.388653 0.478856 -0.005020
MN015 MN -0.147343 -0.021519 -0.004695
MN016 MN 0.358454 -0.037222 -0.004778
0017 O -0.161123 -0.323279 -0.006697
0018 O 0.354500 -0.351247 -0.006586
0019 O 0.115425 0.134968 -0.006489
0020 O -0.391483 0.109845 -0.006667

```

Sodium, Three Waters

data_BG_Na2Mn408_6_H2O.SLAB.MnECP.wat2wat3wat6.01.out

```

_cell_length_a 5.874017

```

_cell_length_b	5.142437	_atom_site_type_symbol
_cell_length_c	500.000000	_atom_site_fract_x
_cell_angle_alpha	90.000000	_atom_site_fract_y
_cell_angle_beta	90.000000	_atom_site_fract_z
_cell_angle_gamma	94.090440	H001 H -0.173776 0.128135 0.006834
_symmetry_space_group_name_H-M	'P 1'	H002 H 0.410319 0.044057 0.007372
_symmetry_Int_Tables_number	1	NA003 NA 0.231402 -0.341227 0.003454
		NA004 NA -0.291501 -0.389554 0.005630
loop_	0005 O -0.017721 0.206619 0.006795	
_symmetry_equiv_pos_as_xyz	'x, y, z'	0006 O -0.467277 -0.006605 0.006226
		H007 H 0.024734 0.214481 0.004859
		H008 H -0.449837 0.159067 0.003880
loop_	0009 O -0.107253 -0.212508 0.002134	
_atom_site_label		H010 H -0.129865 -0.287244 0.000375
_atom_site_type_symbol		H011 H -0.055773 -0.023659 0.001792
_atom_site_fract_x		H012 H 0.195662 0.188599 0.000756
_atom_site_fract_y		H013 H -0.260370 0.278083 0.001815
_atom_site_fract_z		0014 O 0.064793 0.255260 0.001668
H001 H 0.277528 0.150446 0.007316	0015 O -0.417776 0.298686 0.002346	
NA002 NA 0.245353 -0.239996 0.002924	H016 H -0.032126 0.348777 -0.001125	
NA003 NA -0.320485 0.493134 0.001522	H017 H 0.486709 0.333134 -0.000944	
0004 O 0.352170 0.141894 0.005613	0018 O 0.161791 -0.120634 -0.003166	
H005 H 0.249344 0.232440 0.004171	0019 O -0.333812 -0.109565 -0.003097	
0006 O -0.118328 -0.114007 0.002121	0020 O -0.077391 0.380860 -0.003032	
H007 H -0.061991 -0.144770 0.000220	0021 O 0.436746 0.361469 -0.002791	
H008 H -0.047197 0.064307 0.002435	MN022 MN 0.166032 -0.445831 -0.005271	
H009 H 0.216281 0.322181 0.000405	MN023 MN -0.333377 -0.444285 -0.005064	
0010 O 0.125864 0.340396 0.002100	MN024 MN -0.086153 0.039432 -0.005170	
H011 H -0.056781 0.274092 -0.000849	MN025 MN 0.421701 0.038792 -0.005083	
0012 O 0.055921 -0.176133 -0.002554	0026 O -0.107866 -0.265246 -0.007081	
0013 O -0.436055 -0.185711 -0.002638	0027 O 0.419072 -0.280125 -0.006937	
0014 O -0.151760 0.294758 -0.002428	0028 O 0.177077 0.209140 -0.006862	
0015 O 0.337675 0.304272 -0.002510	0029 O -0.330612 0.210735 -0.006861	
MN016 MN 0.066234 0.487308 -0.004855		
MN017 MN -0.446314 0.486573 -0.004817		
MN018 MN -0.182975 -0.029552 -0.004690		
MN019 MN 0.317764 -0.016009 -0.004540		
0020 O -0.199987 -0.335085 -0.006569		
0021 O 0.294777 -0.323739 -0.006587		
0022 O 0.077665 0.133075 -0.006445		
0023 O -0.421892 0.141213 -0.006374		

Sodium, Five Waters

data_BG_Na2Mn408_6_H2O.SLAB.MnECP.wat3.out

_cell_length_a	5.881914	_cell_length_a	5.983525
_cell_length_b	5.063799	_cell_length_b	5.079525
_cell_length_c	500.000000	_cell_length_c	500.000000
_cell_angle_alpha	90.000000	_cell_angle_alpha	90.000000
_cell_angle_beta	90.000000	_cell_angle_beta	90.000000
_cell_angle_gamma	92.106316	_cell_angle_gamma	92.550882
_symmetry_space_group_name_H-M	'P 1'	_symmetry_space_group_name_H-M	'P 1'
_symmetry_Int_Tables_number	1	_symmetry_Int_Tables_number	1
loop_		loop_	
_symmetry_equiv_pos_as_xyz	'x, y, z'	_atom_site_label	
'x, y, z'		_atom_site_type_symbol	
		_atom_site_fract_x	
		_atom_site_fract_y	
		_atom_site_fract_z	
H001 H -0.039525 -0.017979 0.007152	H001 H -0.039525 -0.017979 0.007152		
H002 H 0.370953 -0.004053 0.006395	H002 H 0.370953 -0.004053 0.006395		
NA003 NA 0.261289 -0.393056 0.004271	NA003 NA 0.261289 -0.393056 0.004271		
NA004 NA -0.250662 -0.337937 0.003808	NA004 NA -0.250662 -0.337937 0.003808		

0005	O	0.075523	-0.048033	0.005862	0016	O	-0.362838	-0.062692	-0.002896
0006	O	-0.470235	-0.010271	0.005887	0017	O	-0.089948	0.419044	-0.002642
H007	H	0.060904	0.133677	0.003671	0018	O	0.410232	0.419703	-0.002637
H008	H	-0.455655	0.119078	0.004258	MN019	MN	0.138026	-0.392153	-0.004948
H009	H	0.194302	0.209293	0.000977	MN020	MN	-0.363622	-0.392671	-0.004960
H010	H	-0.320210	0.219021	0.000929	MN021	MN	-0.110472	0.091876	-0.004880
0011	O	0.074213	0.270303	0.002094	MN022	MN	0.389756	0.093455	-0.004861
0012	O	-0.431204	0.300757	0.002012	0023	O	-0.130361	-0.214820	-0.006791
H013	H	-0.043082	0.381595	-0.000815	0024	O	0.369622	-0.213199	-0.006788
H014	H	0.465986	0.389099	-0.000776	0025	O	0.148811	0.262952	-0.006599
0015	O	0.136238	-0.062551	-0.002892	0026	O	-0.351485	0.262394	-0.006603